Climate Change and Water Resources Management:
Adaptations for Flood Control and Water Supply

By

TINGJU ZHU
B.S. (Wuhan University of Hydraulic and Electric Engineering, China) 1995
M.S. (Tsinghua University, China) 2001

DISSERTATION

Submitted in partial satisfaction of the requirements for the degree of

DOCTOR OF PHILOSOPHY

in

Engineering

in the

OFFICE OF GRADUATE STUDIES

of the

UNIVERSITY OF CALIFORNIA

DAVIS

Approved:

_____

_____

_____

Committee in Charge

2004

Acknowledgements

I would like to thank Professor Jay R. Lund, my major advisor and committee chairman, for his help, support, encouragement, and guidance throughout the past three years. His kindness, enthusiasm and insight make working with him full of joy. I would also like to thank Professor Richard E. Howitt, committee member, for his valuable advice on my research. I am grateful to Professor Miguel A. Mariño for his useful advice while severing on my committee. Thanks go to Professor Michael R. Caputo for his valuable helps on optimal control. Thanks go to Dr. Marion W. Jenkins for helping me understand CALVIN and California hydrology. I would like to thank the former and current research group members, in particular, Guiherme F. Marques, Manuel Pulido Velazquez, Roberto Garcia Alcubilla, Stacy K. Tanaka, Sarah Null, David E. Rosenberg, Julien Harou, and John T. Hickey, for their many helps.

Mr. Maury Roos at the California Department of Water Resources, and Dr. Norman Miller and Dr. Kathy Bashford at the Lawrence Berkeley National Laboratory are thanked for their useful comments on the hydrology study summarized in Chapter 1. Mr. Darryl Davis at the US Army Corps of Engineers Hydrologic Engineering Center is thanked for his valuable comments on the study summarized in Chapter 4. I also thank the U.S. Army Corps of Engineers, Sacramento District, for providing the lower American River channel geometry data in a UNET model.

Finally, I would like to thank my family. My grandfather, Zhanren Zhu, my parents, Zibin Zhu and Dongmei Wang, were always supportive and understanding. I particularly want to thank my wife, Linlin Qi, for her love, patience and understanding.

Abstract

This dissertation focuses on flood control and water supply adaptations to climate change. For water supply, potential climate warming impacts on surface runoff, groundwater inflows and reservoir evaporation for distributed locations in the inter-tied water system of California are analyzed. Increasing winter flows and decreasing spring snowmelt runoff are identified in a statewide. The potential magnitude of water supply effects of climate warming can be very significant. Integrated water resources management is a promising way for water supply adaptation to climate change. A multiple stage stochastic optimization model is formulated to integrate water demand, water conservation, conjunctive use of surface and ground waters and water transfers in an irrigated district and an urban area. The results provide optimal long-term and short-term crop mix, optimal permanent and temporary urban conservation measures, and conjunctive use and water transfer decisions. It is illustrated that conjunctive use and water transfers can complement each other and significantly improve water management flexibility. For flood control adaptations, optimal tradeoff of levee setback for height and flood levee re-design rules are first analyzed under static climatic and economic conditions. Under dynamic conditions, optimal levee height over time is examined with optimal control. A stochastic dynamic programming model is developed for long-term floodplain planning under climate change and urbanization, with levee height and setback as decision variables. The results demonstrate climate change and urbanization can have major combined effects on flood damage and optimal long-term flood management. The case study shows there is likely to be economic value to expanding lower American River setbacks and levee heights over long periods of time, and making present-day zoning decisions to preserve such options.

Table of Contents

List of Figures

List of Tables

Chapter 1 Introduction

1.1 Motivation

Climate change impacts on water resources have been widely recognized and a variety of regional assessments of such impacts have been done over the past two decades. The Intergovernmental Panel on Climate Change Third Assessment Report (IPCC, 2001) illustrates various water resources impacts due to climate change: accelerated glacier retreat, shift in the timing of streamflow, sea level rise, intensified floods and droughts, and changes in evapotranspiration, etc. Among those natural phenomena, floods and droughts are classical problems in water resources management, and have been intensively studied. Traditional analysis methods attribute floods and droughts to hydrologic variability, which can be quantified with various time invariant probability functions. With evolving climate change, however, a time dependent change is involved in hydrology as well as inherent variability. Such trends can be considered in water resources planning and management, particularly for long-lived infrastructure and development decisions.

Besides effects on hydrology, climate change affects other water resource system components (due to temperature and precipitation changes), including water demand side, which should be considered. Meanwhile, as a result of population growth and economic development, water demand and urbanization generally increase. These nonclimatic changes complicate flood protection and drought management in many areas. Both the climatic and nonclimatic changes are dynamic. This dissertation first tries to quantify the regional water resources impacts (a California example) and then accounts for the evolutionary aspects of adaptation for flood control and water supply to climate change through theoretical analysis and illustrative case studies. Two kinds of approaches are explored for analyzing evolving adaptation for water excess and scarcity. One employs cross-sector water transfer analysis with multiple hydrologic year types. The other uses dynamic optimization techniques to examine evolving optimal adaptations over time.

1.2 Organization

This chapter introduces the organization of the dissertation. In *Chapter 2*, spatially disaggregated estimates of over 131 streamflow, groundwater, and reservoir evaporation monthly time series in California have been created for 12 different climate change scenarios for a 72-year period. Such disaggregated hydrologic estimates of multiple hydrologic cycle components are important for impact and adaptation studies of California's water system. A statewide trend of increased winter and spring runoff and decreased summer runoff is identified. Without operation modeling, approximate changes in water availability are estimated for each scenario. Most scenarios with even increased precipitation result in less available water because of the current storage systems' inability to catch increased winter streamflow in compensation for reduced summer runoff. These water availability changes are then compared with estimated changes in urban and agricultural water uses in California between now and 2100. The methods used

in this study are simple, but the results are qualitatively consistent with other studies focusing on the hydrologies of simple basins or surface water.

Chapter 3 presents analytical results of flood levee optimization under static and dynamic hydrologic and economic conditions. It first addresses the optimal trade-off of levee setback and height where a new levee is built, then develops levee re-design rules for cases where there is an existing levee. Under dynamic hydrologic and economic conditions, optimal control models are developed to find optimal time path of levee height over a long period. Theoretical insights are discussed under both static and dynamic conditions.

Chapter 4 examines flood management for an urbanizing floodplain with increasing flood risk due to climate change. The lower American River floodplain in the Sacramento, California metropolitan area, is used as a preliminary example. The modeling focus on levee setback and height of a river reach and detailed hydrologic analysis, hydraulic modeling, and economic evaluation are involved. A conventional stochastic dynamic programming model is employed to generate initial global optimal solution of levee heights and setback over a long planning period, and the discrete differential dynamic programming (DDDP) is then used to improve the accuracy of optimal solution. The results suggest economically desirable adaptations for floodplain levee systems given simultaneous changes in climate and urban land values. Economic-engineering optimizations were done for several climate change and urbanization scenarios. Methodological and policy conclusions are drawn, based on the results, for floodplain planning considering interaction of climate, costs, and regional economic growth.

Chapter 5 examines the potential benefits of water transfers between an agricultural region and an urban region in various hydrologic year types. Two stages are considered in each sector, representing long-term (permanent) and short-term (temporary) decisions, respectively. The analytical evaluation provides some insight into the general characteristics of regional water transfers. Then, an economic-engineering optimization model is employed to maximize the overall expected net benefit. The results demonstrate that the integrated water allocation policy results in apparent net benefit increase when it is compared with the independent decisions made separately by the agricultural and urban regions without interregional transfers. The application of such a market mechanism would be limited by different political, economic and social concerns. This study focus on the economic consequence of such kinds of transfers, with third party effects simply reflected in transaction costs. Climate warming effects on water transfers and potential adaptations are studied through implementing cross sectional analysis with the multistage optimization model for different year levels.

Chapter 6 summaries and concludes the findings throughout the dissertation.

References

IPCC (Intergovernmental Panel on Climate Change) (2001), *Climate Change 2001: The Scientific Basis*, Cambridge University Press, 881 pp.

Chapter 2 Estimated Impacts of Climate Change on California Water Availability under Future Climate Scenarios

2.1 Introduction

Much of California has cool, wet winters and warm, dry summers, and a resulting water supply that is poorly distributed in time and space. On average, 75% of annual precipitation of 584 mm occurs between November and March, while urban and agricultural demands are highest during the summer and lowest during the winter. Spatially, more than 70% of California's 88 bcm (billion cubic meters) average annual runoff occurs in the northern part of the state. However, about 75% of urban and agricultural water use is south of Sacramento (CDWR, 1998).

In terms of runoff and temperature, great consistency and variability are evident in California's climate during the last few thousand years (Haston et al. 1997; Meko et al. 2001; Stine 1994). Perhaps the most-debated form of climate change for California is climate warming, usually attributed to increasing concentrations of carbon dioxide and other gasses from industrialization (Snyder et al 2002; Wigley et al. 2001). The Intergovernmental Panel on Climate Change Third Assessment Report (IPCC, 2001) summarizes projections for future climate and the consequences on many sectors including water resources for which more serious floods and droughts are expected to occur. There have been many studies of the potential effects of climate warming on streamflows in California (Cayan et al. 1993; Gleick et al. 1999; Lettenmaier et al. 1990; Lettenmaier et al. 1991; Miller et al. 2003; Vanrheenen et al. 2004). The degree of change is usually estimated based on the results of general circulation models (GCMs). These studies all indicate that climate warming would change the seasonal distribution of runoff, with a greater proportion of runoff occurring during the wet winter months, and less snowmelt runoff during spring. Spatial changes of hydrologic factors were also identified (Synder et al. 2002). There is some reason to think that seasonal shifts in runoff patterns from spring to winter are already occurring in California (Aguado et al. 1992; Dettinger et al. 1995).

However, almost all existing studies of California's hydrologic responses to climate change focus exclusively on streamflow changes, either macroscopically or for a few selected streams (Vanrheenen et al. 2004; Brekke et al. 2004; Dettinger et al. 2004; Miller et al. 2003; Carpenter et al. 2001; Cayan et al. 1993; Lettenmaier et al. 1990; Lettenmaier et al. 1991). Such studies are not of sufficient breadth or detail for understanding how management of California's vast integrated surface and groundwater system might adapt to climate change. Water management analysis across California's complex highly integrated and inter-tied (inter-connected) system requires a more integrated and complete hydrologic representation (Draper et al. 2003; Lund et al. 2003).

To this end, spatially disaggregated estimates of streamflow, groundwater inflow, and reservoir evaporation time series for 131 inflow and evaporation locations have been created for 12 different climate warming scenarios over a 72-year period (Zhu et al.

2003). Each hydrology represents a permutation of the 72-year (October 1921 through September 1993) historically based monthly time series used in an economic-engineering optimization model of California's inter-tied water system, CALVIN (Draper et al. 2003; Lund et al. 2003). Each hydrologic time series is used to represent hydrologic variability within each California climate scenario. While the approaches used here are simple, they allow for the more detailed spatial representation of several aspects of the hydrological cycle needed for more realistic studies of climate change impact and adaptation.

2.2 Twelve Climate Warming Scenarios

In this study, spatially distributed climate warming impacts on hydrology are based on streamflow estimates for six index basins in California ("watersheds" in Figure 2.1) and distributed statewide temperature shifts and precipitation change ratios that Miller et al. (2003) generated for 12 climate scenarios. Those index basins spread from the northernmost area to the east-central region of the state, providing broad information for spatial estimates of the overall response of California's water supply and the potential range of hydrologic impacts. Besides the six index basins, Figure 2.1 also shows the CALVIN model's inflow, local runoff, and reservoir locations as well as 28 groundwater basin centroids.

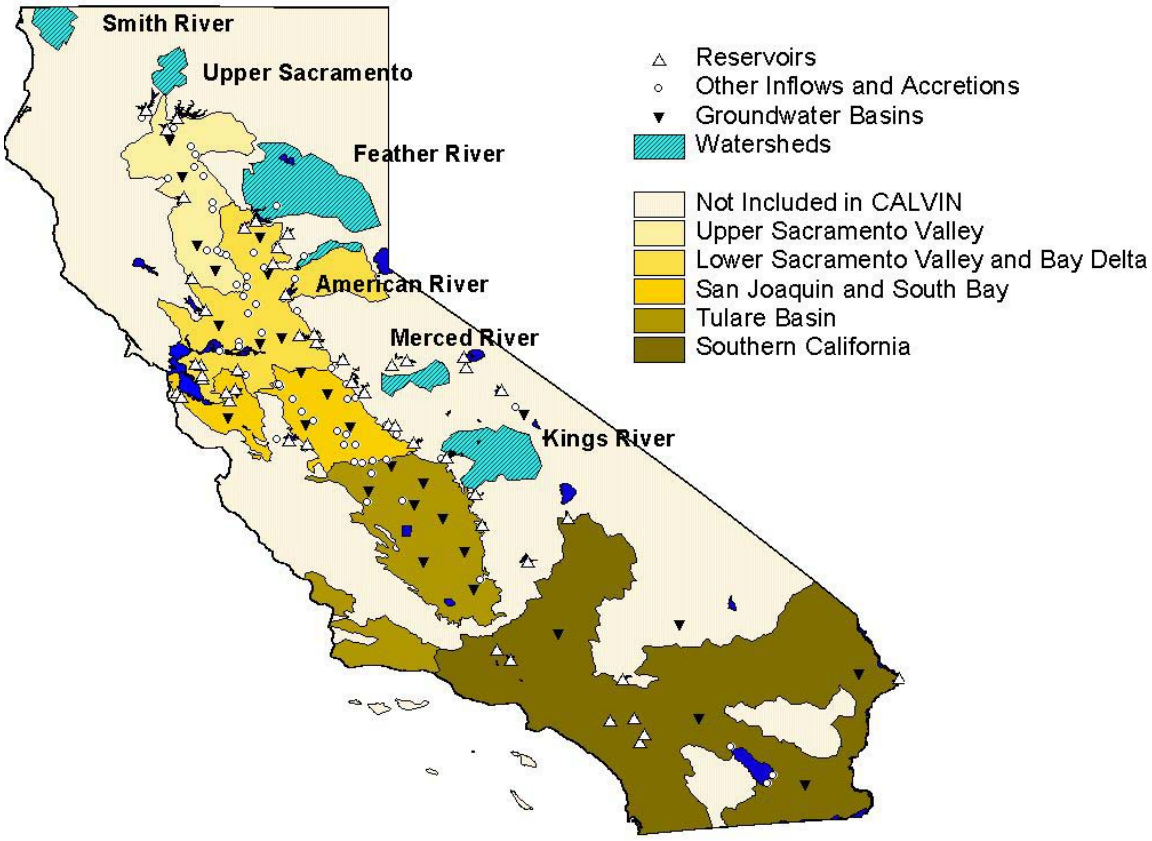

Figure 2.1. Map of California showing the six index basins ("watersheds" in legend) and distributed hydrologic components of the CALVIN model.

In Miller et al. (2003), two GCM projections for three projected future periods (2010 to 2039, 2050 to 2079, and 2080 to 2099) were used, based on 1 percent per year increase of CO_2 relative to late 20th Century CO_2 conditions. These future periods are labeled by their mid-points: 2025, 2065 and 2090. The two GCM projections were statistically downscaled and interpolated to a 10 km resolution, representing the relatively warm/wet (the Hadley Centre's HadCM2 run 1) and warm/dry (NCAR PCM run B06.06) scenarios for California, compared to the GCM projections in the Third Assessment Report by IPCC (2001). Limiting this study to two GCM scenarios was based on the recommendations of the California Climate Change Panel and other constraints (Miller et al., 2003).

Because of the uncertainty inherent in projecting future climate, Miller et al. (2003) applied an additional set of specified incremental temperature (shifts) and precipitation (ratios) changes to fully bracket the possibility of changes, though such uniform parametric changes seem unlikely. Streamflow simulation of GCM scenarios and uniform change scenarios are based on the National Weather Service River Forecast

System (NWSRFS) Sacramento Soil Moisture Accounting (SAC-SMA) Model and Anderson Snow Model, partly because of its dependence on only precipitation and temperature.

The 12 climate warming scenarios are described below. The average temperature increases (in ºC) and precipitation changes marked in the six GCM-based scenarios are averaged spatial changes.

(1) 1.5 ºC temperature increase and 0% precipitation increase (1.5 T; 0% P)
(2) 1.5 ºC temperature increase and 9% precipitation increase (1.5 T; 9% P)
(3) 3.0 ºC temperature increase and 0% precipitation increase (3.0 T; 0% P)
(4) 3.0 ºC temperature increase and 18% precipitation increase (3.0 T; 18% P)
(5) 5.0 ºC temperature increase and 0% precipitation increase (5.0 T; 0% P)
(6) 5.0 ºC temperature increase and 30% precipitation increase (5.0 T; 30% P)
(7) HadCM2025 (1.4 T ; 26% P)
(8) HadCM2065 (2.4 T ; 32% P)
(9) HadCM2090 (3.3 T ; 62% P)
(10) PCM2025 (0.4 T ; -2% P)
(11) PCM2065 (1.5 T; -12% P)
(12) PCM2090 (2.3 T; -26% P)

For all 12 scenarios, a larger proportion of the annual streamflow volume occurs in winter months because fewer freezing days allow less storage of water in snowpack. The hydrologic response varies for each scenario and the resulting hydrologic data sets provide bounds to the range of likely changes in streamflow, snowmelt, snow water equivalent, and the change in the magnitude of annual high flow days.

2.3 Methods

Hydrologic components considered in this study include rim inflows, groundwater, local runoff and reservoir evaporation. Flux time series for each component are constructed under climate warming scenarios with the following approaches.

2.3.1 Rim Inflows

Those major inflows into the Central Valley from the surrounding mountains are commonly called rim inflows. For each scenario, climate change impacts on 37 rim inflows are estimated with hydrologic response ratios (simulated monthly flows under a climate change scenario divided by corresponding simulated historical flows) developed by Miller et al. (2003) for the six index basins. To identify the appropriate index basins for each rim inflow, first, monthly and annual correlation coefficients between historical runoff of the rim inflow from 1963 to 1993 and simulated historical runoff of the six index basins for the same period are calculated. The index basin that has the best annual correlation with the rim inflow is chosen as the best index basin for mapping, if most of its monthly correlation coefficients (e.g., eight months out of twelve) with the rim inflow also are the largest among those of the six index basins. Another method is applied to the remaining rim inflows to find appropriate index basins. It calculates summed square

errors (SSE) of streamflow monthly percentages in wet and dry seasons (October to March and April to September, respectively) between each rim inflow and each index basin. The best index basin (when wet and dry seasons share the same index basin) or index basins (when wet and dry seasons use different index basins) are determined by choosing those with the least SSE. This method partitions a water year into a wet season and a dry season to facilitate finding the best fit for snowmelt-dominant runoff and rainfall-dominant runoff regimes. Thus, for each of 37 rim inflows the best index basins for wet and dry seasons are obtained, resulting in a 37(rim inflow)×2(season) mapping matrix. This mapping matrix provides index information to apply hydrologic response ratios to each rim inflow. For example, the wet season monthly ratios of the Kings River and dry season monthly ratios of the Merced River under the "HadCM2025" scenario are applied to the "present climate" monthly time series of the Kaweah River streamflows from 1921 to 1993 to generate corresponding "HadCM2025" streamflows. This approach extends a similarly simple approach used by Brekke et al. (2004).

To compare climate change impacts on index basin streamflows and constructed climate change rim inflows, the percent changes (from historical) of annual and seasonal mean flows due to climate change are calculated for all index basins and rim inflows for each of the 12 climate change scenarios. To assure that climate change impacts on index basins are mapped to corresponding rim inflows, it is required that, under the same climate change scenario, the percent changes of each rim inflow should be similar to the changes of its index basins. Where constructed rim inflows did not meet this criterion, two measures are applied to improve fits: (1) Watershed conditions were further examined and their historical streamflow patterns were visually compared with those of the index basins; and (2) One-month lags in the hydrologic response ratios of some index basins were used to represent snowmelt timing changes on the east side of the Sierras. Of the 37 rim inflows, seven are mapped by examining temporal correlation (the first method), 18 are mapped by finding the least SSE, and 12 are identified by detailed analysis and use of lags.

2.3.2 Groundwater and Local Runoff

To estimate climate change impacts on groundwater inflows and local runoff, we partition precipitation changes into local runoff and deep percolation portions for each groundwater sub-basin. These changes are then added to corresponding historical groundwater and local runoff time series. The unsaturated layer water balance and changes in stream-aquifer exchanges are not considered.

A cubic regression equation is employed to represent the nonlinear relationship between monthly deep percolation and precipitation volumes for each groundwater sub-basin (Zhu et al. 2003). These empirical equations were established based on the Central Valley Ground and Surface Water Model (CVGSM) simulated data over the 1922-1990 period (USBR, 1997). Deep percolation changes are estimated for each groundwater sub-basin with its empirical equation based on precipitation changes for each climate change scenario. A cubic form is chosen because it fits the empirical data well for most groundwater basins, and equations have peak plateaus which can represent infiltration

capacities. For the six parametric scenarios, the specified uniform precipitation changes are applied for each month. For the six GCM scenarios, different monthly precipitation change ratios are available for each groundwater sub-basin.

Natural groundwater inflows or recharge, excluding recharge from operational deliveries to agricultural and urban demand areas, for each groundwater sub-basin in the Central Valley from CVGSM can be represented as

$$GW = DP + SA + BF + SS + LS + AR$$

where DP is deep percolation of precipitation, SA denotes gain from streams, BF represents gain from boundary flows (from outside the CVGSM modeled area), SS is gain in the sub-basin from subsurface flows across basin boundaries, LS denotes seepage from lake beds and bedrock in the sub-basin, and AR is seepage from canals and artificial recharge. Assuming other components of groundwater inflow are unchanged, changes in groundwater inflow are equivalent to changes in deep percolation from changes in rainfall over each groundwater sub-basin, that is

$$GW^P = GW + \Delta DP$$

where GW^P represents perturbed groundwater inflow for the groundwater sub-basin, and ΔDP is change in deep percolation.

To connect groundwater inflow with local runoff, each groundwater sub-basin is associated with a local accretion area that coincides with the groundwater sub-basin. Local runoff associated with a groundwater sub-basin can be represented as

$$LR = R + AG$$

where LR represents net local runoff, R denotes direct runoff, and AG is gain from the aquifer. Incremental local runoff over a groundwater sub-basin equals incremental precipitation minus incremental deep percolation, so that

$$LR^P = LR + \Delta P - \Delta DP$$

where LR^P is climate change perturbed local runoff and ΔP is increased precipitation volume. This equation assumes a negligible change in evaporation from changed precipitation, which is probably not a major error in most wet months.

2.3.3 Reservoir Evaporation

Changes in evaporation rate and total evaporation for each reservoir, assuming similar operations, were estimated for each climate scenario. A linear form is employed to regress monthly average net evaporation rate against monthly average air temperature and precipitation at each surface reservoir (Zhu et al. 2003). In the parametric climate scenarios (1 to 6), the temperature shifts and precipitation change ratios are uniform across months. The GCM scenarios have average temperature and precipitation shifts that

vary by month. The monthly incremental net evaporation rate at each reservoir is then added to the historical monthly net evaporation rate time series for that reservoir. Next, the monthly net evaporation quantity, based on current storage operations, is obtained from the perturbed net evaporation rate using simulated historical reservoir monthly surface areas.

2.4 Results

2.4.1 Rim Inflows

There are 37 major inflows into the Central Valley. Historically, these rim inflows average 34.9 bcm/yr, accounting for 72% of all inflows into California's inter-tied water system. Table 2.1 shows total quantities and changes for rim inflows under the 12 climate change scenarios. Considerable range in rim inflow changes is presented. Total annual rim inflows could be 76.5% more than historical under the wettest scenario HadCM2090, and 25.5% less under the driest scenario PCM2090. Except for the three PCM scenarios, inflows increase in the wet season. In all but the HadCM2 scenarios, dry season inflows decrease. Even in HadCM2 scenarios, winter inflows increase much more significantly than in summer, resulting in an overall shift in annual runoff from the dry to the wet season in all scenarios except PCM2025.

Table 2.1. Overall rim inflow quantities and changes.

Climate Scenario	Annual		October to March		April to September	
	Quantity (bcm)	Change (%)	Quantity (bcm)	Change (%)	Quantity (bcm)	Change (%)
Historical (1921-1993)	34.8	0	17.5	0	17.3	0
1) 1. 1.5 T 0% P	35.3	1	20.3	16	15.0	-13
2) 2. 1.5 T 9% P	40.0	15	23.1	32	16.9	-3
3) 3. 3.0 T 0% P	35.2	1	22.4	28	12.7	-27
4) 4. 3.0 T 18% P	44.7	28	28.8	64	15.8	-9
5) 5. 5.0 T 0% P	34.5	-1	24.0	37	10.5	-40
6) 6. 5.0 T 30% P	50.1	44	35.7	104	14.4	-17
7) 7. HadCM2025	47.5	36	27.2	55	20.4	18
8) 8. HadCM2065	51.0	46	31.9	82	19.1	10
9) 9. HadCM2090	61.5	77	41.1	134	20.5	18
10) 10. PCM2025	32.7	-6	16.3	-7	16.4	-6
11) 11. PCM2065	30.1	-14	16.9	-4	13.3	-24
12) 12. PCM2090	26.0	-26	15.0	-14	10.9	-37

Monthly mean overall rim inflows for the 12 climate scenarios and historical inflows are plotted in Figure 2.2. It shows all the climate change scenarios would significantly shift the peak runoff of catchments where the annual hydrograph is currently dominated by spring snowmelt. Much more runoff would occur in winter and less in spring and summer. Therefore, reservoirs would have to maintain more empty space to

maintain current levels of flood protection from increased winter storm runoff. This empty space would then be less likely to refill at the end of the flooding season, because of reductions in snowmelt after the storm season's end.

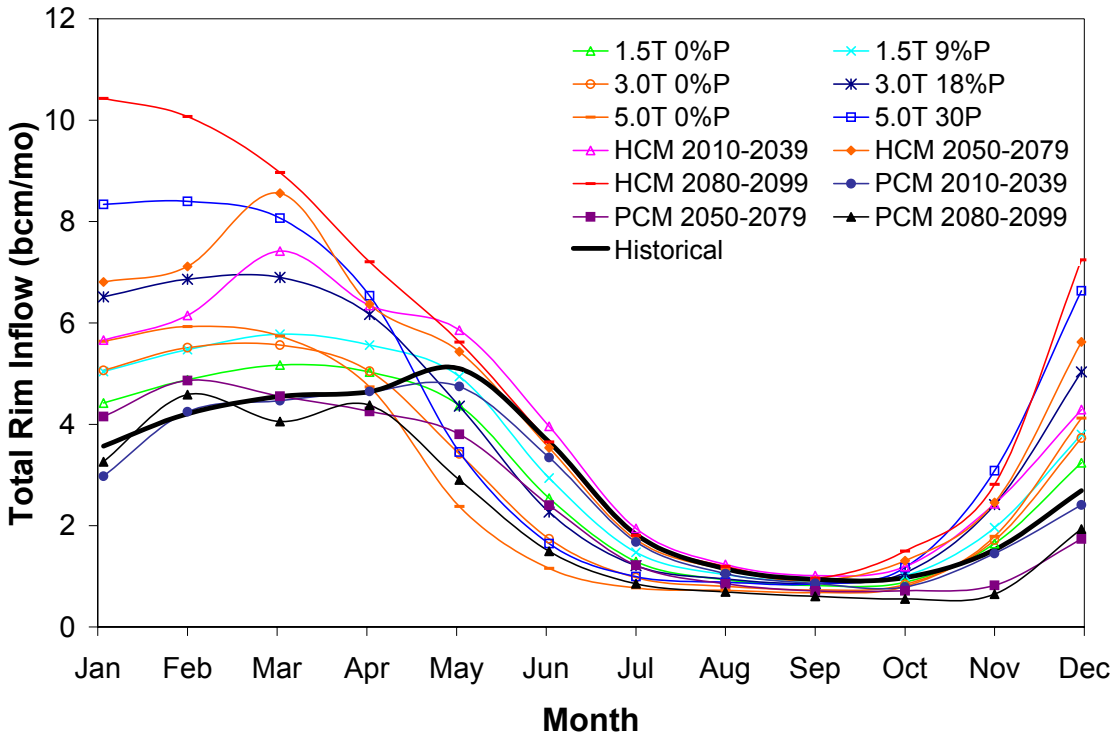

Figure 2.2. Mean annual total rim inflow for 12 climate change scenarios and historical record.

Regional analyses show rim inflows in the south increase relatively more than in the north with the extreme warm and wet climate HadCM2090. With the dry PCM2090 scenario, rim inflows decrease in all regions. Seasonally, wet season rim inflows increase for all the regions and scenarios, except the PCMs. Dry season rim inflows decrease for all regions and scenarios, except HadCM2090. For most cases, rim inflows in the north decrease relatively more than in the south during dry season. These regional conclusions should be tempered by understanding that mapping inflows to index basins tended to be poorer further south, where there were fewer index basins.

Figure 2.2 demonstrates the monthly average of 72 year perturbed rim inflows for the 12 climate change scenarios presents a range of hydrological responses to climate change in California. Essentially, as statistical interpolations and extrapolations of the changes projected for the six index basins, the perturbed rim inflows present a set of possibilities under different climate change scenarios. However, for a few rivers, particularly in southern parts of California, their annual and seasonal mean flow changes deviate changes of their corresponding index basins under the same climate change scenarios. Flow quantity of these problematic rim inflows accounts for a small portion (<

15%) of the total. However, they indicate that climate change impact simulations of more southern index basins, along the coast and in the Central Valley floor would be useful. In addition, the SAC-SMA results also appear to have some problems representing increased evapotranspiration with increased temperature and do not include vegatation changes which could induce additional evapotranspiration effects of climate change.

2.4.2 Groundwater and Local Runoff

The CALVIN model has 28 groundwater inflows and 35 local runoff inflows (Figure 2.1). Due to limited data, the seven groundwater sub-basins located outside the Central Valley are not studied although these tend to have relatively small natural inflows. The 21 groundwater sub-basins and 21 corresponding nodes of local runoff in the Central Valley have been perturbed for climate warming. Total groundwater inflow and local runoff account for 8.4 and 5.5 bcm/yr, respectively, of all inflows into California's inter-tied water system, representing about 17% and 11%, respectively, of all inflows. Deep percolation of rainfall accounts for about 2.1 bcm/yr of the total 8.4 bcm/yr of average groundwater inflow in the Central Valley. Under the historical climate, this volume represents only about 12% of precipitation falling over groundwater sub-basins in the Central Valley. Figure 2.3 shows quantity and changes of average annual groundwater inflows over the modeled sub-basins. Figure 2.4 shows average annual changes in local runoff.

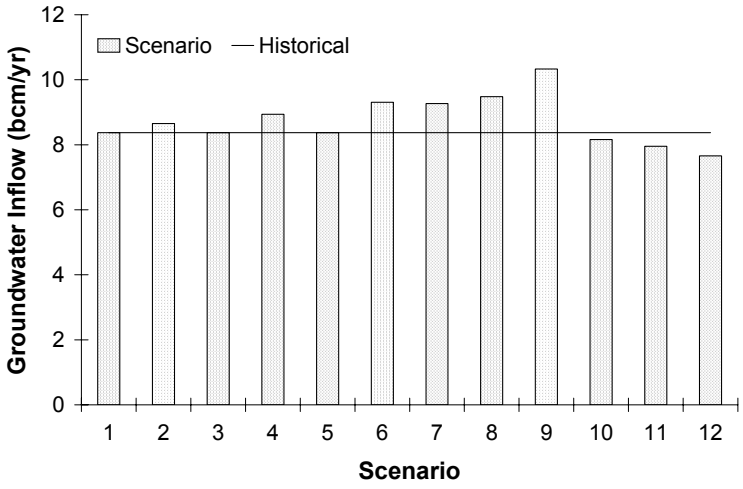

Figure 2.3. Average annual groundwater inflow changes.

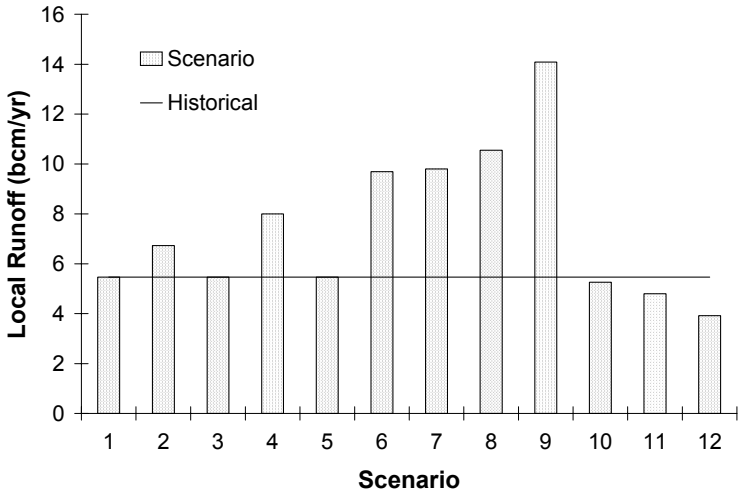

Figure 2.4. Average annual local runoff changes.

For all the three GCM periods, groundwater inflows and local runoff increase with HadCM2 scenarios and decrease with PCM scenarios. These trends continue over time. Most increased precipitation contributes to direct local runoff because infiltration capacity limits deep percolation. On average, local runoff in the wet season accounts for 80% of annual local runoff. Winter season groundwater inflow accounts for 53% of annual groundwater inflow. The proportions of winter season local runoff and groundwater inflow increase with more-precipitation scenarios (parametric changes and HadCM2) and decrease with less-precipitation scenarios (PCM).

2.4.3 Reservoir Evaporation

The CALVIN model has 47 surface reservoirs for which evaporation is calculated. Historically, over the 72-year hydrology used in CALVIN, 2.0 bcm/yr of water is lost from these reservoirs as net evaporation under current reservoir operations, which represents about 4% of all inflows.

The regression equations of most of the 47 reservoirs have high significance levels, with net evaporation rates being more sensitive to temperature than precipitation. Figure 2.5 shows the surface reservoir evaporation results for the 12 scenarios, with relative increases between 3.6% and 41.3%.

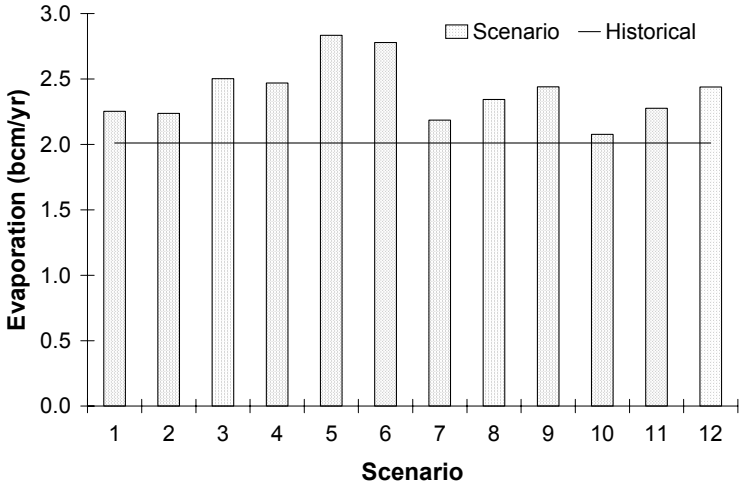

Figure 2.5. Changes of average annual surface reservoir evaporation.

2.4.4 Statewide Annual and Seasonal Inflows

Total water quantity available to California's inter-tied system is the sum of rim inflows, local runoff, and groundwater inflows, minus evaporation losses. Among these components, rim inflows account for most of the overall water quantity. Groundwater and local runoff also contribute significantly to overall water quantity.

In general, statewide results (Table 2.2 and Figure 2.6) show that climate warming would result in significant shifts in the peak season of water quantity. Snowmelt would come much earlier than historically. Relatively more annual runoff would occur in the wet season and less in the dry season. The three wet and warm HadCM2 scenarios indicate that future decades might experience much more water, and water quantity might increase over time. The drier PCM scenarios indicate less water will be available and conditions will worsen with time. Compared with the historical average, drought years (1928-1934, 1976-1977, and 1987-1992) are expected to experience serious water decreases under the climate warming scenarios, though the HadCM2090 scenario shows only moderate reductions.

Table 2.2. Overall water quantities and changes.

Climate scenario	Annual		October-March		April-September	
	Quantity (bcm)	Change (%)	Quantity (bcm)	Change (%)	Quantity (bcm)	Change (%)
Historical (1921-1993)	46.7	0	25.9	0	20.8	0
1. 1.5 T 0% P	46.8	0	28.5	10	18.3	-12
2. 1.5 T 9% P	53.1	14	32.6	26	20.5	-2
3. 3.0 T 0% P	46.5	0	30.6	18	15.9	-23
4. 3.0 T 18% P	59.1	27	39.5	53	19.6	-6
5. 5.0 T 0% P	45.5	-3	32.0	24	13.5	-35
6. 5.0 T 30% P	66.3	42	48.0	86	18.3	-12
7. HadCM2025	64.4	38	39.2	52	25.2	21
8. HadCM2065	68.7	47	45.4	76	23.3	12
9. HadCM2090	83.5	79	58.7	127	24.8	19
10. PCM2025	44.1	-6	24.1	-7	20.0	-4
11. PCM2065	40.6	-13	24.2	-7	16.4	-21
12. PCM2090	35.1	-25	21.1	-19	14.0	-33

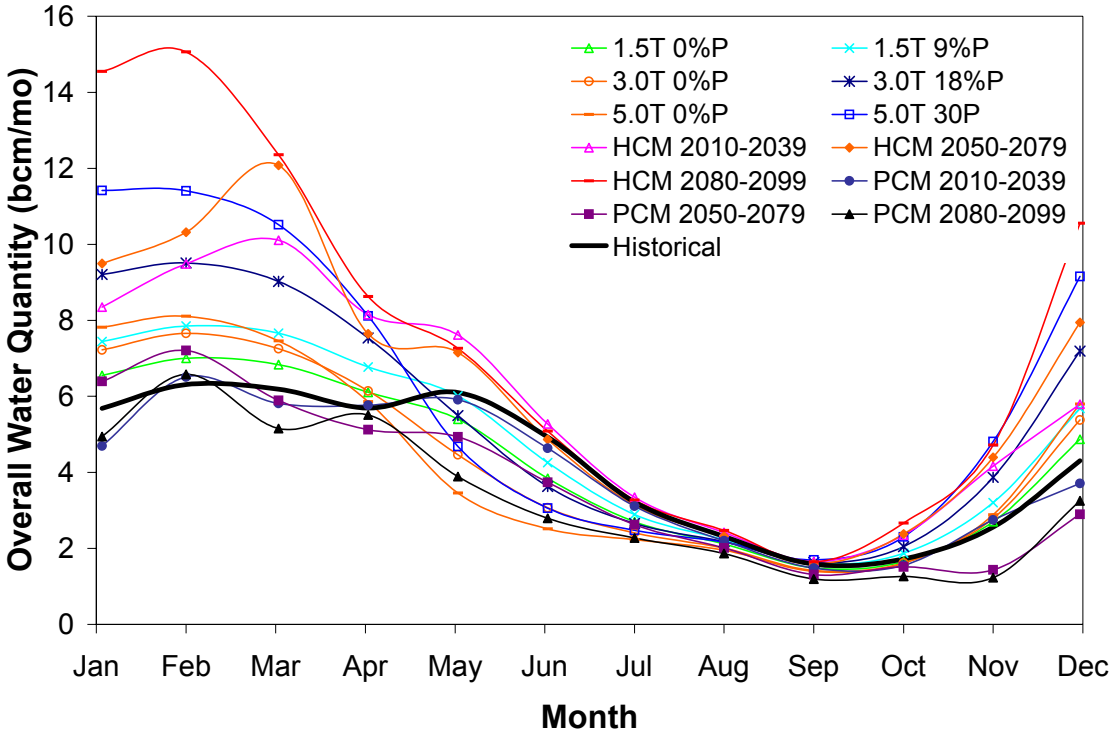

Figure 2.6. Mean annual overall water quantity for 12 climate change scenarios and historical record.

Figure 2.7 shows annual exceedence probabilities of statewide total water quantities, based on historical and selected perturbed 72-year hydrologies, among which the HadCM2090 and the PCM2090 form the upper and lower bounds of those curves.

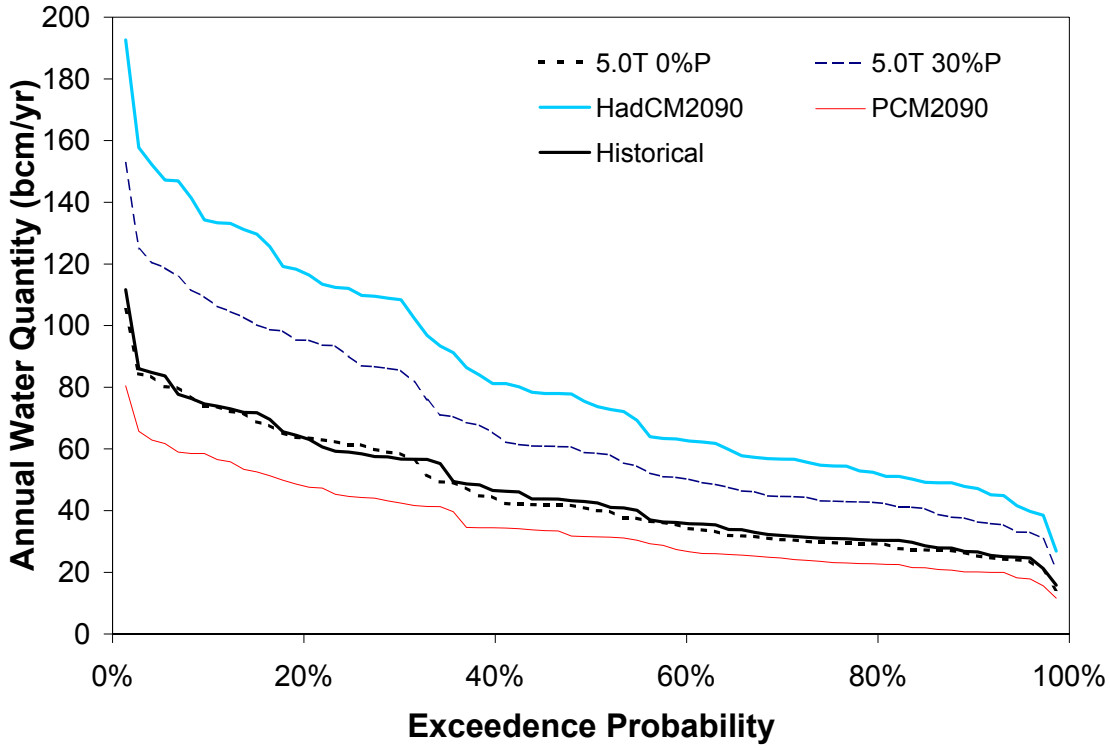

Figure 2.7. Overall Water Quantity exceedence probability.

Regional analyses indicate southern regions are more sensitive to climate changes under HadCM2 scenarios, with increased water quantity even in the dry season. Under PCM scenarios, water quantity decreases for all seasons in all regions. No significant spatial trend was identified for PCM scenarios.

2.4.5 Statewide Water Supply Availability

Approximate water supply changes with climate warming are estimated without modeling facility operations (Table 2.3). We assume: (1) All changes in dry season inflows directly affect water deliveries (because water is most easily managed during the dry season); (2) Increases in wet season surface inflows are lost because of low water demand and low surface storage flexibility resulting from flood control; and (3) changes in wet season groundwater inflows directly affect water supply availability because they directly affect groundwater storage. Since there is likely to be more wet season storage

flexibility than is assumed here, the resulting estimates are likely to be more dire than more realistic results from operations modeling.

As Table 2.3 shows, on average, water availability decreases for nine of the twelve scenarios, the exceptions being the three HadCM2 scenarios, in which water availability increases even in the dry season. For the three uniform precipitation and temperature increase scenarios (scenarios 2, 4, 6 in Table 2.3) water availability decreases though overall water quantities increase (Table 2.2). It was estimated elsewhere that urban and agriculture demand changes from year 2020 to 2100 are 10.1 bcm/yr and -3.3 bcm/yr respectively (Lund et al. 2003). The net demand increase of 6.8 bcm/yr is challenging to the system, even exceeding water availability increases of the three HadCM2 scenarios. These are important for identifying potential long-term water supply problems.

Table 2.3. Estimated raw water supply availabilities and changes.

Climate Scenario	Volume (bcm/yr)	Change (bcm)	Change (%)
Historical	46.7	0.0	0
1. 1.5 T 0% P	44.1	-2.6	-6
2. 1.5 T 9% P	46.5	-0.2	0
3. 3.0 T 0% P	41.6	-5.1	-11
4. 3.0 T 18% P	45.8	-0.9	-2
5. 5.0 T 0% P	39	-7.7	-16
6. 5.0 T 30% P	44.7	-2.0	-4
7. HadCM2025	51.7	5.0	11
8. HadCM2065	50	3.3	7
9. HadCM2090	52.3	5.6	12
10. PCM2025	44.1	-2.6	-6
11. PCM2065	40.6	-6.1	-13
12. PCM2090	35.2	-11.5	-25

Considering that most wet season groundwater inflows are stored for dry season consumption, the sum of dry season water availability plus wet season groundwater inflows decreases much less significantly than either rim inflows or overall water availability in the dry season under the parametric and PCM scenarios (when the dry season experiences serious water decreases). This indicates groundwater inflow helps to dampen overall fluctuations in water availability. Efficient groundwater management, such as conjunctive use and groundwater banking could be crucial to meet increasing water demand under climate change conditions.

2.5 Limitations

By including multiple hydrologic components (particularly many rim inflows, local inflows, groundwater inflows, and reservoir evaporation) over the entire system, this work has a more complete representation of hydrology for California's water system than previous climate change studies. However, this required great simplicity in the methods used to represent climate change effects for each individual component. In particular, groundwater inflow and local inflows are estimated solely based on deep percolation changes, with other influencing factors treated as unchangeable. Furthermore, deep percolation for each groundwater sub-basin is calculated with empirical historical relationships, with unsaturated layer water balance neglected. Climate change rim inflows are estimated using monthly percent changes of index basin streamflows under climate warming scenarios. Index basin coverage for the many rim inflows is less than ideal, and the approach relies on rainfall runoff models for the individual index basins.

While quite simple, the methods used here do seem able to represent the essential signals of climate warming for California's water system, in patterns and magnitudes similar to those found applying more sophisticated methods for a few basins or hydrologic components. Nevertheless, we see several areas where more detailed hydrologic investigations would be particularly desirable. For instance, climate change impact simulation of more southern index basins, along the coast and in the Central Valley floor, and better representation of evapotranspiration in the precipitation-runoff model would be useful.

The application of more sophisticated methods to such an extensive and complex hydrologic system would be difficult, expensive, and embody uncertainties in many hydrologic details, as well as the significant uncertainties in the climatic boundary conditions driving any hydrologic representation of the system (which our methods share). It was felt that a simpler approach would allow the development of a wider range of generally reasonable climate warming scenarios with an extensive scale, a greater number of important hydrologic components, with a spatial representation commensurate with water resource system management and performance assessment models. This work is not the final step in representing California's hydrology with climate change.

A non-technical advantage of employing permutation of the 72-year historically-derived time series as our basic approach is that the resulting climate change fluxes are more explicitly comparable with hydrologic fluxes commonly employed for understanding and modeling water management and policy in California (Brekke et al. 2004).

2.6 Conclusions

Inflows to California's entire inter-tied water system are estimated over a range of annual hydrologic conditions, represented by a systematic modification of the 1922-1993 historical period. Such comprehensive representations of inflows to a water management system are needed for impact, management, and adaptation studies of climate change.

This study generalizes and confirms findings of significant climate warming effects of increased winter flows and decreased spring snowmelt runoff found in earlier climate warming studies of California. Groundwater flows are especially important for such studies, given their significant proportion of total water availability and use, ability to shift water availability seasonally, and ability to store water for drought periods. The potential magnitude of water supply effects of climate warming can be very significant, both positive and negative. These changes can be significant even relative to estimates of increased water demands due to population growth.

For more credible climate change impact and adaptation studies, more comprehensive and system-wide examination of hydrologic processes is needed. Additional GCM-driven hydrologies might better characterize the range and likelihood of climate changes. A larger number and diversity of index basins and better evapotranspiration representation in the rim inflow runoff model also would be useful. Changes in drought persistence with climate change are only modestly captured in this study. Finally, the results of this study are limited by the simplicity of approaches employed although it is not yet clear that more sophisticated methods would yield very different results. Further work will be valuable here.

References

Aguado, E., D. Cayan, L. Riddle, and M. Roos (1992), Climate fluctuations and the timing of west coast streamflow, *J. Climate*, 5, 1468-1483.

Brekke, L. D., N. L. Miller, K. E. Bashford, N. W. T. Quinn, and J. A. Dracup (2004), Climate change impacts uncertainty for water resources in the San Joaquin river basin, California, *J. Am. Water Resour. Assoc.*, 40(1), 149-164.

Carpenter, T. M. and K. P. Georgakakos (2001), Assessment of Folsom Lake response to historical and potential future climate scenarios: 1. Forecasting, *J. Hydrology*, 249, 148-175.

Cayan, D. R., L. G. Riddle, and E. Aguado (1993), The influence of precipitation and temperature on seasonal streamflow in California, *Water Resour. Res.,* 29(4), 1127-1140.

Dettinger, M. D. and D. R. Cayan (1995), Large-scale atmospheric forcing of recent trends toward early snowmelt runoff in California, *J. Climate*, 8(3), 606-623.

Dettinger, M. D., D. R. Cayan, M. K. Meyer, and A. E. Jeton (2004), Simulated hydrologic responses to climate variations and change in the Merced, Carson, and American river basins, Sierra Nevada, California, 1900-2099, *Climatic Change*, 62, 283-317.

Draper, A. J., M. W. Jenkins, K. W. Kirby, J. R. Lund, and R. E. Howitt (2003), Economic-engineering optimization for California water management, *J. Water Resour. Plann. Manage.,* 129(3), 155-164.

CDWR (California Department of Water Resources) (1998), *The California water plan update*, Bulletin 160-98, Volume 1, California Department of Water Resources, Sacramento, Calif.

Gleick, P. H. and E. L. Chalecki (1999), The impact of climatic changes for water resources of the Colorado and Sacramento-San Joquin river systems, *J. Am. Water Resour. Assoc.*, 35(6), 1429-1441.

Haston, L. and J. Michaelsen (1997), Spatial and temporal variability of Southern California precipitation over the last 400 yr and relationships to atmospheric circulation patterns, *J. Climate*, 10(8), 1836-1852.

IPCC (Intergovernmental Panel on Climate Change) (2001), *Climate Change 2001: The Scientific Basis*, Cambridge University Press, 881 pp.

Lettenmaier D. P. and T. Y. Gan (1990), Hydrologic sensitivity of the Sacramento-San Joaquin river basin, California, to global warming, *Water Resour. Res.*, 26(1), 69-86.

Lettenmaier, D. P. and D. P. Sheer (1991), Climate sensitivity of california water resources, *J. Water Resour. Plann. Manage.*, 117(1), 108-125.

Lund, J.R. et al. (2003), *Climate warming and California's water future*, Center for Environmental and Water Resources Engineering, University of California, Davis, Calif. *Available at*: http://cee.engr.ucdavis.edu/faculty/lund/CALVIN/ReportCEC/AppendixA.pdf. *Accessed in* March 2004.

Meko, D. M., M. D. Therrell, C. H. Baisan and M. K. Hughes (2001), Sacramento River flow reconstructed to A. D. 869 from tree rings, *J. Am. Water Resour. Assoc.*, 37(4), 1029-1039.

Miller, N.L., K.E. Bashford and E. Strem (2003), Potential impacts of climate change on California hydrology, *J. Am. Water Resour. Assoc.*, 39(4), 771-784.

Stine, S. (1994), Extreme and persistent drought in California and Patagonia during medieval time, *Nature*, 369, 546-549.

Snyder, M. A., J. L. Bell, L. C. Sloan, P. B. Duffy, and B. Govindasamy (2002), Climate responses to a doubling of atmospheric carbon dioxide for a climatically vulnerable region, *Geophys. Res. Lett.*, 29(11), 9-1 to 9-4.

USBR (United States Bureau of Reclamation) (1997), *Central Valley Project Improvement Act Programmatic Environmental Impact Statement*, United States Bureau of Reclamation, Sacramento, Calif.

Vanrheenen, N. T., A. W., Wood, R. N., Palmer, and D. P., Lettenmaier (2004), Potential implications of PCM climate change scenarios for Sacramento-San Joaquin river basin hydrology and water resources, *Climatic Change*, 62, 257-281.

Wigley, T. M. L. and S. C. B. Raper (2001), Interpretation of high projections for global mean warming, *Science*, 293, 451-454.

Zhu, T., M. W., Jenkins, J. R., Lund (2003), *Appendix A: Climate Change Surface and Groundwater Hydrologies for Modeling Water Supply Management*. Center for Environmental and Water Resources Engineering, University of California, Davis. Davis, CA. *Available at* http://cee.engr.ucdavis.edu/faculty/lund/CALVIN/ReportCEC/AppendixA.pdf. *Accessed in* March 2004.

Chapter 3 Theoretical Economic-Engineering Analysis of Flood Levee Height and Setback under Static and Dynamic Conditions

3.1 Introduction

Levee systems have been built for flood protection in numerous rivers, lakes and coasts in the world over the long human history. Early flood levees usually were designed with scant quantitative analysis, relying primarily on occasional observations of flood stages and empirical judgments on required project scales. The achievements in experimental and theoretical hydraulics since the 18th century (Hunter and Simon, 1957), reational estimation of storm discharge in the mid 19th century (Biswas, 1970) and the emerging of early economic-engineering analysis (Humphreys, 1861) made possible the "modern sense" designs of flood levees. In recent decades, several studies have addressed the economic aspects of flood levee design, usually with benefit-cost analysis and optimization techniques (Davis et al., 1972; Tung and Mays, 1981; Wurbs, 1983; Goldman, 1997; Olsen et al., 1998; Jaffe and Sanders, 2001; Lund, 2002).

There is sometimes considerable controversy over whether flood channel capacity should be obtained more from levee heightening or from greater levee setbacks. This issue has received increased public attention due to public concern for riparian recreation and environmental uses of unprotected floodplain land.

This chapter examines the optimal levee height and levee setback decisions from a theoretical and analytical perspective. First, detailed analyses are conducted for static conditions when hydrology and the local economy are stationary. Next, for dynamic hydrologic and economic conditions, such as climate warming induced flood frequency changes and urbanization, an optimal control approach is introduced to determine economically optimal levee heights over a planning horizon. The approach taken here is to examine designs based on overall economic efficiency, considering both flood control action costs and flood damages. Flood warning systems are assumed to allow us to neglect, for now, losses of life from these evaluations. Hypothetical river and levee types are explored.

3.2 Flood Levee and Floodplain Optimization under Static Conditions

Economic design of a levee system for flood protection involves balancing costs of levee building (height), the losses of land value sacrificed for floodway expansion (setback) and flood damages from inadequate channel capacity. The most common economic objective for floodplain management is minimization of expected annual damages and flood management expenses (Lund, 2002; Olsen, 2000). Under static conditions, the flood frequency distribution is stationary and economic factors, such as the value of damageable property, construction cost, and floodplain land values, are constant. Optimality conditions can be applied to examine flood levee designs under static conditions. The methods developed here apply to relatively simple cases where the expected total cost function is convex with levee setback and levee height. A proof is

given in Appendix A demonstrating the convexity nature of the expected total cost function under certain conditions, however there are other cases where the cost function is not convex. Some economic-engineering insights are developed for this problem.

3.2.1 Optimal Static Tradeoff of New Levee Setback for Height

A static model is formulated to minimize the sum of expected flood damage, annualized levee construction cost and resultant annual land value loss due to floodway occupancy. This simple model allows preliminary quantitative examination of the tradeoff between optimal setback and optimal height in designing a new levee. The objective function is

$$Min\ EC(X_s, X_h) = P(X_s, X_h)\cdot D + C(X_h) + B(X_s, X_h) \tag{3.1}$$

where

$EC(.)$ = expected annualized total cost
X_s = designed levee setback
X_h = designed levee height
$P(\cdot)$ = overtopping probability with levee height X_h and setback X_s
D = damageable property value (potential loss in a flood disaster)
$C(\cdot)$ = annualized cost to build a levee of height X_h
$B(\cdot)$ = annual loss of floodplain land value due to floodway occupancy

Even if not overtopped by floods, levees may fail for geotechnical reasons. Such failures can be examined through geotechnical reliability modeling, which leads to a relationship between water height and probability of geotechnical failure (USACE, 2002). For simplicity, in the above formulation levee breach and the loss of property are assumed to occur only when river stage becomes high enough to overtop the levee. Average flood damage is applied to different flood events, equaling the abovementioned damageable property value. The land value loss function $B(\cdot)$ depends not only on levee setback but also on levee height because the bottom width of levee cross-section may change with levee height (e.g., a trapezoid cross-section).

The first order condition for minimizing the expected total cost of flood control is that the first partial derivatives of $EC(X_s, X_h)$ with respect to X_s and X_h equal zero.

$$\frac{\partial EC}{\partial X_h} = \frac{\partial P}{\partial X_h}\cdot D + \frac{\partial (C+B)}{\partial X_h} = 0 \tag{3.2}$$

$$\frac{\partial EC}{\partial X_s} = \frac{\partial P}{\partial X_s}\cdot D + \frac{\partial B}{\partial X_s} = 0 \tag{3.3}$$

Given a levee overtopping flow $Q(X_s, X_h)$, we have

$$\frac{\partial P}{\partial X_h} = \frac{\partial P}{\partial Q} \cdot \frac{\partial Q}{\partial X_h} \tag{3.4}$$

$$\frac{\partial P}{\partial X_s} = \frac{\partial P}{\partial Q} \cdot \frac{\partial Q}{\partial X_s} \tag{3.5}$$

Embedding Equation (3.4) into Equation (3.2), Equation (3.5) into Equation (3.3), then deleting $\frac{\partial P}{\partial Q}$ by combining equations (3.2) and (3.3) result in

$$\frac{\partial Q}{\partial X_h} \Big/ \frac{\partial Q}{\partial X_s} = \frac{\partial (C+B)}{\partial X_h} \Big/ \frac{\partial B}{\partial X_s} \tag{3.6}$$

Equation (3.6) holds for the optimal levee height X_h^* and setback X_s^*. The optimal levee height X_h^* and setback X_s^* can be found by numerically solving combined equations (3.2) and (3.3) and verifying that a minimum has been found, even though the expected total cost function in Equation (3.1) is not convex. In Equation (3.6), the left hand side is the Marginal Substitution Rate (hereafter referred to as MSR) of levee setback for height for the optimal overtopping flow $Q(X_s^*, X_h^*)$; the right hand side (RHS) is the ratio of marginal construction cost and land value loss in X_h to marginal land value loss in X_s. Equation (3.6) implies that optimal economic efficiency occurs where the MSR of levee setback for height equals the ratio of marginal levee construction cost plus marginal land value loss in X_h to marginal land benefit loss in X_s. In Equation (3.6), neither flood hydrology nor value of potential flood damages affect the optimal MSR, although these factors do affect the optimal flood channel capacity. Thus, when changes occur in flood hydrology (e.g. climate change, human activity impacts on watershed, or structure measures in upstream) and/or damageable property value (e.g. floodplain zoning, flood warning, or urbanization), the MSR between levee height and setback will not change as the optimally designed overtopping flow changes.

Rearranging Equation (3.6) leads to

$$\frac{\partial B}{\partial X_s} \Big/ \frac{\partial Q}{\partial X_s} = \frac{\partial (C+B)}{\partial X_h} \Big/ \frac{\partial Q}{\partial X_h} \tag{3.6'}$$

If we define $\frac{\partial B}{\partial X_s}$ and $\frac{\partial (C+B)}{\partial X_h}$ as cost efficiencies of setback and height, and $\frac{\partial Q}{\partial X_s}$ and $\frac{\partial Q}{\partial X_h}$ as hydraulic efficiencies of setback and height, Equation (3.6') means the ratio of cost efficiency to hydraulic efficiency of levee setback should equal that of levee height.

3.2.2 Levee Re-design under Static Conditions

Flood levee construction involves large irreversible investments, so rigorous examination is desirable before an implementation decision is made. The above analysis assumes no levee currently exists for flood protection. Given an existing levee, a decision must be made among three choices: do nothing to the existing levee, raise the existing levee to the optimal height for current setback, or build a new levee with optimal height at optimal setback for the river reach. The decision should minimize expected total cost.

Let X_{s0} and X_{h0} represent current levee setback and height of an existing levee. For a given X_{s0}, the optimal levee height X_{h0}^{*} associated with current setback can be found with Equation (3.2). Here, X_{h0}^{*} is the optimal height for building a new levee at current setback X_{s0}. We first consider the case that current levee height is less than the optimal levee height associated with current setback, namely $X_{ho} \le X_{h0}^{*}$. Supposing the levee should be raised instead of being relocated, the optimal height $\overline{X}_{h0}$ that the levee should be raised to is found by minimizing expected total cost

$$ETC(\overline{X}_{h0}) = EC(X_{s0}, \overline{X}_{h0}) - C(X_{h0}) \tag{3.7}$$

The RHS of Equation (3.7) represents the expected annualized total cost of raising the current levee height X_{h0} to an optimal flood protection height $\overline{X}_{h0}$. The levee construction cost is assumed to be linear with levee volume. Retaining the same levee setback, minimization of $ETC(\overline{X}_{h0})$ requires $\frac{dETC(\overline{X}_{h0})}{d\overline{X}_{h0}} = 0$, namely

$$\frac{dP(\overline{X}_{h0}; X_{s0})}{d\overline{X}_{h0}} \cdot D + \frac{d\left[C(\overline{X}_{h0}) - B(\overline{X}_{h0}; X_{s0})\right]}{d\overline{X}_{h0}} = 0 \tag{3.8}$$

The current setback X_{s0} is a fixed parameter in Equation (3.8). Therefore, Equation (3.8) leads to the same solution as Equation (3.2), that is $\overline{X}_{h0} = X_{h0}^{*}$. Whenever an existing levee should be raised, it should be raised to its optimal height associated with the current setback.

For the case $X_{h0} \le X_{h0}^{*}$, to determine whether the existing levee should be raised or relocated, the difference of annualized expected cost between the two options is defined as

$$G_1(X_{s0}, X_{h0}; X_s^{*}, X_h^{*}) \overset{def}{=} \left\{EC(X_{s0}, X_{h0}^{*}) - C(X_{h0})\right\} - EC(X_s^{*}, X_h^{*}) \tag{3.9}$$

Equation (3.9) is a function of current setback and height of the existing levee, in which X_s^{*} and X_h^{*} are parameters and X_{h0}^{*} depends on X_{s0}. For short, this equation is called the "cost difference function". Similar to Equation (3.7), the first two terms in the

RHS of Equation (3.9) represent the annualized total cost of raising the current levee height to the optimal flood protection height X_{h0}^*. The third term in the RHS is the expected annualized total cost of building a new levee with the optimal setback and height for the river reach.

If $G_1(X_{s0}, X_{h0}; X_s^*, X_h^*) > 0$, the overall cost to raise the existing levee exceeds that of a new levee. Thus, a new levee should be built at a new location. Otherwise, the existing levee should be raised to height X_{h0}^*.

If the current levee height exceeds the optimal height for current setback ($X_{h0} > X_{h0}^*$), the levee should not be further raised because with the convexity nature of the expected total cost with respect to levee height, further raising an over-constructed levee increases expected total cost. However, this does not mean the levee should not be relocated. Define the expected cost difference between the existing levee and a new levee with the optimal setback and height as

$$G_2(X_{s0}, X_{h0}; X_s^*, X_h^*) \overset{def}{=} \{EC(X_{s0}, X_{h0}) - C(X_{h0})\} - EC(X_s^*, X_h^*) \qquad (3.10)$$

If $G_2(X_{s0}, X_{h0}; X_s^*, X_h^*) < 0$, it is more costly to relocate the levee than retaining it, so the levee should remain at setback X_{s0} and height X_{h0}; otherwise, the levee should be moved to the optimal setback X_s^* with optimal height X_h^*.

Where $G_1(X_{s0}, X_{h0}^c; X_s^*, X_h^*) = 0$, the annualized overall cost to raise the existing levee equals that of a new levee. This is the critical case when either option is economically equivalently acceptable. Such a levee height X_{h0}^c is called the "critical height" for the current levee setback since it is the partitioning point for levee re-design options. As assumed, the expected total cost function is convex in levee height with an minimum at X_{h0}^*; thus where $X_{h0} \le X_{h0}^*$ and $X_{h0} \ge X_{h0}^c$, the levee should remain with setback X_{s0} but rise to height X_{h0}^*. Otherwise, the levee should be moved to the optimal setback X_s^* and raised to the optimal height X_h^*.

However, a critical height less than the optimal height associated with current setback might not exist when the current setback is too small or too large. For a very small setback, a very high levee is desirable to provide the channel capacity, therefore expected flood control cost with an existing levee at the optimal height could be much higher than that of relocating the levee. However, for very large setbacks, annual loss of land value is high, thus the saving from having an existing levee at optimal height may not be able to compensate the loss of land value from suboptimal setback.

From the definition of critical height we know that at the optimal setback X_s^* the critical height is zero. The more a setback deviates from the optimal setback, the more its corresponding critical height approaches its optimal height until they overlap. At a

setback X_s^c where the levee's optimal height coincides with its critical height X_h^c, X_s^c and X_h^c would simultaneously satisfy both $\left[\frac{\partial P}{\partial X_h}\cdot D+\frac{\partial(C+B)}{\partial X_h}\right]_{\substack{X_s=X_s^c\\X_h=X_h^c}}=0$, and $G_1(X_s^c, X_h^c)=0$. Such a setback X_s^c is called the "critical setback" of a river reach. It is a constant for given hydrologic, hydraulic and economic conditions, independent of current levee location or height. Theoretically, a river reach could have two critical setbacks, one should be small, identifying the critical point below which an existing setback would be "too small"; the other one should be large, beyond which an existing setback would be "too large". However, with large main channel a river reach might have only a large critical setback.

When a levee setback exceeds the critical setback (on either direction) for the study river reach, even if the current height equals the optimal height for this location, the levee should be relocated. For such a case, the height of an existing levee has to exceed the optimal height for current location to avoid being relocated. The critical height for such cases can be derived by solving $G_2(X_{s0}, X_{h0}^c; X_s^*, X_h^*)=0$. The decision criterion becomes: If current levee height exceeds the critical height, no action should be taken to the existing levee; otherwise, the levee should be relocated to the optimal X_s^* and raised to the corresponding optimal height X_h^*.

Table 3.1 summarizes these theoretical decision-making rules for re-design of a levee. For generality, we assume there are two critical setbacks, the small one X_{s1}^c and the larger one X_{s2}^c.

Table 3.1. Flood levee re-design rules under static conditions.

Height \ Setback	$\mathbf{X_{s1}^c < X_{s0} < X_{s2}^c}$	$\mathbf{X_{s0} < X_{s1}^c}$ or $\mathbf{X_{s0} > X_{s2}^c}$
$\mathbf{X_{h0} < X_{h0}^c}$	Move to (X_s^*, X_h^*) [a]	Move to (X_s^*, X_h^*) [a]
$\mathbf{X_{h0}^* > X_{h0} > X_{h0}^c}$	Raise current levee to X_{h0}^*	Impossible
$\mathbf{X_{h0} > X_{h0}^*}$	Do nothing	Depends on X_{h0} vs. $\mathbf{X_{h0}^c}$
$\mathbf{X_{h0} > X_{h0}^c}$	Depends on X_{h0} vs. $\mathbf{X_{h0}^*}$	Do nothing

Note a: Relocate levee to the optimal setback for the river reach X_s^* and raise to the optimal height X_h^*.

3.3 Examples for Static Analysis

The theory developed here is now applied to some common special cases.

3.3.1 Optimal Tradeoff of Levee Setback for Height Examples

The first set of special cases is for a new levee, first for a wide prismatic channel, then for a trapezoid channel.

3.3.1.1 Prismatic Wide Rectangular Channel

As Figure 3.1 shows, for an ideal prismatic wide shallow rectangular channel with width X_s and levee height X_h, the overtopping flow is given by Manning's Equation

$$Q = \frac{k}{n} S^{1/2} X_s X_h^{5/3} \tag{3.11}$$

where n is Manning roughness, S is longitudinal channel bed slope, k equals 1.49 for English units and 1 for metric units. In Equation (11), let $\alpha = \frac{k}{n} S^{1/2}$ and the partial derivatives with respect to X_s and X_h are

$$\frac{\partial Q}{\partial X_h} = \frac{5}{3} \alpha X_s X_h^{2/3} \tag{3.12}$$

$$\frac{\partial Q}{\partial X_s} = \alpha X_h^{5/3} \tag{3.13}$$

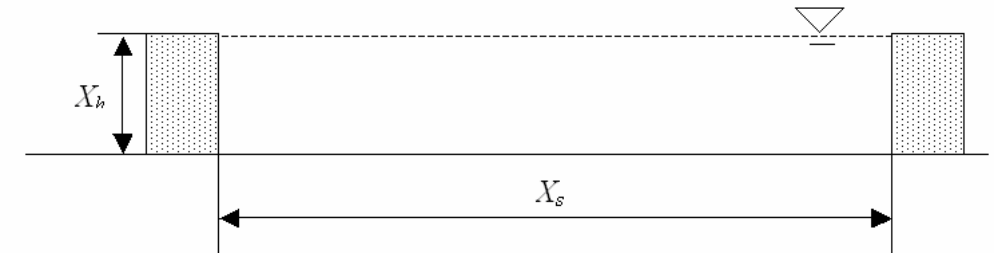

Figure 3.1. Rectangular channel and levee cross section.

Assuming levee width does not change with levee height (e.g., a flood wall), land value loss will depend on setback only, leading to linear cost functions $B(X_s) = \gamma L X_s$ and $C(X_h) = \beta_0 L w_0 X_h$, where L is the length of levee reach, w_0 is the width of levee, and γ is unit land value loss per year. Embedding these cost functions and equations (3.12) and (3.13) into Equation (3.6) leads to:

$$\frac{X_s^*}{X_h^*} = \frac{3\beta_0 w_0}{5\gamma} \tag{3.14}$$

where β_0 is annualized unit construction cost. Equation (3.14) shows the optimal ratio of levee setback to height is a constant for idealized wide shallow rectangular channel and rectangular cross-section levee under static conditions. The ideal ratio of levee setback to height is the ratio of marginal hydraulic effectiveness of levee setback to height in producing channel capacity (3/5 in this case) multiplied by the ratio of the relative economic cost of levee setback and height ($\beta_0 w_0 / 5\gamma$). The optimal ratio of X_s to X_h is unaffected by hydrology or the value of protected properties (which do however affect optimal channel capacity). In addition, Manning roughness and channel longitudinal slope also do not influence the optimal ratio of X_s to X_h.

3.3.1.2 Prismatic Trapezoid Channel

This type of analysis can be done for different channel and levee forms. In Figure 3.2, for instance, a compound channel is assumed consisting of a trapezoidal main channel with depth *d*, bottom width b_0, and side slope *m*, which normally contains flow within bank-full conditions, and a trapezoidal floodplain section over the main channel, which carries overbank flow during floods. The left and right bank setbacks are X_s and b_1 respectively. The levee also has trapezoid cross section with top width *w* and side slope *m*.

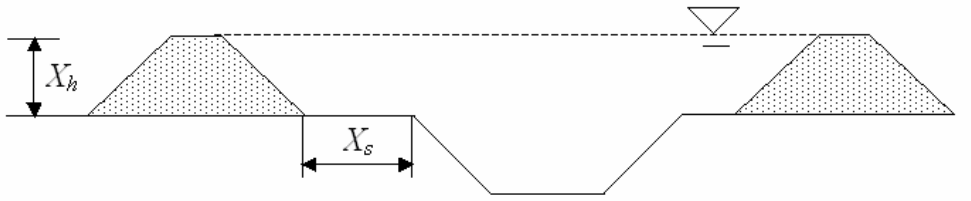

Figure 3.2. Trapezoid channel and levee cross section.

With Manning equation, the overtopping flow is

$$Q = kS^{1/2}\left\{\frac{\left(X_s X_h + \frac{mX_h^2}{2}\right)^{5/3}}{n_f\left(X_s + X_h\sqrt{1+m^2}\right)^{2/3}} + \frac{\left[b_0(d+X_h)+md(d+2X_h)\right]^{5/3}}{n_m\left(b_0 + 2d\sqrt{1+m^2}+2X_h\right)^{2/3}} + \frac{\left(b_1 X_h + \frac{mX_h^2}{2}\right)^{5/3}}{n_f\left(b_1 + X_h\sqrt{1+m^2}\right)^{2/3}}\right\} \tag{15}$$

where n_f and n_m are Manning roughness coefficients for floodplains and main channel respectively. The meaning of *k* and *S* are the same as in Equation (3.11). Embedding

(3.15) and the land value loss function $B(X_s)=\gamma X_s$, construction cost function $C(X_h)=\beta_0 L(mX_h^2+wX_h)$ into Equation (3.6), where L is length of levee reach, β_0 is unit construction cost of levee, we obtain

$$\left\{\left[5(X_s+mX_h)f_1^{2/3}-2\sqrt{1+m^2}\,f_1^{5/3}\right]+\frac{n_f}{n_m}\left[5(b_0+2md)f_2^{2/3}+4f_2^{5/3}\right]+\left[5(b_1+mX_h)f_3^{2/3}-2\sqrt{1+m^2}\,f_3^{5/3}\right]\right\}$$
$$\Big/\left(5X_h f_1^{2/3}-2f_1^{5/3}\right)=\frac{\beta_0(2mX_h+w)}{\gamma}+2m \tag{3.16}$$

where

$$f_1=\frac{X_sX_h+\frac{mX_h^2}{2}}{X_s+X_h\sqrt{1+m^2}},\quad f_2=\frac{b_0(d+X_h)+md(d+2X_h)}{b_0+2d\sqrt{1+m^2}+2X_h},\quad f_3=\frac{b_1X_h+\frac{mX_h^2}{2}}{b_1+X_h\sqrt{1+m^2}}$$

Equation (3.16) gives the relationship of the optimal levee height and setback for the channel and levee with trapezoid cross sections. Equation (3.16) demonstrates that the relationship of optimal levee setback and height does not depend on flood hydrology and longitudinal channel slope but does depend on the relative Manning roughness of main channel and floodplain. The relative roughness of floodplain vs. main channel would affect the physical and economic efficiency of levee height vs. setback expansion.

3.3.2 Static Levee Relocation for Rectangular Channels

The following presents an analysis of the levee re-design decision for the wide shallow rectangular channel and rectangular cross-section levee shown in Figure 3.1. Assuming the floods have mean μ and standard deviation σ, and fit a lognormal distribution, the mean and standard deviation of this lognormal distribution should be

$$M=\frac{1}{2}\ln\left(\frac{\mu^2}{\left(\frac{\sigma}{\mu}\right)^2+1}\right) \tag{3.17}$$

$$S=\sqrt{\ln\left(\left(\frac{\sigma}{\mu}\right)^2+1\right)} \tag{3.18}$$

For a given levee overtopping flow Q, the probability of flooding is

$$P(Q)=\int_{Q}^{+\infty}\left[\frac{1}{qS\sqrt{2\pi}}e^{-[\ln(q)-M]^2/2S^2}\right]dq \tag{3.19}$$

Differentiating P with respect to Q results in

$$\frac{\partial P}{\partial Q}=\frac{-1}{QS\sqrt{2\pi}}e^{-[\ln(Q)-M]^2/2S^2} \tag{3.20}$$

Combining equations (3.4), (3.12), (3.20), embedding them and the land value loss function $B(X_s)$ and construction cost function $C(X_h)$ into Equation (3.2), we obtain

$$\frac{e^{-\left[\ln\left(\alpha X_s X_h^{3/5}\right)-M\right]^2/2S^2}}{X_h S\sqrt{2\pi}}-\frac{3\beta_0 L w_0}{5D}=0 \tag{3.21}$$

The meanings of parameters in Equation (3.21) are the same as in section 3.1.1. Combining (3.21) and (3.14), the optimal levee setback X_s^* and height X_h^* for given hydrologic, hydraulic and economic conditions can be found. With an existing levee setback X_{s0}, the optimal levee height X_{h0}^* for this existing setback can be solved from Equation (3.21). With X_{h0}^*, X_s^* and X_h^*, for the existing setback X_{s0}, the "critical" levee height X_{h0}^c can be solved by solving $G_1(X_{s0}, X_{h0}; X_s^*, X_h^*)=0$ in Equation (3.9).

Table 3.2 gives the parameters of five cases to examine various factors' effects on critical levee height. Economic and hydraulic parameters are taken from Table 3.2. Case 1 and Case 2 show larger flood magnitudes increase the optimal setback, optimal height, and critical setback. Case 3 indicates increased unit levee construction cost increases optimal setback, smaller optimal height and greater critical setback. Case 4 demonstrates larger Manning roughness increases optimal setback, optimal height, and critical setback. Case 5 shows more damageable property also increases optimal setback, optimal height, and critical setback.

Table 3.2. Hydrologic, hydraulic and economic parameters, and resultant optimal and critical values.

Case	Parameters							Results		
	μ (cfs)	σ (cfs)	β_0 ($/ft^3.yr)	γ ($/ac.yr)	w_0 (ft)	n	D ($10^8)	X_s^* (ft)	X_h^* (ft)	X_{s2}^c (ft)
1	20000	20000	0.05	10000	150	0.035	1	519	27	1442
2	10000	10000	0.1	10000	150	0.035	1	410	21	1138
3	20000	20000	0.1	20000	200	0.035	1	767	20	2134
4	20000	20000	0.1	20000	200	0.045	1	565	29	1570
5	20000	20000	0.1	20000	200	0.035	2	553	28	1533

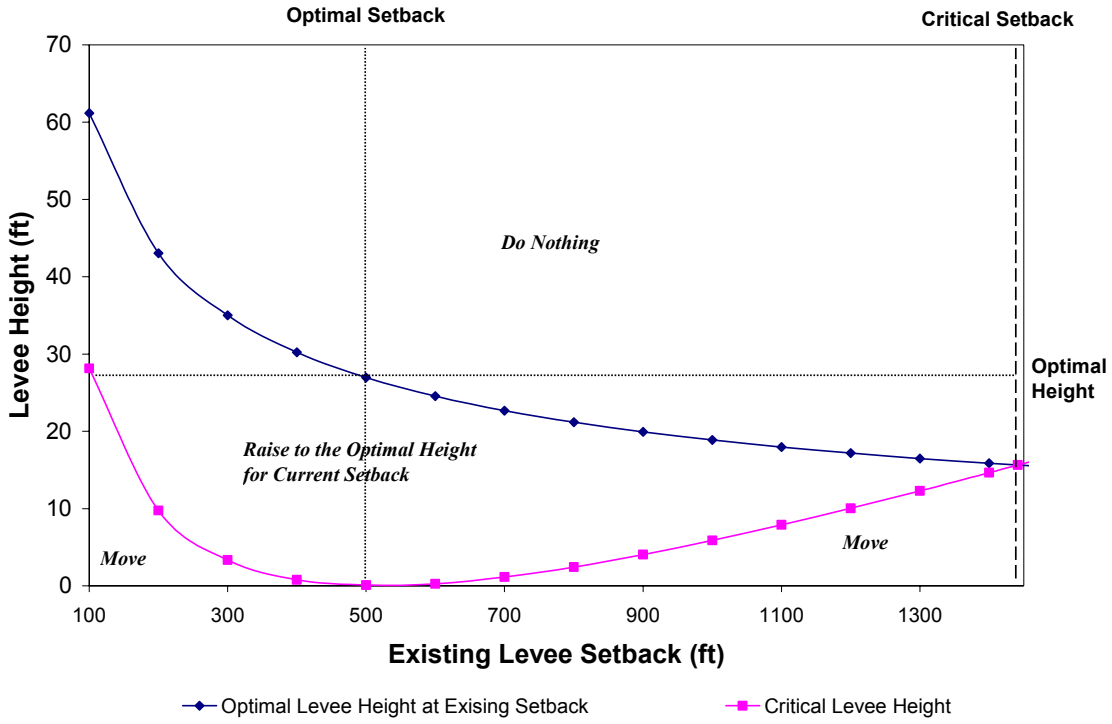

Figure 3.3. Optimal and critical levee height for existing setbacks (Case 1)

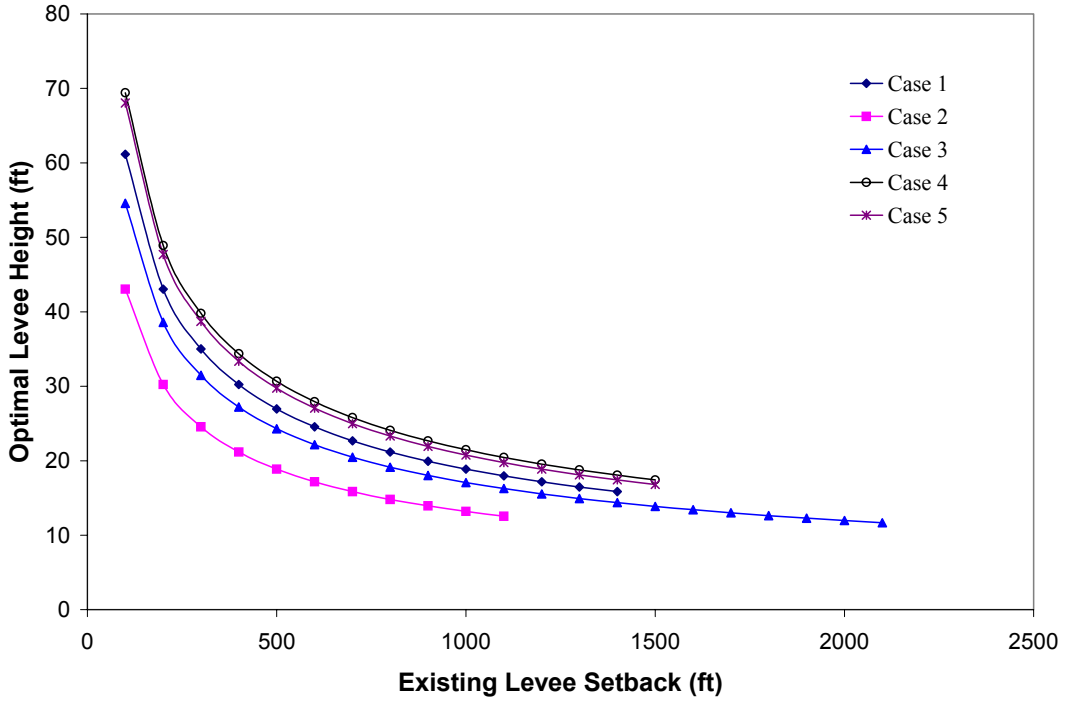

Figure 3.4. Optimal levee height for existing setback.

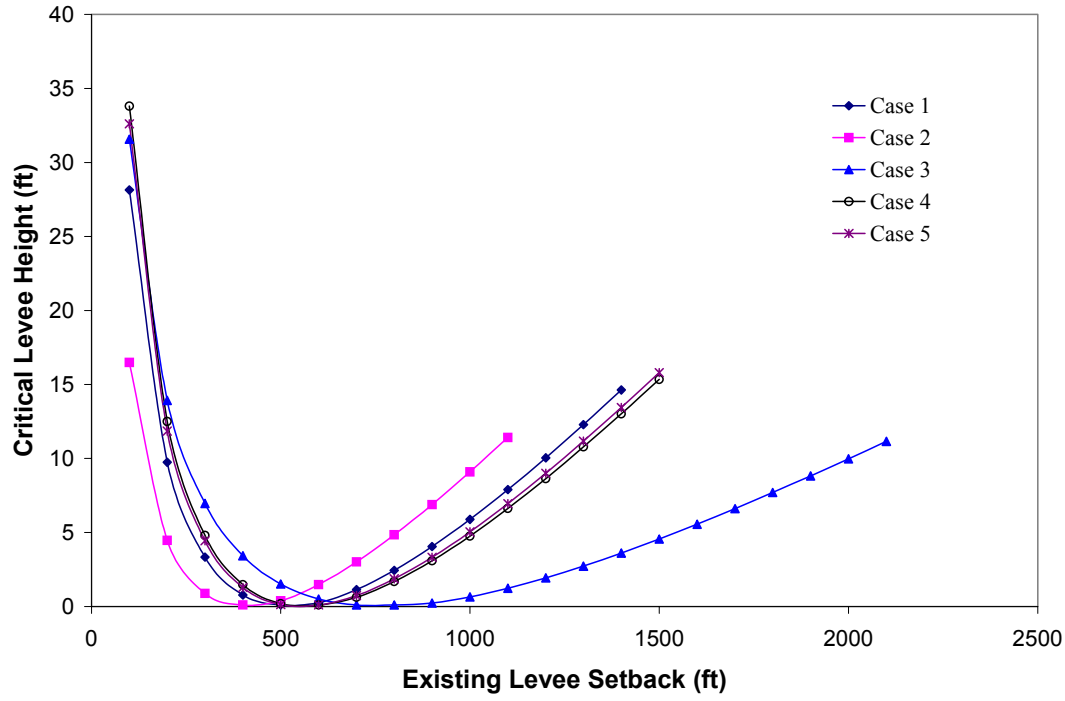

Figure 3.5. Critical levee height for existing setback.

Figure 3.3 presents the optimal and critical levee heights with various setbacks for Case 1. The optimal levee height decreases as existing setback increases. The critical height is convex with levee setback and it attains its minimum, zero, at the optimal setback of the river reach, about 520 ft. If an existing levee is located at its optimal setback it is not economical to move it to somewhere else and the levee should be raised to its optimal height. If levee setback deviates from the optimal setback, whether increased or decreased, an existing levee greater than the critical height is needed to avoid relocating the levee.

In Figure 3.4, comparison of Case1 and Case 2 shows smaller flood magnitude results in smaller optimal levee height for existing setback. Other Cases demonstrate that increases of unit levee construction cost, Manning roughness or damageable property would increase optimal levee height for existing setback.

In Figure 3.5, each critical height curve crosses at one point with Case 1. The crossing point of any curve with Case 1 is located between the two points associated with their minimum critical levee heights. For instance, the smaller flood magnitude in Case 2 leads to smaller critical setback before the crossing point of Case 1 and Case 2, and bigger critical setbacks after the crossing point. Intuitively, when the existing setback is less than the optimal setback the floodway capacity is constrained and smaller flood magnitude can improve the condition of constrained capacity and thus the system needs a smaller critical height to compensate the loss from deviating from the optimal setback; when the existing setback exceeds the optimal setback the floodway tends to have additional flood capacity and smaller flood magnitudes would lead to a solution where the property value losses exceed savings in levee construction costs, so a greater critical height is needed to compensate for property value losses from exceeding the optimal setback.

Case 2 to Case 5 demonstrate that increases of unit levee construction cost, Manning roughness or damageable property would increase the critical setback before crossing points with Case 1, and reduce critical setback after the crossing point. Explanation of these effects is similar to that for reduced flood magnitude.

3.4 Optimal Levee Raising with Dynamic Climatic and Economic Conditions

The above static analysis approach is less useful with dynamic hydrologic and economic conditions, such as climate warming induced flood frequency changes and urbanization in protected regions. The following provides a framework for an optimal control approach to derive optimal levee raising plans under dynamic conditions. Analysis of levee setback is neglected in the time being, with setback being fixed.

3.4.1 Linear Construction Cost

3.4.1.1 Model Development

The objective of optimal levee height planning is to minimize the total expected present value of floodplain management costs, including expected flood damage and levee construction costs. With a given initial levee height and a construction rate limit, the optimal control problem is formulated as follows, where levee height is the state variable and levee rising rate is the control.

$$\underset{u(.),\, x_T}{Maximize}\ J[x(.), u(.)] = \int_0^T -\left[P_t(x) D_t + \frac{\partial C_t(x)}{\partial x} u \right] \cdot e^{-rt}\, dt \tag{3.22}$$

$$\text{st.} \qquad \dot{x} = u\,, \quad x(0) = x_0\,, \ x(0) = x_0 \tag{3.23}$$

$$0 \le u(t) \le \bar{u} \quad \forall\, t \in [0, T] \tag{3.24}$$

Parameters in the above model are explained below:

$x(t)$ = levee height at time t;
$u(t)$ = levee height increase rate at time t;
$P_t(x)$ = overtopping probability at time t when levee height is $x(t)$;
D_t = damageable property value at time t;
$C_t(x)$ = cost to build a levee of height $x(t)$ at time t;
r = discount factor;
x_0 = initial levee height;
$\bar{u}$ = levee building capacity, maximum construction rate.
T = time horizon for the analysis

Define the Lagrangian as

$$L(t, x, u, \lambda, w_1, w_2) = -\left[P_t(x) D_t + \frac{\partial C_t(x)}{\partial x} u \right] \cdot e^{-rt} + \lambda u + w_1 u + w_2 (\bar{u} - u) \tag{3.25}$$

With the Maximum Principle (Kamien et al., 1981), an optimal solution satisfies

$$L_u(t, x, u, \lambda, w_1, w_2) = -\frac{\partial C_t(x)}{\partial x} \cdot e^{-rt} + \lambda + w_1 - w_2 = 0 \tag{3.26}$$

where

$$\begin{aligned} w_1 \ge 0, &\quad w_1 u = 0 \\ w_2 \ge 0, &\quad w_2 (\bar{u} - u) = 0 \end{aligned} \tag{3.27}$$

$$\dot{\lambda} = -L_x\left(t, x, u, \lambda, w_1, w_2\right) = \left[\frac{\partial P_t(x)}{\partial x} D_t + \frac{\partial^2 C_t(x)}{\partial x^2} u\right] \cdot e^{-rt},\ \lambda(T) = 0 \tag{3.28}$$

$$\dot{x} = L_\lambda\left(t, x, u, \lambda, w_1, w_2\right) = u,\ x(0) = x_0 \tag{3.29}$$

The condition (3.27) is equivalent to either

$$\lambda < \frac{\partial C_t(x)}{\partial x} \cdot e^{-rt} \text{ and } w_1 > 0,\ w_2 = 0 \text{ so } u = 0 \tag{3.30a}$$

or

$$\lambda = \frac{\partial C_t(x)}{\partial x} \cdot e^{-rt} \text{ and } w_1 = 0,\ w_2 = 0 \text{ so } u \in [0, \bar{u}] \tag{3.30b}$$

or

$$\lambda > \frac{\partial C_t(x)}{\partial x} \cdot e^{-rt} \text{ and } w_1 = 0,\ w_2 > 0 \text{ so } u = \bar{u} \tag{30c}$$

In equations (3.30a), (3.30b) and (3.30c), λ is the marginal benefit of levee height to the system, $\frac{\partial C_t(x)}{\partial x} \cdot e^{-rt}$ is the marginal construction cost. Hence, $\lambda - \frac{\partial C_t(x)}{\partial x} \cdot e^{-rt}$ represents net marginal benefit (NMB) of levee raising at time t. Equation (3.30a) and Equation (3.30c) uniquely define the levee building rate as a function of the costate variable (no building and full capacity building respectively). Equation (3.30b) represents a singular building regime. Hence, the optimal control solution could include both bang-bang and singular controls.

The maximum principle requires H_u to vanish identically on any extremal arc where u is the interior of its allowed region. In the singular case, this does not directly determine u, since H_u is independent of u by the linearity assumption. However, it determines u indirectly, via the time derivatives of H_u. Equation (3.30b) assured by the identical vanishing of H_u, gives the condition

$$\dot{\lambda} = \frac{d}{dt}\left[\frac{\partial C_t(x)}{\partial x} \cdot e^{-rt}\right] \tag{3.31}$$

Combining equations (28) and (31) results in

$$\left[\frac{\partial P_t(x)}{\partial x} D_t + \frac{\partial^2 C_t(x)}{\partial x^2} u\right] \cdot e^{-rt} = \frac{d}{dt}\left[\frac{\partial C_t(x)}{\partial x} \cdot e^{-rt}\right] \tag{3.32}$$

Equation (3.32) can be used to derive state values on a singular arc.

3.4.1.2 Numerical Example

For an ideal prismatic wide-shallow rectangular channel (Figure 3.6), the overtopping flow is approximated by

$$Q = \alpha x^{5/3} \tag{3.33}$$

where α is a constant, and x is levee height.

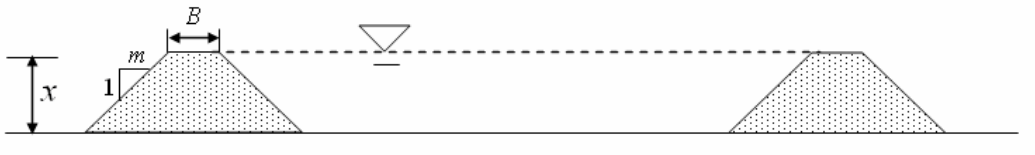

Figure 3.6. Prismatic wide shadow channel and trapezoid levee.

Assuming the flood frequency fits a lognormal distribution with mean M_t and standard deviation S_t, the overtopping probability is

$$P_t(x) = \int_{Q(x)}^{+\infty} \left[\frac{1}{qS_t\sqrt{2\pi}} e^{-[\ln(q)-M_t]^2/2S_t^2} \right] dq \tag{3.34}$$

hence

$$\begin{aligned} \frac{\partial P_t(x)}{\partial x} &= \frac{\partial P_t(x)}{\partial Q}\frac{dQ}{dx} \\ &= \frac{-5}{3xS_t\sqrt{2\pi}} e^{-\left[\ln\left(\alpha x^{5/3}\right)-M_t\right]^2/2S_t^2} \end{aligned} \tag{3.35}$$

Assuming we have a trapezoidal levee cross-section with a top width B, side slopes m, and length L. If the unit construction cost at time 0 is $C_{0,}$ with an annual growth rate of ρ, then the cost to build a new levee of height x at time t is

$$C_t(x) = \left(mx^2 + Bx\right)LC_0e^{\rho t} \tag{3.36}$$

The damageable property value at time t is

$$D_t = D_0e^{\delta t} \tag{3.37}$$

where D_0 denotes initial damage and δ is growth rate of unit construction cost. Substituting equations (3.35), (3.36) and (3.37) into Equation (3.32), we have

$$\frac{-5}{3xS_t\sqrt{2\pi}}e^{-\left[ln\left(\alpha x^{5/3}\right)-M_t\right]^2/2S_t^2}=\frac{LC_0(\rho-r)}{D_0}(2mx+B)e^{(\rho-\delta)t} \tag{3.38}$$

The solution of the algebraic equation (3.38) gives the necessary condition of the optimal levee height on single or multiple singular arcs (depending on parameters), however, it does not provide any information for the switching points when levee construction starts or pauses.

Equation (3.38) implies that singular arcs exist only if $r > \rho$. While $r < \rho$, the present value unit construction cost in a future year will exceeds that at present, so all the levee construction will occur instantaneously at the beginning, and the levee will not be raised over the remaining planning horizon.

3.4.2 Diseconomies of Scale in Levee Construction

For many practical cases, unit construction cost is not constant, but has economy or diseconomy of scale. For instance, if required levee raising is too small, unit construction cost would be relatively high because of insufficient use of contractor's construction capacity; on the other hand, if required raising in a limited time is huge, the construction contractor may have to purchase new facilities, recruit new employees, and improve its management to adapt to the new task which is beyond its existing capacity.

The building task, which matches the contractor's current construction capability, represents the most economical building activity. The relationship between unit construction cost and building rate (m^3/yr) can be obtained through investigating market and production data. For theoretical illustration, the unit construction cost $\eta(t,\dot{V})$ is assumed to be quadratic with respect to construction rate $\dot{V}=\frac{dV(x)}{dt}$, where $V(x)$ is levee volume at height x.

The objective of optimal levee height planning is to minimize the total discounted expected value of floodplain management costs, including expected flood damage and levee building expenditures. The levee height at time t and levee height increase rate u at time t are chosen as state and control variables respectively, for the following optimal control problem.

$$\underset{u(.),\,x_T}{Maximize}\ J[x(.),u(.)]=\int_0^T-\left[P(t,x)\cdot D(t)+\frac{dV(x)}{dx}\cdot u\cdot\eta(t,\dot{V})\right]\cdot e^{-rt}\,dt \tag{3.39}$$

$$\text{st.}\qquad \dot{x}=u,\ x(0)=x_0,\ x(T)=x_T,\ u\geq 0 \tag{3.40}$$

where,

$x(t)$ = levee height at time t;
$u(t)$ = levee height increase rate at time t;
$P(t,x)$ = overtopping probability at time t when levee height is $x(t)$;
$D(t)$ = damageable property value at time t;
$V(x)$ = levee volume at height x;
$\eta(t,\dot{V})$ = unit construction cost at time t;
$\dot{V}$ = levee building rate (volume increase rate)
r = discount rate;
x_0 = initial levee height.

The current value Hamiltonian is defined as

$$H(t,x,u,\lambda) = -\left[P(t,x)D(t) + \dot{V}\cdot\eta(t,\dot{V})\right] + \lambda u \tag{3.41}$$

where the levee building rate $\dot{V} = \frac{dV(x)}{dt} = \frac{dV(x)}{dx}\cdot u$.

Since the control is constrained and the optimal control may occur at the boundary, the Maximum Principle requires

$$\max_{u\geq 0} H(t,x,u,\lambda) \tag{3.42}$$

$$\dot{\lambda} = r\lambda - H_x = r\lambda + \left[\frac{\partial P}{\partial x}D + \frac{dV^2}{dx^2}u\eta + \frac{dV}{dx}\frac{\partial \eta}{\partial x}u\right],\ \lambda(T) = 0 \tag{3.43}$$

$$\dot{x} = u\ ,\ x(0) = x_0 \tag{3.44}$$

The expression (3.42) is equivalent to

$$\max_{u\geq 0}\left[\left(\lambda - \frac{dV}{dx}\eta\right)u\right] \tag{3.45}$$

For a quadratic unit construction cost function $\eta(\cdot)$ and known t, x and λ, (3.45) is to maximize a cubic function of u by choosing the most appropriate value for u. Equations (3.43), (3.44) and (3.45) can be combined and numerically solved to obtain the optimal trajectories of x, u and λ.

The unit construction cost has a quadratic form and increases at rate ρ over time

$$\eta(t,u) = \left(a\dot{V}^2 + b\dot{V} + c\right)e^{\rho t} \tag{3.46}$$

where the coefficients a>0, b<0 and c>0. Substituting (3.46) into (3.45) we have

$$\max_{u\geq 0}\left\{-\frac{dV}{dx}\cdot e^{\rho t}\cdot\left[a\left(\frac{dV}{dx}\right)^2 u^3+b\frac{dV}{dx}u^2+\left(c-\lambda\cdot e^{-\rho t}\Big/\frac{dV}{dx}\right)u\right]\right\} \tag{3.47}$$

Because $\frac{dV}{dx}$ is positive (levee volume increase with height), to find the optimal u, (3.47) can be replaced by

$$\min_{u\geq 0} f(u) \tag{3.48}$$

where $f(u)=a\left(\frac{dV}{dx}\right)^2 u^3+b\frac{dV}{dx}u^2+\left(c-\lambda\cdot e^{-\rho t}\Big/\frac{dV}{dx}\right)u$. According to Appendix 3B, the optimal choice of u that satisfies (3.47) as well as (3.48) is

$$u=\begin{cases}\dfrac{-b\frac{dV}{dx}+\phi^{1/2}}{3a\left(\frac{dV}{dx}\right)^2}, & \phi>0 \text{ and } f\left(\dfrac{-b\frac{dV}{dx}+\phi^{1/2}}{3a\left(\frac{dV}{dx}\right)^2}\right)<0\\ 0, & \textit{elsewhere}\end{cases} \tag{3.49}$$

where $\phi=\left(\frac{dV}{dx}\right)^2\left[b^2-3a\left(c-\lambda\cdot e^{-\rho t}\Big/\frac{dV}{dx}\right)\right]$.

With (3.43), (3.44) and (3.49), assuming an initial costate $\lambda(0)=\lambda_0$, the values of *x*, u and λ for each time t can be solved numerically, and the final solution is obtained when $\lambda(T)=0$ is approached through adjusting the initial costate to an appropriate level according to the feedback from end of period costate value in each iteration. Adjustment of the initial costate value can be conducted with the golden section search method. The flow chart is shown in Figure 3.7.

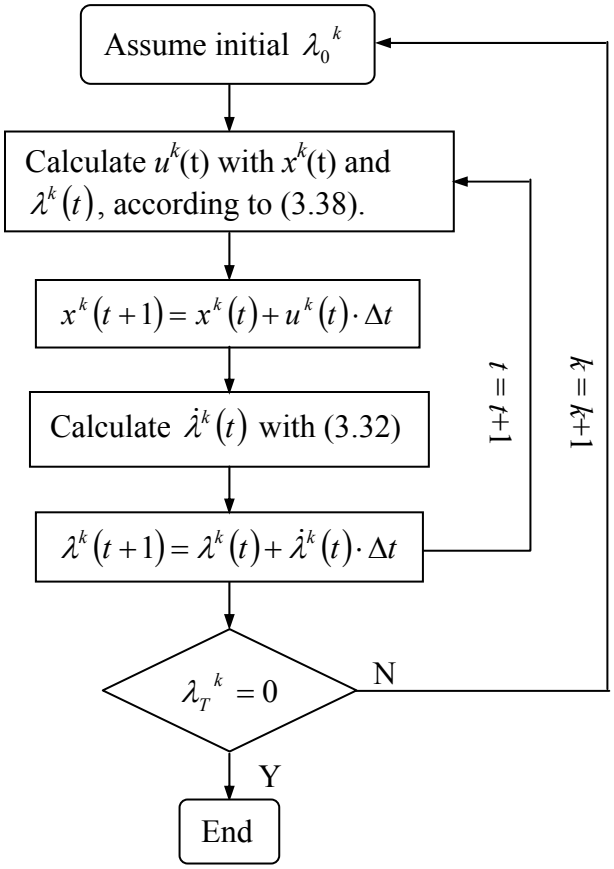

Figure 3.7. Flow chart for numerically solving the optimal control problem.

3.5 Conclusions

This chapter analyzes some theoretical aspects of simplified flood levee planning problems under static and dynamic hydrologic and economic conditions. The following conclusions are drawn from the theoretical analysis and numerical examples:

1) Under static hydrologic and economic conditions, the optimal tradeoff of levee setback for height is determined by hydraulic factors, annualized unit levee construction cost and annual unit floodplain land value loss due to floodway occupation or expansion. Neither flood frequency nor damageable property value influences the tradeoff rate, though they affect the optimal overall channel capacity.

2) Levee re-design decision rules are developed for static conditions where a levee already exists. The *critical height* for a setback and *critical setback* for a river reach are defined and analyzed. The critical setbacks are constant for a given river reach, depending on hydrologic, hydraulic and economic factors. Levee re-design decision rules are given based on these optimal and critical values of a given problem.

3) Theoretical analyses are conducted for dynamic optimization of flood levee height for two cases: a) linear construction cost, and b) nonlinear construction cost. For the first case, three types of levee raising patterns were identified: no action, gradual rising, and abrupt raising. At any time within the planning horizon, the pattern depends on relative present values of marginal construction cost and marginal benefit of levee raising to the remaining period. In particular, if the increase rate of unit construction cost exceeds the discount rate, levee raising only occurs at the very beginning of the planning horizon. For the second case, a numerical approach is given to calculate the optimal marginal benefit of levee construction as well as levee height and building decision at each time step. The construction patterns include no action and gradual levee raising. Different from the first case, no abrupt levee raising occurs when the unit construction cost depends on construction rate.

While these results are unlikely to provide directly useful quantification for actual levee problems, such theoretical formulations and results should help provide qualitative and conceptual insights for levee and floodplain management problems.

References

Biswas, A. K. (1970), *History of Hydrology*, North-Holland Pub. Co.; Amsterdam and American Elsevier Pub. Co., New York, 336 p.

Davis, D. R., C. C. Kisiel, and L. Duckstein (1972), Bayesian decision theory applied to design in hydrology, *Water Resour. Res.*, 8(1), 33-41.

Goldman, D. (1997), Estimating expected annual damage for levee retrofits, *J. Water Resour. Plann. Manage.*, 123(2), 89-94.

Humphreys, A. A. (1861), *Report upon the physics and hydraulics of the Mississippi river; upon the protection of the alluvial region against overflow; and upon the deepening of the mouths ... Submitted to the Bureau of Topographical Engineers, War Department, 1861*. Prepared by Captain A. A. Humphreys and Lieut. H. L. Abbot**,** J.B. Lippincott & Co., Philadelphia, 456 p.

Jaffe, D. A. and B. F. Sanders (2001), Engineered levee breaches for flood mitigation, *J. Hydraulic Engr.*, 127(6), 471-479.

Kamien, M. I. and Schwartz, N. L., 1981, *Dynamic Optimization: The Calculus of Variations and Optimal Control in Economics and Management*, North Holland, Amsterdam, 186-191.

Lund, J. R. (2002), Floodplain planning with risk-based optimization, *J. Water Resour. Plann. Manage.*, 128(3), 202-207.

Novshek, W. (1993), *Mathematics for Economists*, Academic Press, Inc., San Diego, 308 p.

Olsen, J. R., P. A. Beling, and J. H. Lambert (2000), Dynamic models for floodplain management, *J. Water Resour. Plann. Manage.*, 126(3), 167-175.

Olsen, J. R., P. A. Beling, J. H. Lambert, Y. Y. Haimes (1998), Input-output economic evaluation of system of levees, *J. Water Resour. Plann. Manage.*, 124(5), 237-245.

Robbins, H. M., 1967, A Generalized Legendre-Clebsch Condition for the Singular Cases of Optimal Control, *IBM Journal*, July, 361-372.

Rouse, H. and S. Ince (1957), *History of Hydraulics*, Iowa Institute of Hydraulic Research, State University of Iowa, Iowa City, Iowa, 269 p.

Tung, Y. Y. and L. W. Mays (1981), Optimal risk-based design of flood levee systems, *Water Resour. Res.*, 17(4), 843-852.

U.S. Army Corps of Engineers (USACE) (2002), *Sacramento and San Joaquin River Basins Comprehensive Study Technical Studies Documentation, Appendix E. Risk Analysis*, *Available at*: http://www.compstudy.org/docs/techstudies/appendix_e_riskanalysis.pdf, *accessed in* July 2004.

Wurbs, R. A. (1983), Economic feasibility of flood control improvements, *J. Water Resou. Plann. Manage.*, 109(1), 29-47.

Appendix 3A. Convexity of the Expected Cost Function under Particular Conditions

This appendix proves for longnormal flood frequency and a wide shallow channel, the following are sufficient conditions to assure the expected cost function of Equation (1) is convex in levee height:

- The construction cost function is quadratic or linear with respect to levee height;
- The land value loss function does not depend on, or linearly depend on levee height; and
- The designed overtopping flow exceeds the mean of the lognormal distribution.

For trapezoid or rectangular (flood wall) cross-section levees, as commonly used, the first two conditions are satisfied. Most flood levees have designed protection level of at least ten years for which the third condition can be met. Detailed proof is illustrated as follows.

Assuming the expected total cost function in Equation (1) of this chapter, $EC(X_s, X_h)$, is twice differentiable with respect to X_s and X_h, if the Hessian of $EC(X_s, X_h)$ is positive definite for all $X_s \geq 0$ and $X_h \geq 0$, then $EC(X_s, X_h)$ is strict convex.

The second order partial differential of the expect cost function with respect to X_h is

$$\frac{\partial^2 EC}{\partial X_h^{\,2}} = \frac{\partial^2 P}{\partial X_h^{\,2}} D + \frac{\partial^2 C}{\partial X_h^{\,2}} + \frac{\partial^2 B}{\partial X_h^{\,2}} \tag{3A.1}$$

If the construction cost function $C(X_h)$ is quadratic with X_h and the coefficient of the quadratic term is positive (e.g. trapezoid cross-section flood levee), we have $\frac{\partial^2 C}{\partial X_h^{\,2}} > 0$. If $C(X_h)$ is linear with X_h (e.g. rectangular cross-section flood wall), we have $\frac{\partial^2 C}{\partial X_h^{\,2}} = 0$. Assuming the land value of floodplain behind a levee is homogeneous, annual land value loss due to floodway occupancy is proportional to the lost acreage. So, if levee bottom width does not depend on levee height, or is linearly dependent on levee height, we have $\frac{\partial^2 B}{\partial X_h^{\,2}} = 0$.

The second order partial differential of the overtopping probability in X_h is

$$\frac{\partial^2 P}{\partial X_h{}^2} = \frac{\partial^2 P}{\partial Q^2}\left(\frac{\partial Q}{\partial X_h}\right)^2 + \frac{\partial P}{\partial Q}\frac{\partial^2 Q}{\partial X_h{}^2} \tag{3A.2}$$

Since floods fit a lognormal distribution, with Equation (3.19) in this chapter, we have

$$\frac{\partial^2 P}{\partial Q^2} = \frac{\ln Q - M + S^2}{Q^2 S^3 \sqrt{2\pi}} e^{-[\ln(Q)-M]^2/2S^2} \tag{3A.3}$$

For the wide and shallow flood channel, Equation (3.12) of this chapter gives the overtopping flow. Embedding equations (3.19), (3A.3) and (3.12) into (3A.2) leads to

$$\frac{\partial^2 P}{\partial X_h{}^2} = \frac{5}{9}\frac{5(\ln Q - M) + 3S^2}{X_h{}^2 S^3 \sqrt{2\pi}} e^{-[\ln(Q)-M]^2/2S^2} \tag{3A.4}$$

and

$$\frac{\partial^2 EC}{\partial X_h{}^2} = \frac{5}{9}\cdot\frac{5(\ln Q - M) + 3S^2}{X_h{}^2 S^3 \sqrt{2\pi}}\cdot D \cdot e^{-[\ln(Q)-M]^2/2S^2} + \frac{\partial^2 C}{\partial X_h{}^2} \tag{3A.5}$$

Therefore, $\ln Q > M$ is a sufficient condition to assure $\frac{\partial^2 P}{\partial X_h{}^2} > 0$. Since the damageable property value is positive, $\frac{\partial^2 P}{\partial X_h{}^2} > 0$ leads to $\frac{\partial^2 EC}{\partial X_h{}^2} > 0$.

Similarly, the second order derivative of $EC(X_s, X_h)$ with respect to X_s is

$$\begin{aligned}\frac{\partial^2 EC}{\partial X_s{}^2} &= \frac{\partial^2 P}{\partial Q^2}\left(\frac{\partial Q}{\partial X_s}\right)^2 \cdot D + \frac{\partial P}{\partial Q}\frac{\partial^2 Q}{\partial X_s{}^2} \\ &= \frac{\partial^2 P}{\partial Q^2}\left(\frac{\partial Q}{\partial X_s}\right)^2 \cdot D \\ &= \frac{(\ln Q - M + S^2)\cdot D}{X_s{}^2 S^3 \sqrt{2\pi}} e^{-[\ln(Q)-M]^2/2S^2}\end{aligned} \tag{3A.6}$$

The sufficient condition to assure $\frac{\partial^2 P}{\partial X_s{}^2} > 0$ is $\ln Q > M$.

Similarly,

$$\frac{\partial^2 EC}{\partial X_s \partial X_h} = \left(\frac{\partial^2 P}{\partial Q^2} \cdot \frac{\partial Q}{\partial X_s} \cdot \frac{\partial Q}{\partial X_h} + \frac{\partial P}{\partial Q} \frac{\partial^2 Q}{\partial X_s \partial X_h} \right) \cdot D + \frac{\partial B}{\partial X_s \partial X_h}$$
$$= \frac{5}{3} \cdot \frac{(ln\,Q - M) \cdot D}{X_s X_h S^3 \sqrt{2\pi}} e^{-[ln(Q)-M]^2/2S^2} + \frac{\partial B}{\partial X_s \partial X_h}$$
$$= \frac{5}{3} \cdot \frac{(ln\,Q - M) \cdot D}{X_s X_h S^3 \sqrt{2\pi}} e^{-[ln(Q)-M]^2/2S^2}$$

(3A.7)

Therefore

$$\frac{\partial^2 EC}{\partial X_s{}^2} \cdot \frac{\partial^2 EC}{\partial X_h{}^2} - \frac{\partial^2 EC}{\partial X_s X_h} = \frac{25}{9} \cdot \frac{\left(\ln Q - M + \frac{3}{5} S^2 \right) \cdot \left(\ln Q - M + S^2 \right)}{X_s{}^2 X_h{}^2 S^6 \cdot 2\pi} \cdot D^2 \cdot e^{-[\ln(Q)-M]^2/S^2}$$
$$+ \frac{\partial^2 C}{\partial X_h{}^2} \cdot \frac{\left(\ln Q - M + S^2 \right) \cdot D}{X_s{}^2 S^3 \sqrt{2\pi}} e^{-[\ln(Q)-M]^2/2S^2}$$
$$- \frac{25}{9} \cdot \frac{(\ln Q - M)^2}{X_s{}^2 X_h{}^2 S^6 \cdot 2\pi} \cdot D^2 \cdot e^{-[\ln(Q)-M]^2/S^2}$$
$$\geq \frac{25}{9} \cdot \frac{\left(\ln Q - M + \frac{3}{5} S^2 \right) \cdot \left(\ln Q - M + S^2 \right)}{X_s{}^2 X_h{}^2 S^6 \cdot 2\pi} \cdot D^2 \cdot e^{-[\ln(Q)-M]^2/S^2}$$
$$- \frac{25}{9} \cdot \frac{(\ln Q - M)^2}{X_s{}^2 X_h{}^2 S^6 \cdot 2\pi} \cdot D^2 \cdot e^{-[\ln(Q)-M]^2/S^2}$$
$$= \frac{25}{9} \cdot \frac{\left(\ln Q - M + \frac{3}{5} S^2 \right) \cdot \left(\ln Q - M + S^2 \right) - (\ln Q - M)^2}{X_s{}^2 X_h{}^2 S^6 \cdot 2\pi} \cdot D^2 \cdot e^{-[\ln(Q)-M]^2/S^2}$$
$$> 0$$

(3A.8)

under the restrictive condition $ln\,Q - M > 0$.

Since $\frac{\partial^2 EC}{\partial X_s{}^2} > 0$ and $\begin{vmatrix} \frac{\partial^2 EC}{\partial X_s{}^2} & \frac{\partial^2 EC}{\partial X_s X_h} \\ \frac{\partial^2 EC}{\partial X_h X_s} & \frac{\partial^2 EC}{\partial X_h{}^2} \end{vmatrix} = \frac{\partial^2 EC}{\partial X_s{}^2} \cdot \frac{\partial^2 EC}{\partial X_h{}^2} - \frac{\partial^2 EC}{\partial X_s X_h} > 0$, the Hessian of the expected total cost function, $\begin{pmatrix} \frac{\partial^2 EC}{\partial X_s{}^2} & \frac{\partial^2 EC}{\partial X_s X_h} \\ \frac{\partial^2 EC}{\partial X_h X_s} & \frac{\partial^2 EC}{\partial X_h{}^2} \end{pmatrix}$, is positive definite. Hence, the total

expected cost function $EC(X_s, X_h)$ is strict convex with respect to Xs and Xh under the restrictive conditions provided at the beginning of the appendix (Novshek, 1993, p.96).

Appendix 3B. Minimization of Constrained Cubic Function Value

This appendix presents a simple analytical analysis of minimizing a constrained cubic function

$$\begin{aligned} &\min f(x) = ax^3 + bx^2 + cx \\ &st.\ x \geq 0 \end{aligned} \tag{3B.1}$$

where a>0, b<0 and c>0.

Derive the first and the second order derivatives of $f(x)$

$$f'(x) = 3ax^2 + 2bx + c \tag{3B.2}$$

$$f''(x) = 6ax + 2b \tag{3B.3}$$

Let $f'(x) = 0$ and solve the quadratic equation, we get $x_{1,2} = \frac{-b \pm \phi^{1/2}}{3a}$, where $\phi = b^2 - 3ac$. If $\phi > 0$ there exist two different real roots, $x_1 = \frac{-b + \phi^{1/2}}{3a} > -\frac{b}{3a} > 0$ and $0 < x_1 = \frac{-b - \phi^{1/2}}{3a} < -\frac{b}{3a}$ (since $0 < \left(b^2 - 3ac\right)^{1/2} < -b$); if $\phi = 0$ there exists a single real root, $x = \frac{-b}{3a} > 0$; and if $\phi < 0$ the quadratic equation does not have a real root. Similarly, let $f''(x) = 0$ and solve the linear equation, we get $x = \frac{-b}{3a} > 0$. In Equation (3B.3), if $x < \frac{-b}{3a}$, $f''(x) < 0$, $f(x)$ is concave; otherwise if $x > \frac{-b}{3a}$, $f''(x) > 0$, $f(x)$ is convex.

As in Figure 3.8, when $\phi > 0$, the bigger root of Equation (3B.2), $x_2 = \frac{-b + \phi^{1/2}}{3a}$, satisfies both $f'(x) = 0$ and $f''(x) > 0$, so $f(x_2)$ is a minimum. If $f(x_2) < f(0)$, $f(x_2)$ is the global minimum; otherwise, $f(0) = 0$ is the global minimum.

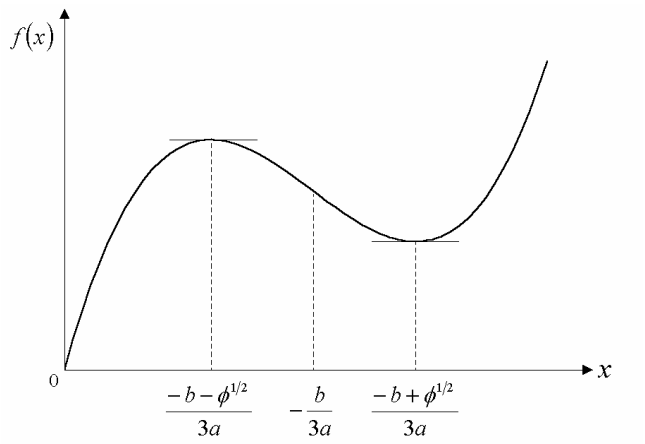

Figure 3.8. Extrema of cubic function: $\phi > 0$

When $\phi = 0$, note $-\frac{b}{3a}$, the single root of $f'(x) = 0$, is also the solution of $f''(x) = 0$. Since $f'\left(\frac{-b}{3a}\right) = -\frac{\phi}{3a} = 0$, $f(x)$ is concave before $x = \frac{-b}{3a}$ and convex after $x = \frac{-b}{3a}$, $f'(x) > 0$ always holds. Hence, the optimal solution for problem (3B-1) is $x = 0$.

When $\phi < 0$, $f'\left(-\frac{b}{3a}\right) = -\frac{\phi}{3a} > 0$. Since $f(x)$ is concave before $x = \frac{-b}{3a}$ and convex after $x = \frac{-b}{3a}$, again, $f'(x) > 0$ holds for any x. Thus $x = 0$ is the optimal solution for problem (3B.1), as illustrated in Figure 3.9.

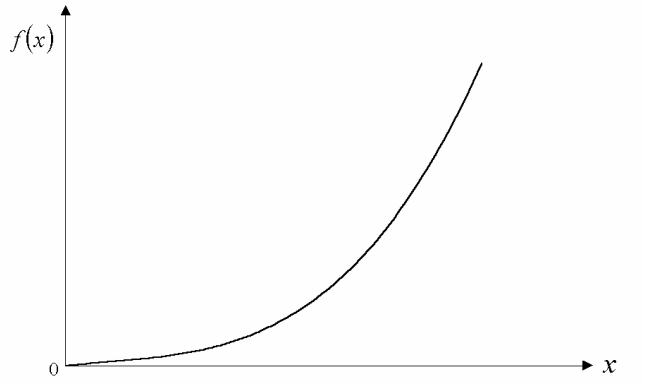

Figure 3.9. Extremum of cubic function: $\phi < 0$

To conclude, the solution for problem (3B.1) is

$$x = \begin{cases} \dfrac{-b + \phi^{1/2}}{3a}, & \phi > 0 \text{ and } f\left(\dfrac{-b + \phi^{1/2}}{3a}\right) < 0 \\ 0, & \text{elsewhere} \end{cases}$$

where $\phi = b^2 - 3ac$.

Chapter 4 Climate Change, Urbanization, and Optimal Long-term Floodplain Protection

4.1 Introduction

Climate change has received considerable attention in recent decades. Most studies have examined the hydrologic potential of climate change and potential impacts of various climate change scenarios on the environment, water, agricultural, and various other human activities. More recently, studies examining the ability and economics of human adaptation to climate change have been undertaken (Venkatesh and Hobbs, 1999; Stakhiv, 1998; Yao and Georgakakos, 2001; Simonovic and Li, 2003; Vanrheenen et al., 2004). Occasionally, the economic and hydrologic impacts of climate change have been compared with those of population growth over long periods (Vörösmarty et al., 2000).

Climate change could make flood control more challenging in many areas of the world (Milly et al., 2002). With continued urbanization of floodplains, future flooding potential and damages also could be much worse than today. Therefore, structurally feasible, economically sound and socially acceptable floodplain management is desirable to reduce vulnerability to damages and balance natural and human uses of floodplains to meet social and economic goals. Towards this end, this study examines the roles of urbanization, climate change, and human adaptation, with a simplified version of flood control problems on California's lower American River near Sacramento, one of the nation's most flood-prone regions. The floodplain management problem is formulated as a long-term optimization problem with stochastic dynamic programming (SDP). Management options also are discussed. Some illustrative results, analyses and conclusions are presented.

4.2 Problem

Climate change is often a relatively slow and significantly uncertain process. The uncertainty of climate change is especially important in the context of slow and uncertain human adaptive responses. In the case of flooding problems, climate change would affect the frequency and severity of floods over long periods of time. However, human use of floodplains and structural and non-structural flood control efforts also evolve over long periods with significant economic and social consequences and potential to buffer climate change effects. Here we examine two questions: (1) how can human use of floodplains adapt economically to changing flood risk and, (2) how might adaptation for climate change compare with adaptation due to floodplain urbanization? We examine these questions preliminarily for the lower American River, California.

At the confluence of the Sacramento and American Rivers, Sacramento is one of the nation's most flood-prone cities. As illustrated in Figure 4.1, the North and South Forks of the American River flow into Folsom Reservoir, with about 1.21 billion cubic meters (bcm) of total storage capacity, of which between 0.49 and 0.82 bcm are kept empty during the winter flood season. Downstream of Folsom Dam, the upper reach of

the lower American River is confined by high ground, which flattens further downstream. The core of the Sacramento metropolis lies south of the American River, behind levees. Large tracts of floodplain north of the American River (North Natomas) are currently undergoing extensive urban development behind levees (NRC, 1995). The Northern Sacramento metropolitan area is the subject of this study.

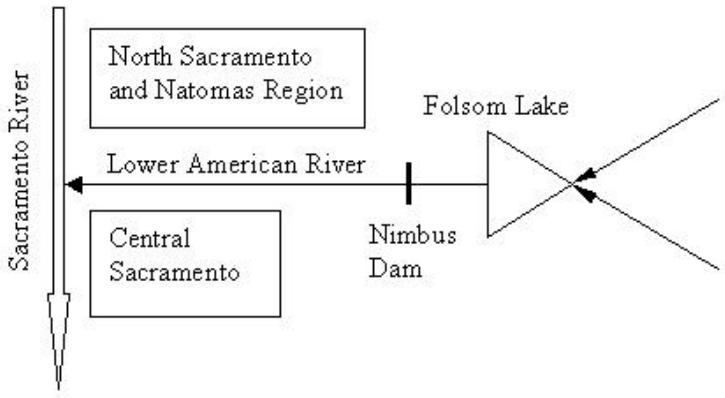

Figure 4.1. Schematic of lower American River flood control.

Over time, the population and value of urban property exposed to potential flooding in this are expected to increase steadily. Population estimates for the Sacramento region by 2100 are as high as four million (Landis et al., 2002). Flooding potential for this region is likely to increase due to climate change (Lettenmaier and Gan, 1990; Miller et al., 2003) as well as increased population and economic activity residing in the floodplain.

4.3 Adaptation Options and Decisions

The Sacramento region has a variety of options for managing floods. To simplify the analysis, we represent the complex of upstream reservoir operation, outlet structure, and reservoir capacity options in terms of their combined resulting flood frequency downstream of Folsom Dam. Options evaluated with the SDP model include:

- Raising Existing Levees. Raising existing levees entails significant construction expense and ongoing maintenance expenses. Raising levees is an expandable option, but construction expenses are irreversible.

- Broadening of the Floodway. Broadening the floodway might expand the current flooding capacity and provide recreational benefits with less risk or cost than having levees of great height. Such re-engineering of the floodway might not be uniform along the river, but would probably occur at particular bottlenecks.

Upstream reservoir control options are not examined explicitly in the model. Downstream Sacramento River options and conditions and their backwater effects are also neglected in this study. Options to reduce flood damage potential, by building codes, zoning, and flood warning and evacuation systems are similarly neglected for now.

Flood management decisions examined in the SDP model include: 1) levee setbacks on the lower American River, and 2) levee heights. In principle, floodplain land use restriction options can be examined by varying urbanization rates for different model runs. As a part of the California water system, Folsom reservoir has several uses other than flood control. To focus on floodplain management, flood control storage decisions are not explicitly included in the SDP model. Adaptation of operating rules for the upstream reservoir is an area for further research (Yao and Georgakakos, 2001).

4.4 Components for Risk-Based Optimization for the Lower American River

Risk-based optimization is used to preliminarily evaluate the economic desirability of various flood management options for the lower American River over a long period of climate change and urbanization. The SDP model has the following components and assumptions, which unavoidably simplifies the basin's true situation.

4.4.1 Flood Frequency Analyses and Levee Failure Probability

Flood frequency analysis, as traditionally practiced, assumes that annual maximum floods conform to a stationary, independent, identically distributed random process. However, with changing flood regime due to climate change, annual maximum floods in this study are treated dynamically. This dynamic process is represented with three climate scenarios of unimpaired annual peak inflows to Folsom Reservoir.

The *stationary history* scenario assumes the peak annual flood distribution is stationary so the future observes the same lognormal distribution as the historical record (NRC, 1999). The historical mean is 962 m^3/s, and historical standard deviation 981 m^3/s.

The *historical trend* scenario assumes the increasing trend of annual floods, identified from the historical record, would continue in the planning period. The 93-year historical record of peak annual 3-day flow from 1905 through 1997 was divided into nine-year fragments, and mean and standard deviation of each fragment were calculated. By regressing these means and standard deviations against median years of corresponding fragments, the linear annual increase rate of mean is identified to be 0.427%, and the linear annual increase rate of standard deviation is 0.675%, on the basis of year 2000 level for which the mean is 1200 m^3/s, and standard deviation is 1338 m^3/s, estimated from the regression equations. Both regression equations for mean and standard deviation satisfy a confidence level of 95%. The means and standard deviations for those nine-year fragments from past record appear in Figure 4.2. The assumed historical trend is plausible in that there is no agreement on what caused the significant increase of flood peaks after 1950. NRC reports (1995; 1999) mentioned the reasons could be climatic changes, nonrandom climatic variability or structural changes in the watershed as well as ordinary random variability, which has a low possibility of explaining these trends.

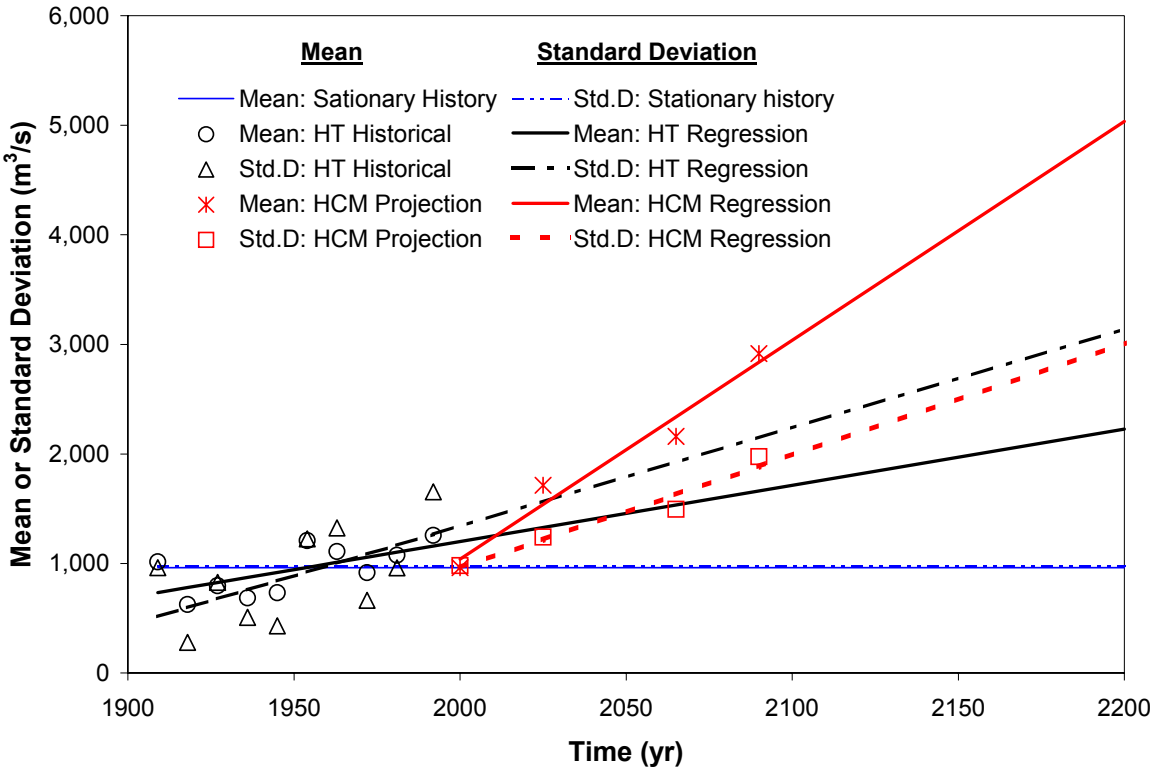

Figure 4.2. Parameterization for mean and standard deviation of 3-day floods into Folsom Reservoir for the *stationary history* scenario, *historical trend* (HT) scenario and HCM scenario, respectively.

The HCM scenario is represented by trend curves of mean and standard deviation of floods parameterized with hydrological results derived from general circulation model (GCM) and precipitation runoff studies by Miller et al. (2003) who developed 30-year of daily flows for the North Fork American River at North Fork Dam for three future periods based on the Hadley Climate Centre's HadCM2 run 1 (referred to as HCM), indicating relatively wet and warm climate trends for California. To construct the HCM scenario, it is required to develop total Folsom Reservoir peak inflows from peak floods at North Fork Dam.

Folsom Reservoir regulates runoff from about 4,820 km^2, receiving drainage from all three forks of the American River (NRC, 1995). A relatively small watershed such as the American River basin would most likely be represented by one grid point in a GCM model, resulting in homogeneous climate change impacts in terms of temperature and precipitation changes. In the meantime, each of the three tributaries is about 130 km long and flood peaks from the three adjoining forks arrive almost simultaneously at Folsom Reservoir (Redmond, 2000). Therefore, climate change perturbed unimpaired flood flows at Folsom can be constructed with GCM hydrology at North Fork Dam. This

mapping logic is further supported by the linear double mass curve comparing total unregulated American River flood flows at Folsom with that at North Fork Dam (NRC, 1999).

With these flow constructions, perturbations for each of the three GCM periods are derived for maximum annual 3-day flows at North Fork Dam, categorized with return periods of historical peak annual flows. These perturbations are then applied as multipliers to Folsom historical maximum annual 3-day flows to generate perturbed floods at Folsom, according to return period of each historical maximum annual 3-day flow. Maximum annual 3-day flow is used to track year-to-year behavior because typically a very heavy flow event will take 2-3 days to fill flood storage at Folsom Reservoir (Redmond, 2000; Goldman, 2001).

Each of the constructed flood series is fitted to a lognormal distribution. Historical and paleoflood data are not considered in curve fitting. In Figure 4.3, from bottom to top the four lognormal curves and their points represent floods in four year levels: 2000, 2025, 2065 and 2090. The means and standard deviations of the four constructed flood series are regressed against year levels and, the results demonstrate that both mean and deviation increase linearly for the coming century (Figure 4.2). These time-dependent flood means and standard deviations represent effects of climate change.

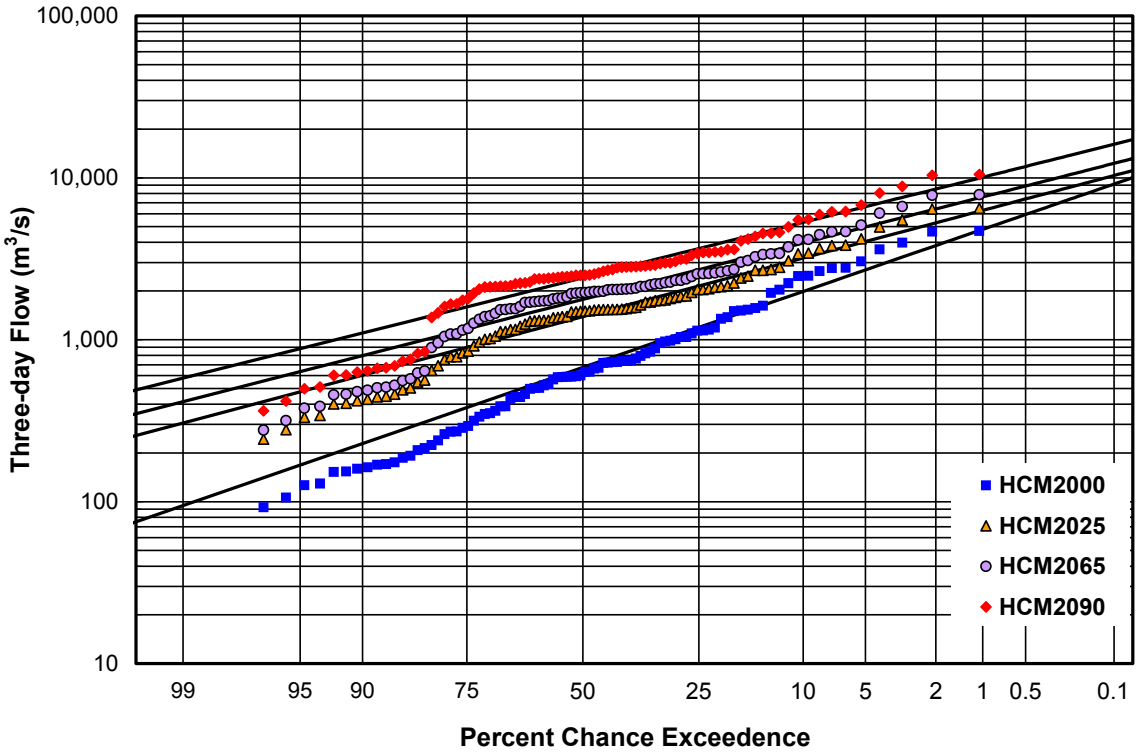

Figure 4.3. Fitting log-normal distributions to HCM scenario data for four different year levels.

As in Figure 4.2, for the HCM scenario the annual linear increase in mean is 1.92%, the annual linear increase in standard deviation is 1.07%. The mean, 1039 m^3/s, and standard deviation, 961 m^3/s, derived from regression equations for year 2000 level, are used for the base year. The extreme effect of the HCM result is chosen for analysis so that the approach and result would be meaningful and interesting. This does not necessarily mean the HCM scenario is more believable than other GCM climate change scenarios.

Climate change is not always gradual. Beyond some threshold, changes can be rapid and long-lasting (Alley et al., 2003). An abrupt change version of the HCM scenario was examined, without particularly noteworthy results, and so is not discussed here.

Flood frequencies of the above scenarios are used to derive levee failure probabilities for the decision analysis model, where floodplain inundation occurs with levee overtopping. Actual levee failure is also affected by other factors not included in this model, such as the duration of flooding (NRC, 1995). For a given channel with a setback and a height, overtopping flow is found from stage-discharge rating curves (Figure 4.4) derived from a HEC-RAS hydraulic modeling of the river (USACE, 2002a).

The upstream Folsom Reservoir discharges the potentially overtopping flow. In this study, present Folsom Reservoir operating rules are used. Though having some limitations, this simplification allows this study to focus on the downstream levee system. The inverse form of the "unregulated inflow and regulated outflow relationship" for Folsom Reservoir 3-day maximum annual floods (Goldman, 2001) is used to derive unregulated Folsom Reservoir inflow for a given downstream levee overtopping flow.

Figure 4.4. Stage-discharge rating curves at 12.5 km from the confluence with Sacramento River (7.75 river mile) for 13 different levee setbacks.

4.4.2 Flood Hydraulics

An existing HEC-RAS hydraulic model was used to create a set of rating curves for critical locations on the lower American River, with a range of levee setbacks covering levee locations available to the optimization model. The total reach length is about 35 km. Thirteen levee setbacks were examined in HEC-RAS for each of 159 cross sections to create stage-discharge relationships as shown in Figure 4.4. Steady flow simulation was done since appropriate operation of Folsom Reservoir can cut the flood peak and result in steadier flow downstream. Hydraulic simulations were made using regulated maximum annual 3-day flows.

This study analyzes 21 km of the north levee upstream from the confluence with the Sacramento River, which is currently leveed. Most of the remaining north bank of the lower American River runs through high ground. Levee setback of the south bank is fixed since it is next to downtown Sacramento, making setback change almost impossible. North bank levee setbacks from 0 to 366 m are examined (Figure 4.4).

HEC-RAS performs a fixed-bed analysis, assuming no geomorphologic change over the study period. Manning's n values ranged from 0.045 to 0.05 overbank and 0.035 in the channel. Downstream boundary conditions for the HEC-RAS model were set at normal depth. A common index point, 12.5 km from the confluence with the Sacramento River (river mile 7.75), was used to evaluate the whole reach. The north bank elevation at this cross section is 9.3 m above mean sea level, which is the assumed levee bottom elevation. The resulting stage-discharge rating curves at the index point cross section is shown in Figure 4.4. In the SDP model, overtopping flows for various setbacks and levee heights are derived from those rating curves through bilinear interpolation.

4.4.3 Benefit and Cost Functions

Philosophically, one of the most difficult steps in planning is summarizing the values of society into a scalar-valued ranking function to allow comparison of engineering alternatives (James, 1965). Economically optimal floodplain management seeks to maximize the annualized economic value of land use minus expected annual flood damage and mitigation costs in this study. The current value of floodplain land protected by the levee is assumed to be $49,422/ha-yr ($20,000/acre-yr); value of floodplain land by the river is $2,471/ha-yr ($1,000/acre-yr).

Expected flood damage functions are estimated from recent flood damage studies (USACE, 2002b). Flood damage is caused when flow stage exceeds levee height. Average damage is estimated to be $11.2 billion at year 2000 level if all land in Sacramento City and Natomas is flooded. This damage is huge but plausible considering there is approximately $40 billion in damageable property in these regions (NRC, 1995; Redmond, 2000).

Implementation costs of various management decisions are estimated from the literature. The base cost for levee building is estimated to be $35.3/m^3 ($1/ft^3). The lower American River area is rapidly urbanizing. A variety of growth rates for floodplain land values are examined. Damageable property values are assumed to increase at the same rate as floodplain land values. Flood warning systems are already quite good for this area. Thus, potential human life loss due to flood hazard is not employed as part of the objective function. We assume an average discount rate over a long planning horizon, with a base case discount rate of 6.5%.

4.5 Model Formulations and Solution Methods

Flood protection in leveed flood control systems has been formulated with various forms of optimization models (Tung and Mays, 1981; Lund, 2002; Olsen et al., 2000; Simonovic and Li, 2003). To incorporate such dynamic factors as climate change and

urbanization requires a structurally flexible and computationally efficient model. Stochastic Dynamic Programming (SDP) was chosen over an alternative Markov chain linear program.

The Stochastic Dynamic Programming formulation uses time t as the decision stage, levee setback and height at the beginning of current period as state variables $\overrightarrow{S_t}$, and the next period's levee setback and height as decision variables $\overrightarrow{X_t}$. For a benefit function $B_{jt}(\overrightarrow{S_t}, \overrightarrow{X_t})$, including flood protection benefits and flood works and damage costs, flooding state probability $P(j|\overrightarrow{X_t})$ over j possible flooding states (e.g., flooded vs. not flooded), and real continuous discount rate r, the recursive function becomes

$$f_t\left(\overrightarrow{S_t}, \overrightarrow{X_t}\right) = \begin{cases} \max\limits_{X_t} \left\{ \left[\sum\limits_j P_t\left(j \mid \overrightarrow{X_t}\right) B_{jt}\left(\overrightarrow{S_t}, \overrightarrow{X_t}\right) \right] + f_{t+1}\left(\overrightarrow{S_{t+1}}, \overrightarrow{X_{t+1}}\right) e^{-r\cdot\Delta t} \right\}, & t < N \\ V\left(\overrightarrow{X_N}\right), & t = N \end{cases} \tag{4.1}$$

where $f_t\left(\overrightarrow{S_t}, \overrightarrow{X_t}\right)$ is the maximized accumulated discounted benefit from time t to time N, the end of the planning period, given the state and decision at time t. Without climate change (i.e., climate is stationary), the time subscript to P can be removed. Without urbanization and construction cost change, the time subscript on the benefit function can be removed. Discounting is handled at each stage with incremental continuous discounting on the second term. We assume climate change and urbanization will persist for N years, followed by a stationary climate, an end to urbanization, and consequently no further change in optimal decisions. For an infinite horizon problem the future value at the end of the N^{th} year becomes

$$V\left(\overrightarrow{X_N}\right) = \left[\sum_j P_N\left(j \mid \overrightarrow{X_N}\right) B_{jN}\left(\overrightarrow{X_N}\right) \right] \frac{e^r}{e^r - 1}$$

where $B_{jN}\left(\overrightarrow{X_N}\right)$ is the constant annual net benefit under flooding event j. The state transition equation is

$$\overrightarrow{S_{t+1}} = \overrightarrow{X_t}$$

The state vector $\overrightarrow{S_t} = \left[h_{1t}, d_{1t,} h_{2t}\right]$, where h_{1t} is north bank levee height, d_{1t} north bank setback, and h_{2t} south bank height, assuming a fixed south bank levee location. To assure overtopping probability in the south bank is less or equal to the north bank, the south bank levee should not be lower than the north bank levee at each stage t. In addition, very high levees are impractical in terms of stability and feasibility, so a maximum levee height is also assumed, limiting this state and decision variable to $h_{\max}$. Hence we have $h_{1t} \le h_{2t} \le h_{\max}$.

The stage benefit function is

$$B_{jt}\left(\overrightarrow{S_t}, \overrightarrow{X_t}\right) = \begin{cases} LB_t\left(\overrightarrow{X_t}\right) - BC_t\left(\overrightarrow{S_t}, \overrightarrow{X_t}\right) & j = 0 \\ -BC_t\left(\overrightarrow{S_t}, \overrightarrow{X_t}\right) - FD_t\left(\overrightarrow{X_t}\right) & j = 1 \end{cases}$$

where LB_t is the annual land benefit or cost resulting from changing levee setback, BC_t levee construction costs, and FD_t flood damage value.

To improve computation speed and represent the infrequency of major flood control system changes, each time step in the model represents several years. The parameters in the model are adjusted for coarsening the time step. For example, if each time step represents n years, the probability of x failures in n years is $p_f^x (1-p_f)^{(n-x)}$, where p_f is the annual probability of flooding and levee failure. Thus, the parameter $P_t(j|i)$ above becomes $1-(1-p_f)^n$, the probability of flooding during an n-year period, where $p_f = P_t(j|i)$ for the one-year time-step. The annual flood damage D_f from a flood or levee failure should be multiplied by the expected value of the number of flood events, $\sum_{i=1}^{n} i(p_f)^i (1-p_f)^{(n-i)}$. The discounting factor e^{-rt} is also expanded to discount to the center of the interval, $e^{-r(t+\Delta t/2)}$.

The SDP algorithm is quite efficient. The time needed to find an optimal policy is polynomial in the number of discrete states in each time step. However, the number of discrete states needs to be quite large to obtain precise results, significantly increasing computation time. Discrete Differential Dynamic Programming (DDDP) is a method to reduce computation time and improve precision (Heidari et al., 1971; Tung and Mays, 1981; Yakowitz, 1982). Here, the conventional SDP was applied with relatively coarse grids of states to get an initial global optimal solution and, then DDDP was used to improve the results, which greatly increases precision and saves computation time compared to the conventional SDP alone. Results show the initial grid size of a SDP run had little influence on the final result refined by DDDP algorithm.

4.6 Base Case Parameters

Table 4.1 contains parameter values for the base case, which assumes a Stationary Historical flood frequency and no urban growth over the 200-year planning horizon.

Table 4.1. Base case parameters for SDP run.

Hydrologic		**Economic**	
Flood frequency distribution	Lognormal	Damageable property (million $)	11,200
Historical mean (m^3/s)	962	Levee construction cost ($/$m^3$)	35.3
Historical standard deviation (m^3/s)	981	Floodplain benefit ($/ha-yr)	49,422
Levee		Benefit of land by river ($/ha-yr)	2,471
Top width (m)	4.9	Discount rate	6.5%
Side slope	3	**Optimization**	
Left bank length (km)	21	Planning horizon (yr)	200
Right bank length (km)	21	Stage length (yr)	5
Initial setback (m)	30.5	Height limit (m)	19.8
Initial height (m)	4.6		

4.7 Results and Analyses

The SDP model was run for a base case and various scenarios. For each comparative analysis, a graph is plotted to demonstrate how parameter perturbations affect the timing and quantities of levee raising and setback changes for the lower American River floodplain. In each graph that shows levee setback and height over a 200 year horizon, the upper half presents levee setback, on the second vertical axis, and the lower half presents levee height, on the primary axis. Only the north bank levee height and setback are discussed since in all runs the north and south bank levee height results were identical.

4.7.1 Climate Change Effects

The three aforementioned climate change scenarios are examined first without growth in urban land values. As shown in Figure 4.5, for all climate change scenarios levee setbacks do not change over the first century. The *stationary history* scenario retains the initial setback, 30.5 m, throughout the entire planning horizon; the HCM scenario expands setback to 305 m at the 110^{th} year; and the *historical trend* scenario expands levee setback to 305 m at the 120^{th} year. These levee setback changes imply that initial setbacks may become economically less than desirable as climate changes and that more land should be occupied by the floodway over long periods.

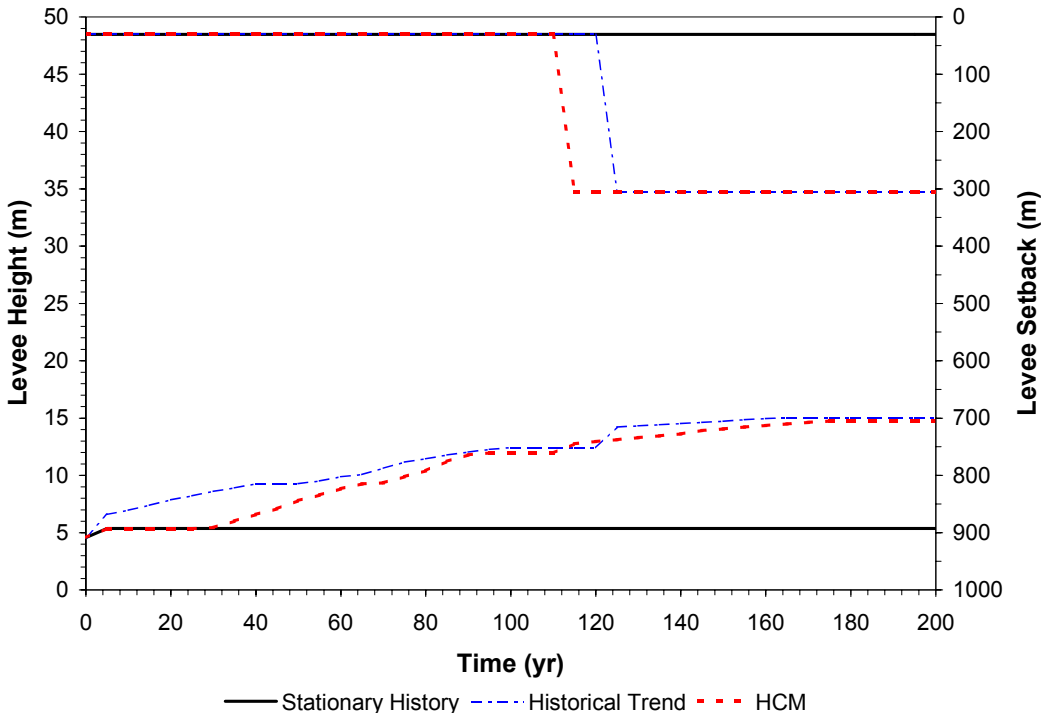

Figure 4.5. Climate change effects on levee setback and height decisions.

In Figure 4.5, levee height for the *stationary history* scenario increases to about 5.4 m at the beginning and has no more change afterwards. For the *historical trend* scenario, levee height increases to 6.6 m at the beginning, then gradually increases to 12.4 m at year 100, and then after 25 years jumps to about 14.2 m at the end of year 125, after that, gradually increases to 15 m in 35 years, and stop increasing.

The HCM scenario raises levee height to 5.4 m at the beginning, followed by about 30 years of "no action", then gradually increases to 11.8 m at year 90, after another 20 years of "no action", jumps to 12 m at year 110, and then gradually increases to 14.7 m followed by another 30 years of "no action" till the end. The different styles of levee height changes between *historical trend* scenario and HCM scenario imply the impacts of starting values and growth rates of flood mean and variance.

Each setback expansion is accompanied by an abrupt levee height increase. These simultaneous increases represent the optimal tradeoff of levee setback for height, as a result of maximizing economic efficiency of the flood control system. Other model runs demonstrate that, however, abrupt levee raising does not necessarily lead to setback change, due to significant discontinuity arising from high cost of changing levee setback.

A conclusion here is that steadily worsening flood frequencies along for a high value urban area lead to an economically optimal dynamic of rising levee heights, punctuated by occasional increases in levee setback.

4.7.2 Urbanization Effects

Three urbanization rates are examined by the optimization model without climate change, as illustrated in Figure 4.6. For the 0%/yr case, no further urbanization, levee setback never changes over the planning horizon; for the 2%/yr increase in urbanization (urban land values) case, levee setback reduces to zero around the 50th year; and for the 5%/yr case, levee setback reduces to zero at about the 20th year.

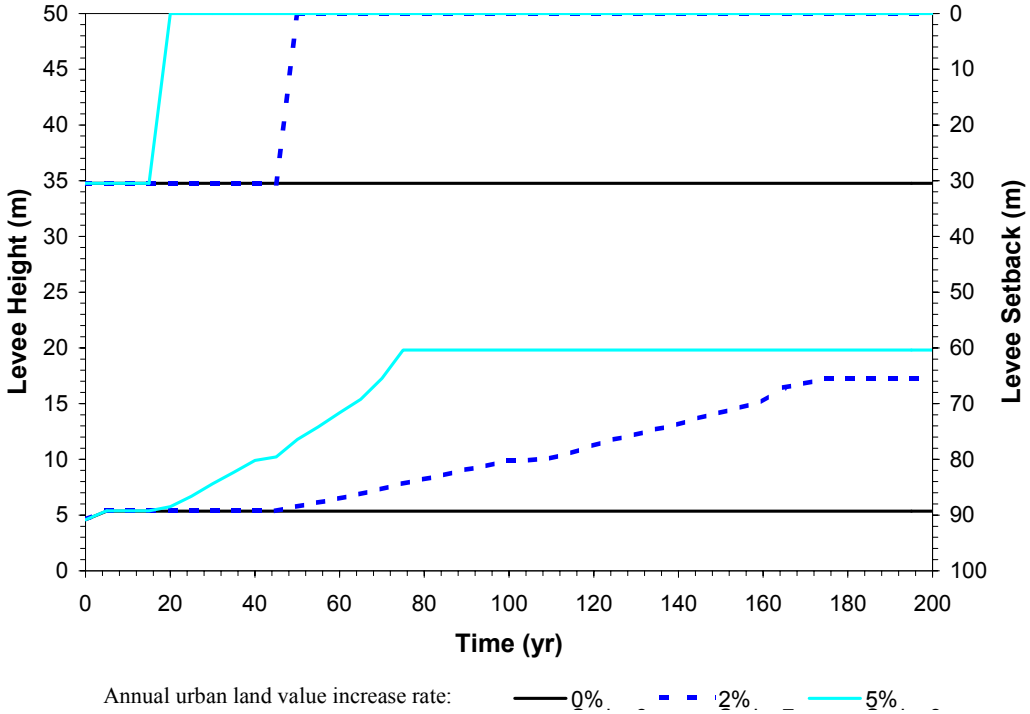

Figure 4.6. Urbanization influence without climate change.

Levee heights for all the three cases increase to 5.4 m at the beginning. After the initial raising, the 0%/yr case never change levee height over the entire remaining period; the 2%/yr case ceases levee construction until the 50th year when levee setback shrinks, followed by a gradually levee raising period of 125 years when the levee is 17.2 m high, and then, stop raising levee until the end; the 5%/yr case experiences a ten-year long "no construction" period after initial levee raising, and raises levee height to 19.8 m in about 60 years, hitting the height limit, and then remains such a height until the end.

The optimal levee behaviors in Figure 4.6 demonstrate the implications of urbanization to long-term flood control planning. Without climate change, urbanization can solely drive levee setback change and levee raising, tending to reduce levee setbacks to increase the protected land at an increased cost of levee height.

4.7.3 Combined Climate Change and Urbanization

Worsening flood frequency climate tends to raise levees and set them back with time, while urbanization tends to raise levees and move them closer to the river. When these two factors are combines, especially in the presence of a maximum levee height, what is the long-term levee strategy?

The *historical trend* and HCM climate change scenarios are combined with three urbanization rates to examine their comprehensive effects on levee construction decisions. With the *historical trend* scenario, as shown in Figure 4.7, the 2%/yr urbanization case expands levee setback twice, first in the 110th year, moving to 158 m from the river bank, and the second in the 170th year, further moving to 219 m from the river bank. The optimal levee heights also differ from the 0%/yr urbanization case. Combined with the *historical trend* climate scenario, the 2%/yr urbanization gradually drives levee height to 19.8 m at the 65th year, hitting the levee height limit. The levee height then remains at 19.8 m until the end, making levee setback expansion the only option available to increase floodway capacity after year 30.

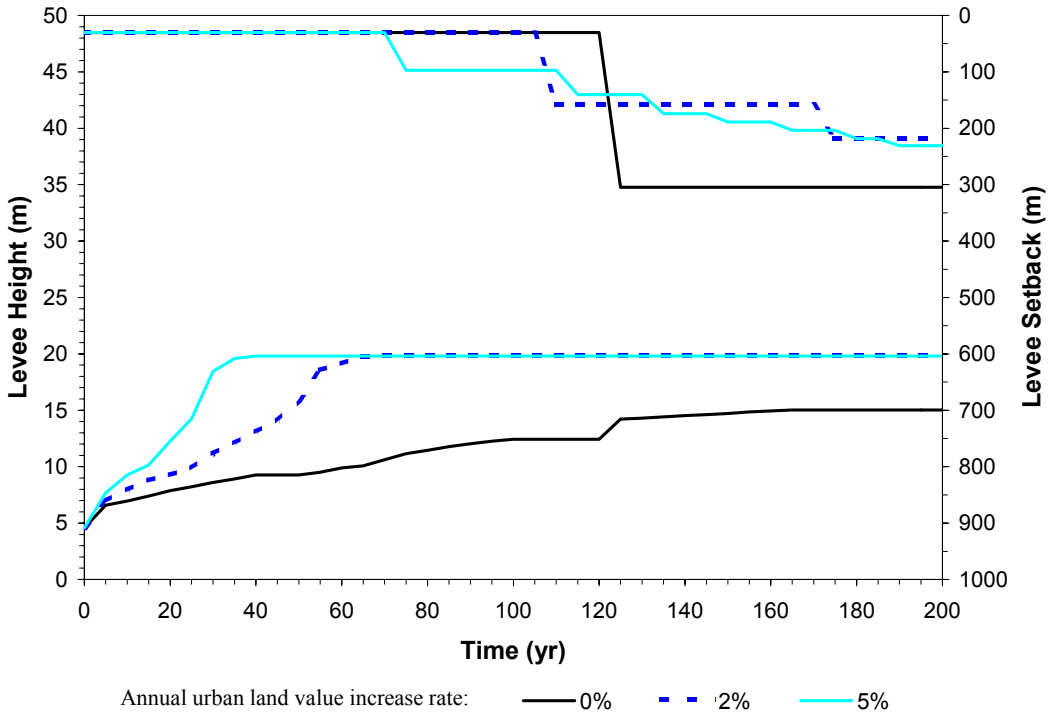

Figure 4.7. Combined effects of *historical trend* scenario and urbanization.

With the *historical trend* scenario and 5%/yr urbanization, levee height is gradually raised to 19.8 m at the 40th year when levee height limit is approached. The levee setback moves to about 97 m in the 75th year, jumps to 140 m in the 115th year, and then further expands to 174 m in the 135th year, followed by frequent moves with an approximate 10-year interval.

These levee setback and height results have implications for long-term floodplain management. First, they show that combined effects of climate change and urbanization are more challenging than the impacts from either factor along, requiring more rigorous flood levee adaptations. Second, with faster urbanization, the optimal decisions prefer building higher levees to sacrificing more urban land for floodway expansions. When levee height is constrained by the height limit (19.8 m), the system must resort to setback expansion. At higher urbanization rates, the levee is relocated more frequently after levee height is constrained. It sounds unacceptable that flood levee should be rebuilt once every ten years, however, it is economically efficient if the construction cost remains at today's level for a very long period and urban land values become very large. The SDP model was also run with different construction cost increase rates. Those results demonstrate that construction cost increase would significantly reduce levee construction, in terms of both levee raising and setback changes. In particular, if the construction cost increase rate is set higher than the urbanization rate, levee construction would be possible only at the beginning of the planning horizon.

With the HCM scenario, as shown in Figure 4.8, the levee heights and setbacks of both 2%/yr and 5%/yr urbanization coincide with that of the 0%/yr urbanization case in the first 15 years. The levee height of the 2%/yr urbanization case gradually increase to the height limit of 19.8 m at the 90th year. Its setback increases to 71 m at the 120th year, moves to 101 m at the 135th year, and finally expands to 156 m at the 175th year.

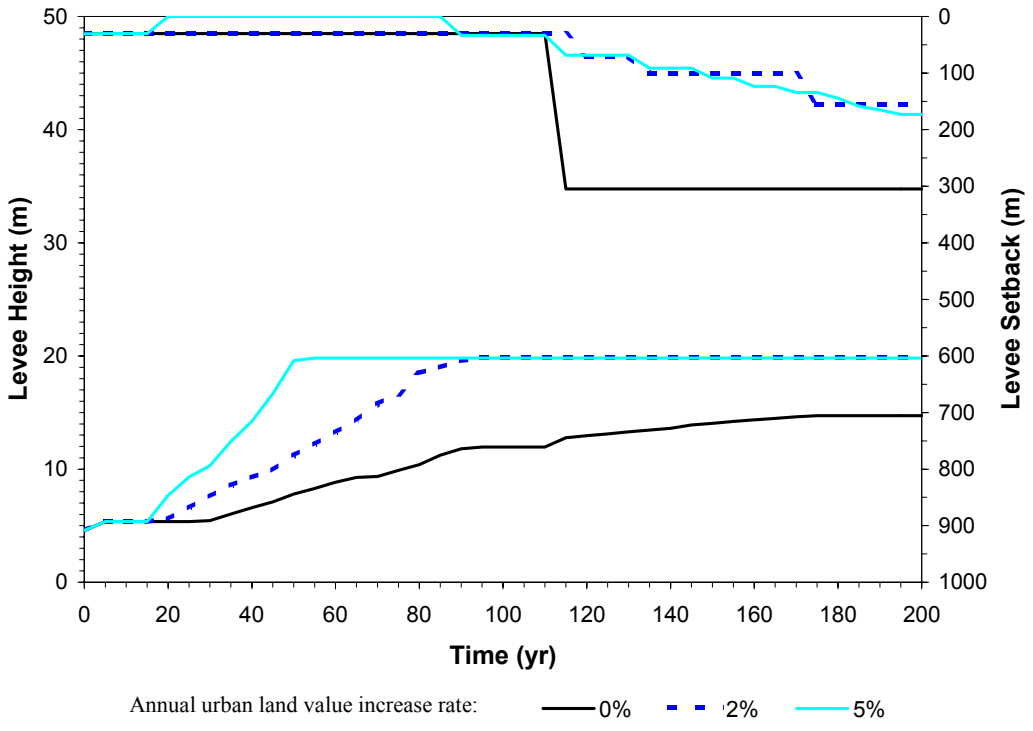

Figure 4.8. Combined effects of HCM climate change scenario and urbanization.

The 5%/yr urbanization case reduces levee setback to zero at the 20th year and the new levee is 7.7 m high. Then, it is gradually raised to 19.8 m in 30 years. In the 90th year, the levee is moved to 33 m, further moved to 68 m in the 115th year, followed by more frequent relocations in the remaining period to compensate the inability to raise levee height, until the levee setback attains 173 m in the end. Apparently, expected annual flood damages are worse when climate change is combined with urbanization.

4.7.4 Result Details

Figure 4.9 shows channel capacity and flooding probability changes over time for the *historical trend* scenario with 2%/yr urbanization. When setback expands, the resulting abrupt river capacity increase would significantly reduce flooding probability. Levee height increases also can significantly reduce flooding probabilities. However, from year 5 to year 25, as levee height and river capacity gradually increases to adapt to climate change and urbanization, the resulting flooding probability does not necessarily go down, due to the tradeoff between construction costs, including land value losses along levee raising, and the expected flooding damages.

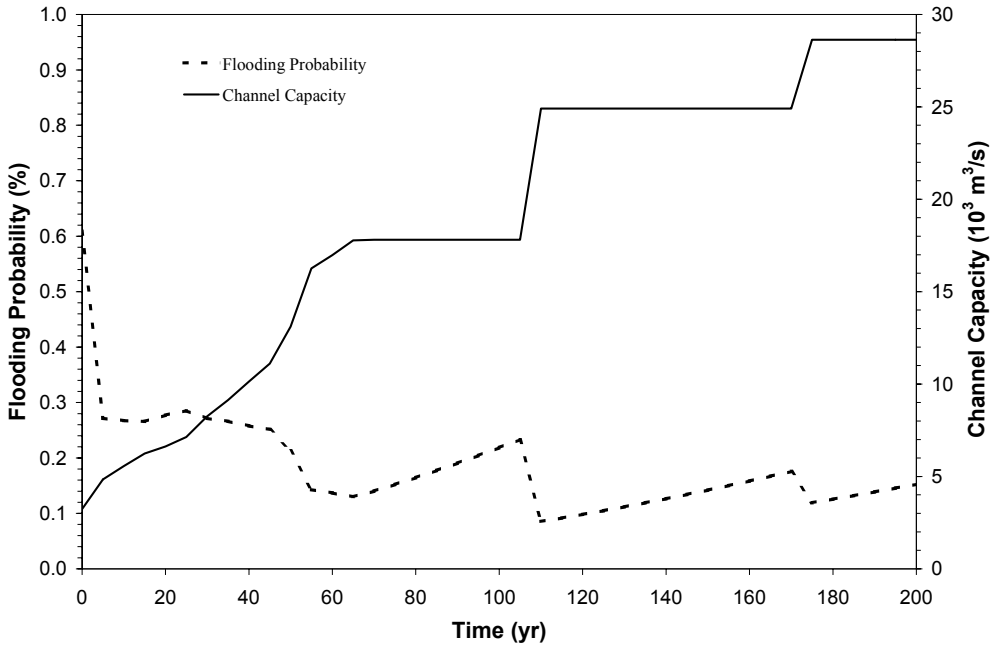

Figure 4.9. River capacity and flooding probability under combined historical trend climate change scenario and 2%/yr urbanization.

4.7.5 Sensitivity Analysis of Major Economic Factors

Sensitivity analysis evaluates sensitivities of levee decisions to such economic factors as damageable property value, urban land value, and discount rate. It was conducted by increasing a single economic factor value by 50% in each run, with the other factor values the same as in the base case (Table 4.1). In all runs the HCM climate change scenario is used to represent the forcing of hydrology. Urbanization is not considered.

As Figure 4.10 demonstrates, levee construction decisions are influenced significantly by perturbing economic factors. For all runs levees remain at the initial setback for more than 100 years. When the damageable property value is increased by 50%, levee setback does not change over the entire planning horizon, but levee heights are higher than that in the base case run. The resulting channel capacities also are greater which reduce flooding probabilities, providing better protection for the increased damageable property value.

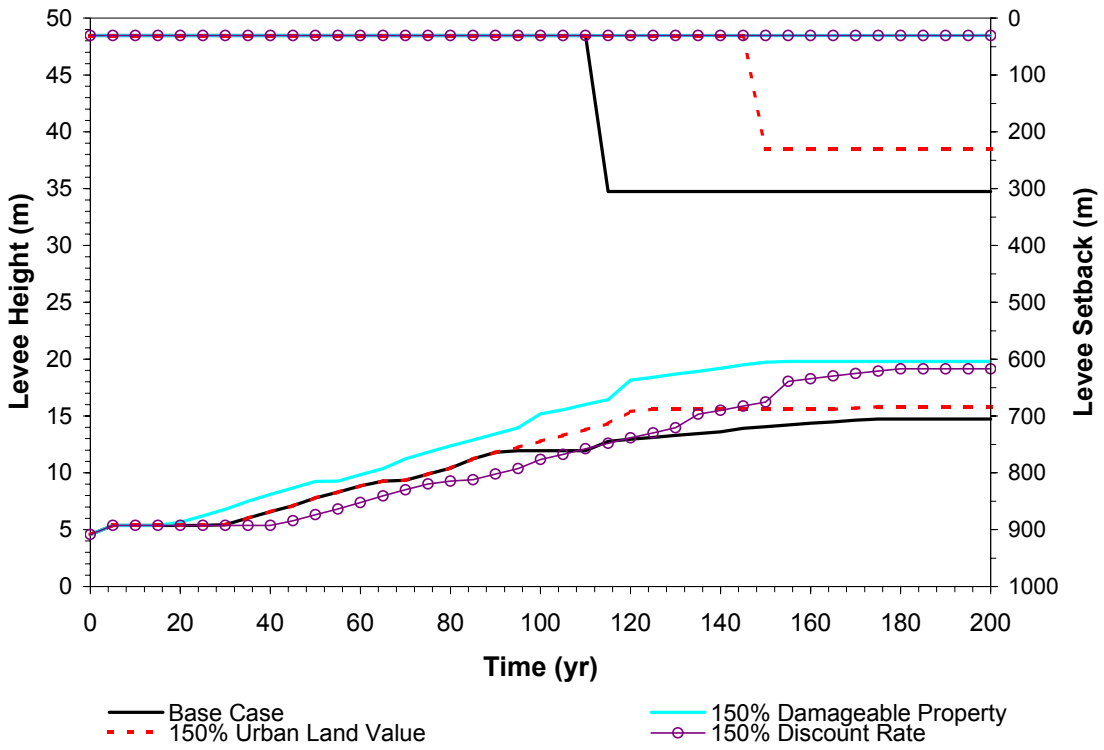

Figure 4.10. Sensitivity analysis for damageable property value, urban land value and discount rate.

When urban land value increases, levee setback expansion takes place later and by a smaller amount and, starting from the 90th year levee heights are greater than in the run with the original urban land value in the base case. Since urban land value is high, it is economically efficient to build a higher levee and protect more land for urban use.

With a 50% higher discount rate, levee setback does not change over the entire planning period. However, a higher discount rate results in lower height in approximately the first half of the planning horizon and higher height in the second half of the planning horizon, except the first 30 years when levee heights in the two runs coincide with each other. It looks like a higher discount rate tends to rotate anticlockwise the optimal time path of levee height. This is because with a higher discount rate the flood control expenditures in the near future are valued more than those in the far future. However, the effect of discount rate is complicated, involving tradeoffs of all other economic factors.

4.7.6 Costs of Flood Control Adaptations

Climate change could worsen flood control problems and significantly increase flood control costs for this system. Table 4.2 shows the costs for different combinations of climate scenarios and urbanization cases. Each cost value represents the accumulated discounted net costs of levee construction, expected flooding damages, and land revenues

or losses due to levee relocating over a 200-year period. Higher urbanization rates lead to higher flood protection costs mainly because of higher damageable property values. Among the three climate scenarios, the *stationary history* leads to the least flood control costs, and the *historical trend* leads to the highest costs. In Figure 4.2 we see that the means of flood frequency distributions for the *historical trend* scenario are higher than that of the HCM only in the first decade, while the standard deviations of the *historical trend* are higher than that of HCM over the entire planning horizon. This implies standard deviations of future floods play a more important role than the means do in flood events and flood protection planning. The more likely extremes in rainfall and floods due to climate change and significant uncertainties in future climate projections would likely result in higher flood protection costs than we see in the model runs.

Table 4.2. Expected present value costs of flood control adaptations (10^6).

Urbanization Rate / Climate Scenario	0%/yr	2%/yr	5%/yr
Stationary history	188	251	332
Historical trend	717	948	1,797
HCM	253	356	740

4.8 Limitations and Extensions

This study employs SDP for very long term flood planning. However, several limitations exist:

1) This method assumes perfect foreknowledge of climate change trends. Climate change projection is far from perfect and there are far more uncertainties in climate and hydrological regime changes than the model can include. Actual flood control planning is bedeviled not only by imperfect forecasting, but also imperfect knowledge of present and future flood climate variability. Nevertheless, this SDP method allows exploration of the implications of potential future trends. The uncertainty in future climate projection can be partly quantified and considered in the SDP model, for instance, through adding an probability density function (PDF) of future climate projection into the stage benefit function in Equation (4.1). The new recursive equation becomes

$$f_t\left(\overrightarrow{S_t}, \overrightarrow{X_t}\right) = \begin{cases} \max\limits_{X_t} \left\{ \sum\limits_j \int P_t\left(j \mid \overrightarrow{X_t}; \theta\right) B_{jt}\left(\overrightarrow{S_t}, \overrightarrow{X_t}\right) f_t(\theta) d\theta + f_{t+1}\left(\overrightarrow{S_{t+1}}, \overrightarrow{X_{t+1}}\right) e^{-r \cdot \Delta t} \right\}, & t < N \\ V\left(\overrightarrow{X_N}\right), & t = N \end{cases}$$

where θ denotes climate change flood frequency parameter or parameters, for example, mean or standard deviation, and $f_t(\theta)$ is the PDF of the flood frequency parameter at a future year t. Presently, such kinds of climate projection PDF is not ready for use in flood control planning, but some research works have been conducted to develop the PDFs of future climate change hydrology for a few rivers in California (Dettinger, 2003).

2) Flood frequency may not fit a lognormal distribution when climate and hydrologic regime change. And, parameter changes may not follow linear trends. We are unlikely to actually know the form and rates of these trends until a long history of floods have been endured.

3) Flood control operations for Folsom Reservoir and upstream reservoirs are not well represented in this study. These could have important influences on the results, and greatly simplifies the range of upstream options for flood management for this practical case. This is a topic for further study.

4) This study employs steady flow hydraulic routing with normal flow depth downstream to derive rating curves. Unsteady flow routing of properly designed hydrographs might provide better representation of stage-discharge relationships. Stochastic analysis of downstream elevations at the confluence with the American River might be valuable.

5) The north bank setback is dealt with a unique state variable. In reality, levee relocation may be impossible in some important locations, and different setbacks for different reaches may be optimal given varying hydraulic and economic conditions. It is also a simplification to use the water elevation at a common index point to represent the whole reach of the levee being studied. Theoretically, multiple reaches can be represented by more state variables, at a cost of much longer computational time.

The results presented in this chapter for the lower American River are very preliminary, given these limitations in method and in parameter estimation. However, these results illustrate possible trends in climate change and potential economic effects and promising adaptation directions over long periods.

4.9 Conclusions

Optimal long-term flood protection for urban areas is affected by many climatic, hydraulic, economic and societal factors. For long-term planning these interactions can be examined by optimization methods, providing some insights into this planning problem. The following conclusions are drawn for this study:

1) The SDP method developed here provides a framework for long term flood control planning and analysis with climate change and urbanization. The method appears useful for exploratory analysis within its limitations.

2) This study demonstrates the economically optimal interaction of multiple flood control decisions over long period with changing economic and climatic conditions.

3) Preliminary application of this method to the lower American River examines the effects of climatic and social-economic factors in this region. The results have some implications for long-term floodplain planning and management. Specifically, there is likely to be economic value to expanding lower American River setbacks and levee heights over long periods of time, and making present-day zoning decisions to preserve such options.

4) Climate change and urbanization can have major combined effects on flood damage and optimal long-term flood management. Other factors also have influence. Climate change studies of impacts and adaptations should include future changes in economic conditions and management decisions as well.

Cities and urban land use decisions can endure for hundreds, even thousands of years. So it behooves flood control engineers and urban planners to consider the long-term changes in economic and environmental conditions likely to affect the long-term performance of long-lived infrastructure and land uses. This chapter illustrates the importance of such a long-term perspective and a limited approach for such exploratory examinations of flood control system in a growing urban region.

Over the coming century or so, the core of metropolitan Sacramento appears destined to expand into a major floodplain of the Sacramento and American Rivers. This expanded core, with its benefits of proximity to the existing metropolitan core, will have to cope with increasing flood risk, arising largely from growth of economic activity on vulnerable lands, but also perhaps from growing flood frequencies. If flood climate trends continue and are not otherwise mitigated, there will likely come a time when major land use dislocations are required in the North Natomas region to create a broader floodway for the American River, although the timing and extent of such dislocations remain uncertain.

References

Alley, R. B., J. Marotzke, W. D. Nordhaus, J. T. Overpeck, D. M. Peteet, R. A. Pielke Jr., R. T. Pierrehumbert, P. B. Rhines, T. F. Stocker, L. D. Talley, and J. M. Wallace (2003), Abrupt climate change, *Science*, 129, 2005-2010.

Dettinger, M. D. (2003), Towards a PDF of 21st Century hydroclimate change in California, *Presentation in the California Water and Environmental Modeling Forum Conference, Climate Change and Its Impacts on Water Supply and Water Quanlity in California*, *available at:* http://www.cwemf.org/workshops/ClimateChgWrkshp/Dettinger.pdf, *accessed in:* August, 2004.

Goldman, D. M. (2001), Quantifying uncertainty in estimates of regulated flood frequency curves, in *Proceedings of the World Water and Environmental Resources Congress, Bridging the Gap: Meeting the World's Water and Environmental Resources Challenges*, edited by D. Phelps and G. Sehlke, ASCE, Orlando, Florida.

Heidari, M., V. T. Chow, and P. V. Kokotovic (1971), Discrete differential dynamic programming approach to water resources systems optimization, *Water Resour. Res.*, 7(2), 273-282.

James, L. D. (1965), Nonstructural measures for flood control, *Water Resour. Res.*, 1(1), 9-24.

Landis, J. D. and M. Reilly (2002), *How we will grow: baseline projections of California's urban footprint through the year 2100*, Department of City and Regional Planning, Institute of Urban and Regional Development, University of California, Berkeley. Berkeley, Calif.

Lettenmaier, D. P. and T. Y. Gan (1990), Hydrologic sensitivities of the Sacramento-San Joaquin River basin, California, to global warming, *Water Resour. Res.*, 26(1), 69-86.

Lund, J. R. (2002), Floodplain planning with risk-based optimization, *J. Water Resour. Plann. Manage.*, 128(3), 202-207.

Miller, N. L., K. E. Bashford, and E. Strem (2003), Potential impacts of climate change on California hydrology, *J. Am. Water Resour. Assoc.*, 39(4), 771-784.

Milly, P. C. D., R. T. Wetherald, K. A. Dunne, and T. L. Delworth (2002), Increasing risk of great floods in a changing climate, *Nature*, 415(31), 514-517.

National Research Council (NRC) (1995), *Flood risk management and the American River basin: an evaluation*, NRC Press, Washington, D.C.

National Research Council (NRC) (1999), *Improving American River flood frequency analyses*, NRC Press, Washington, D.C.

Olsen, J. R., P. A. Beling, and J. H. Lambert (2000), Dynamic models for floodplain management, *J. Water Resour. Plann. Manage.*, 126(3), 167-175.

Redmond, K. T. (2000), *American River flood frequencies: a climate-society interaction*, *Available at*: http://meteora.ucsd.edu/cap/kelly_flood.html, *accessed in* September 2003.

Simonovic, S. P. and L. Li (2003), Methodology for assessment of climate change impacts on large-scale flood protection system, *J. Water Resour. Plann. Manage.*, 129(5), 361-371.

Stakhiv, E. Z. (1998), Policy implications of climate change impacts on water resources management, *Water Policy*, 1(2), 159-175.

Schreider, S. Y., D. I. Smith and A. J. Jakeman (2000), Climate change impacts on urban flooding, *Climatic Change*, 47, 91-115.

Tung, Y. Y. and L. W. Mays (1981), Optimal risk-based design of flood levee systems, *Water Resour. Res.*, 17(4), 843-852.

U.S. Army Corps of Engineers (USACE) (2002a), *HEC-RAS river analysis system user's manual*, U.S. Army Crops of Engineers Hydrologic Engineering Center, Davis, Calif.

U.S. Army Corps of Engineers (USACE) (2002b), *Sacramento and San Joaquin River Basins Comprehensive Study Technical Studies Documentation, Appendix F. Economics Technical Documentation*, *Available at*: http://www.compstudy.org/docs/techstudies/appendix_f_economics.pdf, *accessed in* July 2004.

Vanrheenen, N. T., A. W. Wood, R. N. Palmer, and D. P. Lettenmaier (2004), Potential Implications of PCM Climate Change Scenarios for Sacramento-San Joaquin River Basin Hydrology and Water Resources, *Climatic Change*, 62, 257-281.

Venkatesh, B. and B. F. Hobbs (1999), Analyzing investment for managing Lake Erie levels under climate change uncertainty, *Water Resour. Res.*, 35(5), 1671-1683.

Vörösmarty, C. J., P. Green, J. Salisbury, and R. B. Lammers (2000), Global Water Resources: Vulnerability from Climate Change and Population Growth, *Science,* 289(14), 284-288.

Yakowitz, S. (1982), Dynamic programming applications in water resources, *Water Resour. Res.*, 18(4), 673-696.

Yao, H. and A. Georgakakos (2001), Assessment of Folsom lake response to historical and potential future climate scenarios: 2. Reservoir Management, *J. Hydrology*, 249, 176-196.

Chapter 5 Modeling Inter-sector Water Transfers with Stochastic Multiple Stage Optimization

5.1 Introduction

Efficient use and allocation of existing water supplies have been being increasingly important, especially for such areas as California where water are highly valued (Hanak, 2003). The theory and practices of water marketing in American West have evolved in recent decades. Numerous studies illustrated that water transfers alleviate many supply and demand imbalances and result in additional economic benefits through transferring water to more beneficial uses (Vaux and Howitt, 1984; Lund, 1993; Howitt, 1994; Loomis, 1994; Israel et al., 1995; Newlin et al., 2002). Water markets are particularly useful to improve efficiency where perfect information is unavailable to policy makers, and private water rights are well established. Even during a drought, abundant water could be found once the right incentives were in place. However, any operations of water transfers are limited by institutional and physical structures (Johansson et al., 2002).

Water transfers can take many forms, such as a temporary or permanent sale of a water right by the water right holder, a lease of the right to use water from the water right holder, or a sale or lease of a contractual right to water supply. Water transfers also can take the form of a long-term contracts contingent on drought conditions. While, most permanent and long-term transfers are destined for urban users, and farmers purchase water on a year-to-year basis (DWR, 2003).

In California, water transfers have increased significantly over the last twenty years. The 1991 and 1992 California Drought Emergency Water Banks were the first large water transfer programs in the United States (Israel and Lund, 1995). Temporary and long-term transfers between water districts increased from 80,000 acre-feet in 1985 to over 1,250,000 acre-feet in 2001, in which about 80% are short-term transfers, within the same year (DWR, 2003).

Before the mid 1990s, agricultural water districts have been the primary source of water supply, although in some wet years urban districts in Southern California have also transferred water to other users. However, after the mid 1990s, most growth in transfers has been between environmental programs and agriculture, and urban purchases have remained flat (DWR, 2003).

Although an exchange will occur only when its benefits to both parties exceed the transaction costs (Wilchfort et al., 1997), water transfers may indirectly or potentially affect those not directly involved in the transactions. Such third party effects arising from water transfers have been widely discussed (Howitt, 1994; Hanak 2003; Knapp et al., 2003). Hanak (2003) noted two primary aspects of the third party issues in California. The first is a reduction in the quantity or quality of water available to others in source regions, especially as a result of groundwater transfers. The second is land fallowing or

idling cropland to sell water, which may harm the local economy and employment. In California, interregional transfers account for only 25-30% of transfers. Most transfers are within the same county or the same region (DWR, 2003). Among California's 58 counties 22 have adopted ordinances restricting groundwater exports. Without groundwater exports, competition in pumping may not necessarily jeopardize local economy even in a long run (Gisser et al., 1980).

The following of this chapter examines a water market for intersectoral transfers. The application of such a market mechanism would be limited by different political, economic and social concerns. We focus on the economic consequence of such kinds of transfers, with third party effects simply reflected in transaction costs.

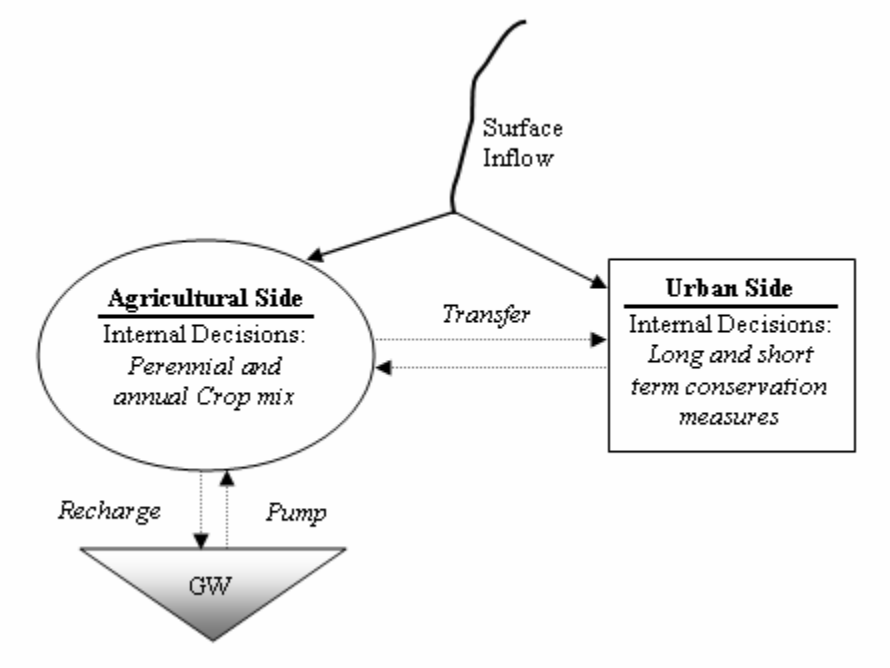

Figure 5.1. Schematics of water transfers.

Modeling of the intersectoral transfers is pictured schematically in Figure 5.1. The agricultural sector and the urban sector share the same surface water supply. Each sector has a predetermined water right, as a percentage of total surface water available in each year. An aquifer with large capacity is available in the agricultural region, enabling artificial recharge in wet years and groundwater pumping in dry years to enhance water supply reliability. A channel connects the two sectors for the purpose of water transfer.

We first examine the problem analytically, which provides some insight into the general characteristics of regional water transfer between two integrated users. Then, an economic-engineering optimization model is employed to maximize the overall expected net benefit. It can be shown that the integrated water allocation policy results in apparent

net benefit increase when it is compared with the independent decisions made separately by the agricultural region and the urban region without interregional transfers.

5.2 Analysis of Water Transfers

Analytical approaches often are not capable of dealing with complicated problems but can provide some useful insights into the features of problem solution. The following analysis follows the approach by Lund (1995) but extends to a system with conjunctive surface and ground water operation and water transfers. The mathematical formulation maximizes the expected value of net benefit, which includes agricultural production benefits, urban water conservation costs, and operating costs of groundwater pumping, artificial recharge, and water transfers.

$$\max Z = \left[f_1(\mathbf{X}_1) + \sum_{j=1}^{h} P(Q_j) f_2(\mathbf{X}_1, \mathbf{X}_{2j}) \right] - \left[g_1(\mathbf{Y}_1) + \sum_{j=1}^{h} P(Q_j) g_2(\mathbf{Y}_1, \mathbf{Y}_{2j}) \right] - \sum_{j=1}^{h} P(Q_j) \left[C_G(G_j) + C_T(T_j) \right] \tag{5.1}$$

Subject to

$$W(\mathbf{X}_1, \mathbf{X}_{2j}) \le \alpha Q_j + G_j - T_j, \quad \forall\ j \tag{5.2}$$

$$D_j - S(\mathbf{Y}_1, \mathbf{Y}_{2j}) \le (1-\alpha) Q_j + T_j, \quad \forall\ j \tag{5.3}$$

$$\sum_{j=1}^{h} P(Q_j) \left[G_j - \beta W(\mathbf{X}_1, \mathbf{X}_{2j}) \right] = 0, \quad \forall\ j \tag{5.4}$$

where

Z = the maximum expected net benefit over the entire discrete hydrologic events
$\mathbf{X}_1$ = vector of planted acreages of perennial crops
$\mathbf{X}_{2j}$ = vector of planted acreages of annual crops in the j^{th} year type
$\mathbf{Y}_1$ = vector of amounts of implementing long-term urban water conservation measures
$\mathbf{Y}_{2j}$ = vector of amounts of implementing temporary (annual) urban water conservation measures in the j^{th} year type
Q_j = total surface water supply in year type j
α = percentage of surface water allocated to agricultural region
β = percentage of total applied irrigation water that percolates to groundwater table
G_j = groundwater pumping (+) or artificial recharge (-) in year type j
T_j = amount of water transferred from agricultural region to urban region in year type j
D_j = full urban water demand in year type j
$P(.)$ = discrete probability function of surface water supply

$f_1(.)$ = annualized benefit of perennial crops

$f_2(.)$ = annualized benefit of annual crops

$g_1(.)$ = annualized long-term urban water conservation cost

$g_2(.)$ = annualized temporary urban water conservation cost

$C_G(.)$ = cost of groundwater pumping or artificial recharge

$C_T(.)$ = transaction cost of water transfer, including operating cost (e.g. rent for using conveyance and storage facilities and energy cost for water pumping) and cost to compensate the third party whose benefit is harmed during the transaction

$W(.)$ = total applied water in agricultural region

$S(.)$ = total water saved with long-term and temporary conservation measures

Constraint (5.2) represents agricultural region water balance. It states that, in each year type j, the total applied irrigation water should not exceed water availability for agricultural region, which equals the surface inflow into agricultural region plus pumped groundwater (or minus the amount of water recharging the aquifer, if $G_j < 0$) and minus export to urban region (or plus import from the urban region, if $T_j < 0$). Similarly, constraint (5.3) represents urban region water balance. It states that, in year type j, the reduced urban demand (full demand minus water saving through implementing conservation measures) should not exceed the sum of urban surface water inflow and water import from agricultural region. Constraint (5.4) describes the stochastic conservation of mass for groundwater storage. It states that the expected amount of net pumping and recharge should equal the expected amount of irrigation water percolation. Besides these constraints, there is an implicit assumption $\sum_{j=1}^{h} P(Q_j) = 1$, a typical feature of probabilistic events.

The above formulation is for the case where land availability is not constraining in agricultural sector and conservation levels are not limited in urban sector. This simplification allows us to focus on effects of water availability. For crops with convex cost functions in cropped acreage and positive urban conservation cost functions, this simplification does not harm the analysis of optimal water allocations within a sector and transfer decisions between agricultural and urban sectors.

The first order solution conditions for this problem can be found using Lagrange multipliers. The Lagrangian for this problem is

$$L = \left[f_1(\mathbf{X}_1) + \sum_{j=1}^{n} P(Q_j) f_2(\mathbf{X}_1, \mathbf{X}_{2j}) \right] - \left[g_1(\mathbf{Y}_1) + \sum_{j=1}^{n} P(Q_j) g_2(\mathbf{Y}_1, \mathbf{Y}_{2j}) \right]$$
$$- \sum_{j=1}^{n} P(Q_j) \left[C_G(G_j) + C_T(T_j) \right] - \sum_{j=1}^{n} \lambda_j \left[W(\mathbf{X}_1, \mathbf{X}_{2j}) - \alpha Q_j - G_j + T_j \right]$$
$$- \sum_{j=1}^{n} \mu_j \left[D_j - S(\mathbf{Y}_1, \mathbf{Y}_{2j}) - (1-\alpha) Q_j - T_j \right] - \eta \sum_{j=1}^{n} P(Q_j) \left[G_j - \beta W(\mathbf{X}_1, \mathbf{X}_{2j}) \right]$$

(5.5)

Deriving the first order solution conditions and simplifying

$$\frac{\partial f_1(\mathbf{X}_1)}{\partial \mathrm{X}_{1\mathrm{i}}} + \sum_{j=1}^{n} P(Q_j)\frac{\partial f_2(\mathbf{X}_1, \mathbf{X}_{2\mathrm{j}})}{\partial \mathrm{X}_{1\mathrm{i}}} = \sum_{j=1}^{n} \lambda_j \frac{\partial W(\mathbf{X}_1, \mathbf{X}_{2\mathrm{j}})}{\partial \mathrm{X}_{1\mathrm{i}}} - \beta\eta \sum_{j=1}^{n} P(Q_j)\frac{\partial W(\mathbf{X}_1, \mathbf{X}_{2\mathrm{j}})}{\partial \mathrm{X}_{1\mathrm{i}}}, \quad \forall\, i \tag{5.6a}$$

$$\frac{\partial f_2(\mathrm{X}_1, \mathrm{X}_{2\mathrm{j}})}{\partial \mathrm{X}_{2\mathrm{jk}}} = \left[\frac{\lambda_j}{P(Q_j)} - \beta\eta\right]\frac{\partial W(\mathrm{X}_1, \mathrm{X}_{2\mathrm{j}})}{\partial \mathrm{X}_{2\mathrm{jk}}}, \quad \forall\, j,k \tag{5.7a}$$

$$\frac{\partial g_1(\mathbf{Y}_1)}{\partial Y_{1\mathrm{i}}} + \sum_{j=1}^{n} P(Q_j)\frac{\partial g_2(\mathbf{Y}_1, \mathbf{Y}_{2\mathrm{j}})}{\partial Y_{1\mathrm{i}}} = \sum_{j=1}^{n} \mu_j \frac{\partial S(\mathbf{Y}_1, \mathbf{Y}_{2\mathrm{j}})}{\partial Y_{1\mathrm{i}}}, \quad \forall\, i \tag{5.8}$$

$$\frac{\partial g_2(\mathrm{Y}_1, \mathrm{Y}_{2\mathrm{j}})}{\partial Y_{2\mathrm{jk}}} = \frac{\mu_j}{P(Q_j)}\frac{\partial S(\mathrm{Y}_1, \mathrm{Y}_{2\mathrm{j}})}{\partial \mathrm{Y}_{2\mathrm{jk}}}, \quad \forall\, j,k \tag{5.9}$$

$$\frac{\lambda_j}{P(Q_j)} = \eta + \frac{\partial C_G(G_j)}{\partial G_j}, \quad \forall\, j \tag{5.10a}$$

$$\frac{\mu_j - \lambda_j}{P(Q_j)} = \frac{\partial C_T(T_j)}{\partial T_j}, \quad \forall\, j \tag{5.11}$$

Equation (5.6a) implies that the marginal expected net benefit of growing permanent crop X_{1i} should equal the marginal expected value of irrigation water increase minus the value of overdrafting the portion of increased irrigation water use that percolates into the aquifer. If we derive the Lagrange multiplier η from Equation (5.10) and substitute it into (5.6a), we have

$$\begin{aligned}\frac{\partial f_1(\mathbf{X}_1)}{\partial \mathrm{X}_{1\mathrm{i}}} + \sum_{j=1}^{n} P(Q_j)\frac{\partial f_2(\mathbf{X}_1, \mathbf{X}_{2\mathrm{j}})}{\partial \mathrm{X}_{1\mathrm{i}}} &= \sum_{j=1}^{n}(1-\beta)\lambda_j \frac{\partial W(\mathbf{X}_1, \mathbf{X}_{2\mathrm{j}})}{\partial \mathrm{X}_{1\mathrm{i}}} \\ &\quad + \beta\sum_{j=1}^{n}\left[P(Q_j)\frac{\partial G_G(G_j)}{\partial \mathrm{G}_{\mathrm{j}}}\frac{\partial W(\mathbf{X}_1, \mathbf{X}_{2\mathrm{j}})}{\partial \mathrm{X}_{1\mathrm{i}}}\right], \quad \forall\, i\end{aligned} \tag{5.6b}$$

Equation (5.6b) states that the marginal expected benefit of growing permanent crop X_{1i} should equal the marginal expected value of the portion of increased irrigation water use that does not percolate into aquifer plus the expected cost to pump that portion of increased irrigation water that percolates into aquifer. This is consistent with intuition. In other word, this shows that the optimal decision of growing each permanent crop requires the marginal expected benefit of plantation equals its marginal expected cost. Since the analysis is conducted under a static framework, temporal discount of values is

not accounted thus the water value and the pumping cost in the future are not different from today.

Literally, Equation (5.7a) means the marginal benefit of growing annual crop X_{2jk} in year type j should equal the value of marginal applied water minus the value of overdrafting the portion of marginal applied water that percolate into aquifer. While, the meaning of the second part in the right hand side (RHS) of Equation (5.7a) is still not quite clear. Deleting η in Equation (5.7a) through embedding Equation (5.10a), we obtain

$$\frac{\partial f_2(X_1, X_{2j})}{\partial X_{2jk}} = (1-\beta)\frac{\lambda_j}{P(Q_j)}\frac{\partial W(X_1, X_{2j})}{\partial X_{2jk}} + \beta\frac{\partial G_G(G_j)}{\partial G_j}\frac{\partial W(X_1, X_{2j})}{\partial X_{2jk}}, \qquad \forall\ j,k \tag{5.7b}$$

Equation (5.7b) states that the marginal benefit of growing annual crop X_{2jk} in year type j should equal the value of the portion of marginal applied water that does not percolate into aquifer plus the cost to pump the rest of marginal applied water that percolates into the aquifer, in year j.

Equations (5.8) and (5.9) are exactly the same as those conditions derived by Lund (1995). Equation (5.8) states that "the marginal expected cost of implementing a particular long-term conservation measure should equal the summed values of water use reductions resulting from implementation."; Equation (5.9) states that the marginal expected cost of implementing a particular short-term conservation measure k during the j^{th} year type of surface water supply should equal the expected value of water conserved from the marginal implementation (Lund, 1995). Equation (5.10a) implies that marginal value of irrigation water in year type j should equal the marginal cost of groundwater pumping or recharge in year type j plus the expected marginal value of groundwater overdraft . Since the expected marginal value of groundwater overdraft η is constant over all year types, difference of the other two terms in Equation (5.10a) also must be a constant for any two different year types, say j_1 and j_2, as illustrated in Equation (5.10b).

$$\frac{\lambda_{j_1}}{P(Q_{j_1})} - \frac{\partial C_G(G_{j_1})}{\partial G_{j_1}} = \frac{\lambda_{j_2}}{P(Q_{j_2})} - \frac{\partial C_G(G_{j_2})}{\partial G_{j_2}}, \qquad \forall\ j_1, j_2 \tag{5.10b}$$

Equation (5.10b) illustrates for any year types j_1 and j_2, the marginal value of irrigation water minus marginal cost of groundwater pumping or recharging in year type j_1 should equal that in j_2. Rearranging Equation (5.10b) leads to

$$\frac{\lambda_{j_1}}{P(Q_{j_1})} - \frac{\lambda_{j_2}}{P(Q_{j_2})} = \frac{\partial C_G(G_{j_1})}{\partial G_{j_1}} - \frac{\partial C_G(G_{j_2})}{\partial G_{j_2}}, \qquad \forall\ j_1, j_2 \tag{5.10c}$$

Equation (5.10c) implies the difference of irrigation water shadow values in two year types is determined by the difference of groundwater pumping or recharging costs in

the two year types. However, aquifer dynamics cannot be included in this model since the stochastic multiple stage optimization examines the problem under a static framework, treating hydrologic uncertainties with discrete year type events without an "order of occurrence". Therefore, the aquifer storage is assumed to be large enough so that pumping and recharge cause only minor groundwater table fluctuation. Consequently, pumping and artificial recharge cost function is piecewise linear (Figure 5.2) and marginal costs of pumping and recharge are constant over all year types. Within this context, an implication of Equation (5.10c) is marginal values of irrigation water equal to each other in all dry years when groundwater pumping is needed. The same conclusions can be drawn for all wet years with artificial recharge and all normal years with neither pumping nor recharge. Note all such conclusions are on the basis of another assumption that farmland is unconstrained.

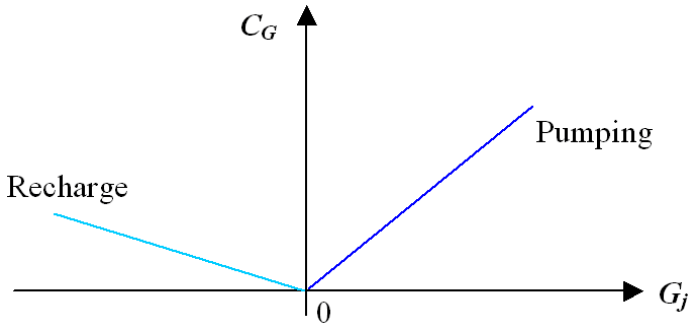

Figure 5.2. Cost function of groundwater pumping and recharge.

Equation (5.11) states that the difference between urban water shadow price and irrigation water shadow price in year type j should equal the marginal cost of water transfer. This further implies that a transfer would occur only if the difference between water marginal values of the two parties exceeds the overall transaction cost. This is similar to the economic implications of regional trade models (Howitt, 2002).

The above analytical analysis does not involve capacity constraints of land, pumping and artificial recharge, conveyance for transfers, and urban conservation measures, etc. The following stochastic two stage mathematical program examines situations with such capacity constraints.

5.3 Two-Stage Mathematical Programming Formulation

5.3.1 Model Development

The following model uses a two-stage stochastic quadratic program to optimize crop production and conjunctive use decisions in an agricultural region, water conservation decisions in an urban region, and water transfers between the two regions. It

optimizes long term, "permanent", decisions in the first stage, and annual "temporary" decisions in the second stage based on stochastic surface water supply.

Urban long term water conservation decisions include retrofitting household fixtures to conserve more water, and short term water conservation decisions include episodic reduction in water use for certain demands. Agricultural long term decisions include permanent crop acreages, and short term decisions include annual crop acreages and conjunctive use operations of artificial recharge and groundwater pumping (Marques, 2004). The urban side seeks to minimize the total expected water conservation cost of permanent and annual measures, while the agricultural side seeks to maximize the total net expected revenue from crop production. Activities in the two sectors are related by water transfer decisions. The objective of the water transfer model is to maximize the total expected value resulting from agricultural benefits minus urban water conservation costs and operating costs of conjunctive operations and water transfers.

In the following objective function, X_{1i} represents the acreage used to grow perennial crop i, which has a unit gross revenue v_{1i}, intercept of supply function α_{1i} and slope γ_{1i}; X_{2lj} represents the acreage used to grow annual crop l in year type j, the crop has a unit gross revenue v_{2l}, intercept of supply function α_{2l} and slope γ_{2l}; Y_{1k} represents the level of implementing permanent conservation measure k, of which the unit implementing cost is c_{1k}; Y_{2lj} represents the level of implementing short-term conservation measure g, of which the unit implementing cost is c_{2g}; e_{1k} is water conservation effectiveness of permanent measure k and e_{2g} is water conservation effectiveness of short-term measure g; p_j represents the probability of the j^{th} hydrologic event of surface water supply; D_j is full service urban demand in year type j; Q_j^{AU}, Q_j^{UA}, Q_j^P represent water transferred to and from urban region and amount of groundwater pumping, respectively; the product of CAP_R and XR_j is the amount of artificial recharge, where CAP_R is recharge capacity per acre of land per year and XR_j is acreage used for artificial recharge; and C_{AU}, C_{UA}, C_P, C_R represent respectively the unit cost of transferring water to and from urban region, groundwater pumping and recharge. The model objective function is

$$
\begin{aligned}
Max\ Z = & \left\{ \sum_{i=1}^{n_P} \left[v_{1i} X_{1i} - \left(\alpha_{1i} + 0.5\gamma_{1i} X_{1i} \right) X_{1i} \right] + \sum_{j=1}^{h} p_j \left[\sum_{l=1}^{n_T} \left(v_{2l} X_{2lj} - \left(\alpha_{2l} + 0.5\gamma_{2l} X_{2lj} \right) X_{2lj} \right) \right] \right\} \\
& - \left\{ \sum_{k=1}^{m_P} c_{1k} Y_{1k} + \sum_{j=1}^{h} p_j \left(\sum_{g=1}^{m_T} c_{2g} Y_{2gj} \right) + \sum_{j=1}^{h} c_{rj} \left(D_j - \sum_{k=1}^{m_P} e_{1k} Y_{1k} - \sum_{g=1}^{m_T} e_{2g} Y_{2gj} \right) \right\} \\
& - \sum_{j=1}^{h} p_j \left(C_{AU} Q_j^{AU} + C_{UA} Q_j^{UA} + C_P Q_j^P + C_R \cdot CAP_R \cdot XR_j \right)
\end{aligned}
\tag{5.12}
$$

Subject to

$$\sum_{i=1}^{n_p} w_{1i} X_{1i} + \sum_{l=1}^{n_t} w_{2l} X_{2lj} \le \alpha Q_j + Q_j^P - CAP_R \cdot XR_j - Q_j^{AU} + Q_j^{UA} \qquad \forall\ j \qquad (5.13)$$

Equation (5.13) describes conservation of mass in the agricultural region in year type j. It states the amount of water used to grow perennial and annual crops should not exceed the surface water supply plus net groundwater pumping and minus net export. In (5.13), w_{1i} is the amount of water required by per acre of perennial crop i; w_{2l} is the amount of water required by per acre of annual crop l; α is percentage of surface water allocated to agricultural region; CAP_R is recharging capacity of per acre of land per year; and XR_j is the acreage used for artificial recharging in year type j. Equation (5.14) describes the urban water balance, that the reduced urban water demand cannot exceed urban surface water supply plus net import for year type j.

$$D_j - \sum_{k=1}^{m_P} e_{1k} Y_{1k} - \sum_{g=1}^{m_T} e_{2g} Y_{2gj} \le (1-\alpha) Q_j + Q_j^{AU} - Q_j^{UA} \qquad \forall\ j \qquad (5.14)$$

Equation (5.15) represents stochastic conservation of mass of groundwater storage, which states that the average net groundwater pumping should equal the average irrigation water percolation.

$$\sum_{j=1}^{h} p_j \left[Q_j^P - CAP_R \cdot XR_j - \beta \left(\sum_{i=1}^{n_p} w_{1i} X_{1i} + \sum_{l=1}^{n_t} w_{2l} X_{2lj} \right) \right] = 0, \qquad \forall\ j \qquad (5.15)$$

In (5.15), β is the percentage of total applied irrigation water that percolates into the aquifer.

The following are capacity constraints. Equation (5.16) states the total acreage of planted perennial and annual crops plus artificial recharging area is limited by the total available land, L. Equations (5.17) and (5.18) are urban permanent and short-term conservation measure constraints. Equation (5.20) states some short-term conservation measures are precluded by some permanent conservation measures. While Equation (5.21) states that some permanent conservation measures Y_{1i^*} are pre-required by some short-term measures Y_{2l^*j} in year type j.

$$\sum_{i=1}^{n_p} X_{1i} + \sum_{l=1}^{n_t} X_{2lj} + XR_j \le L \qquad \forall\ j \qquad (5.16)$$

$$Y_{1i} \le YC_{1i} \qquad \forall\ i \qquad (5.17)$$

$$Y_{2lj} \le YC_{2l} \qquad \forall\ j, l \qquad (5.18)$$

$$Q_j^P \le C_P \qquad \forall\ j \tag{5.19}$$

$$Y_{1i} + Y_{2lj} \le YC_{2l} \qquad \forall\ j, l \tag{5.20}$$

$$Y_{1i^*} - Y_{2l^*j} \ge 0 \qquad \forall\ j \tag{5.21}$$

5.3.2 Illustrative Example

The above optimization problem is written in GAMS (General Algebraic Modeling System), and is solved by using a nonlinear solver, CANOPT, in the GAMS package. The model runs simulate decision making for an urban area with about 83,000 households and a 48,000 acre irrigated district. The urban area and the irrigated district share the same source of surface water supply while the irrigation district also has access to groundwater. The stochastic surface supplies are represented by 12 hydrologic year-types, as shown in Table 5.1. Every year 60% of total surface water supply is allocated to the irrigated district.

A conveyance facility connects the two regions to allow water transfer occur when desirable. Water transfer costs include the costs to negotiate and contract, rent of storage and conveyance facilities, and compensation for the third parties jeopardized by the transaction. The transfer costs from agricultural to urban also include water treatment costs. Agricultural production parameters are shown in Table 5.2, which were taken from Marques (2004). Urban conservation parameters are shown in Table 5.3. All operating costs are given in Table 5.4.

The model was run for different local management alternatives. Water transfer and no-water transfer (transfer capacity is zero) scenarios are developed and compared to evaluate the benefits of transfers to each side and its effect on local decisions. The objective of this analysis is to demonstrate the modeling approach, rather than provide an accurate simulation of the local operations.

Table 5.1. Probability distribution for surface flows[a].

Event	Probability	Quantity (af/yr)
E1	0.01	55286
E2	0.01	70029
E3	0.08	84771
E4	0.32	99514
E5	0.21	114257
E6	0.13	129000
E7	0.09	143743
E8	0.05	158486
E9	0.04	173843
E10	0.03	189814
E11	0.01	209471
E12	0.02	229129

[a]After Knapp and Olson (1995), but the expected annual surface flow is reduced by about 94%.

Table 5.2. Agricultural production parameters.

Crop		Yield (ton/acre)	Price ($/ton)	Intercept	Slope	Water Use (af/acre)
Perennial	Citrus	9.200	747	818.1	6.414	2.70
	Grapes	8.500	900	-583.5	0.336	2.80
	Nuts	1.300	3400	-1993.1	0.644	3.42
Annual	Cotton	0.625	1400	709.1	0.728	3.10
	Field Crops	1.400	500	390.3	0.255	2.97
	Truck Crops	9.000	533	3578.5	3.808	1.78
	Alfalfa	6.350	116	671.7	0.029	4.30
	Grain Crops	3.000	130	228.2	0.343	1.40

Table 5.3. Urban conservation parameters.

Measure		Cost ($/unit)	Effectiveness (af/unit)	Capacity (unit)
Permanent	Replace Toilet	25	0.0591	150000
	Replace Washing Machine	69.9	0.0202	83000
	Replace Dishwasher	40	0.0168	83000
	Avoid Leakage	8.6	0.0198	150000
	Normal Xeriscaping	65.3	0.112	83000
	Advanced Xeriscaping	130.6	0.168	83000
Short-term	Toilet Dam	19	0.056	150000
	Dry Lawn	700	0.112	83000
	Dry Shrub	1500	0.0784	83000

Table 5.4. Operating costs.

Description	Unit	Cost
Groundwater pumping cost	$/af	50
Groundwater recharge cost	$/ac.yr	1500
Urban retail price	$/af	300
Water transfer cost from urban to agricultural	$/af	50
Water transfer cost from agricultural to urban	$/af	60

5.3.3 Results and Discussions

Water transfers would prevent shortages by increasing efficiency and promoting water conservation. It allows more flexible water use by allocating water first to the most economically efficient users. The transfers between the two regions reduce average urban water conservation costs by 16%. The total net benefit of the system is increased by 1.5% through transfer though net agricultural benefit is reduced by 0.85%. Most of this benefit is obtained by eliminating expensive temporary water conservation measures (e.g. dry shrubs) in very dry years when additional water is transferred from the agricultural region.

Table 5.5. Expected value costs and benefits.

Expected values ($M/yr)	Without transfer	With transfer	Change
Agricultural net revenue	127.39	126.30	-0.85%
Urban water conservation cost	-22.76	-19.07	-16.2%
Transfer Cost	0	1.02	-
Total	104.63	106.21	1.5%

Although the agricultural region provides significant supplies to the urban region in the dry years (about 17% of its surface supply in the year type Y3, Table 5.6) it is able to compensate by increasing groundwater use. For example, Table 5.6 and Table 5.7 show in year type Y3, 80% of transferred water is from increased groundwater pumping. This operation allows the agricultural sector to minimize economic losses due to water transfers. However, the groundwater use by the agricultural region in the very dry years is still limited by the pumping capacity, resulting in reduced annual crop acreage, along with a minor reduction in permanent crop acreage.

Table 5.6. Transfer results (in af/yr).

Year type	Surface water supply		Water Transfer	
	Ag	Urban	Ag to Urban	Urban to Ag
Y1	39172	26114	1712	0
Y2	42017	28012	4558	0
Y3	50863	33908	8858	0
Y4	59708	39806	1779	0

Table 5.7. Results of groundwater pumping and recharge (in af/yr).

Year Type	Without Transfer		With Transfer	
	Pump	Recharge	Pump	Recharge
Y1	40000	0	40000	0
Y2	39814	0	40000	0
Y3	30969	0	38114	0
Y4	22123	0	22190	0
Y5	13277	0	11565	0
Y6	8631	0	6919	0
Y7	0	0	0	0
Y8		374	0	2086
Y9		9588	0	11300
Y10		19171	0	20883
Y11		0	0	13119
Y12		30549	0	26237

5.4 Conclusions

This chapter presents a two-stage stochastic optimization model to represent and examine economic-engineering integration of local water demand, conjunctive use, water conservation and water transfer decisions for an agricultural and an urban water districts with probabilistic water availability. Results illustrate how conjunctive use and water markets can function together to improve overall economic performance. Some specific conclusions are:

1) Urban and agricultural water users have significant ability to adjust to imperfect water supply reliability through various water conservation and crop production decisions.

2) Water transfers provide local incentives to facilitate coordinated urban and agricultural water conservation and water transfers to better match a probability profile of water availability.

3) For the example examined, most benefit of water transfer is obtained from avoiding costly urban conservation measures in very dry years.Conjunctive use

and water transfer operations complement each other and increase flexibility in local water management facing uncertain surface water supplies. Groundwater pumping supported by artificial recharge provides additional supply in very dry years allowing surface water transfer to urban regions avoiding expensive temporary water conservation measures.

Like all economic-engineering models, this modeling approach has limitations. First, it assumes urban users have infinite willingness to pay for satisfying demand, violating the truth that urban water demand is also elastic beyond the effects of water conservation. Secondly, groundwater pumping and recharge are greatly simplified by assuming a constant groundwater table and unlimited aquifer storage. A stochastic dynamic formulation of groundwater will improve the transfer model by providing long-term policy implications of transfer and conjunctive operation of surface and groundwater. This kinds of models can be used to develop adaptation measures given supply and demand changes under climatic and nonclimatic changes.

References

Alcubilla, R. G. (2002), *Derived Willingness-to-Pay for Water: Effects of Probabilistic Rationing and Price*, Masters Thesis, University of California, Davis, Calif.

Azaiez, M. N. (2002), A model for Conjunctive use of Ground and Surface Water with Opportunity Costs, *European Journal of Operational Research*, 143 (3), 611-624.

Cai, X. and Rosegrant, M. W. (2004), Irrigation Technology Choice under Hydrologic Uncertainty: A Case Study from Maipo River Basin, Chile, *Water Resour. Res*., 40W04103, doi: 10.1029/2003WR002810.

DWR (2003), California Water Plan Update 2003 (Draft)

Gisser, M. and Sanchez, D. A. (1980), Competition Versus Optimal Control in Groundwater Pumping, *Water Resour. Res.*, 16(4), 638-642.

Griffin, R. C. and Mjelde J. W. (2000), Valuing Water Supply Reliability, *Amer. J. Agr. Econ.*, 82, 414-426.

Hanak, E. (2003), *Who Should be Allowed to Sell Water in California? Third –Party Issues and the Water Market*, Public Policy Institute of California.

Howitt, R. E., Watson, W. D., and Adams, R. M. (1980), A Reevaluation of Price Elasticities for Irrigation Water, *Water Resour. Res.*, 16(4), 623-628.

Howitt, R. (1994), Empirical analysis of water market institutions: The 1991 California water market, *Resour. Energy Econ.*, 16(4), 357-371.

Howitt, R. E. (2002), *Optimization Model Building in Economics*, Department of Agricultural and Resource Economics, University of California, Davis, Calif.

Israel, M. and Lund, J. R. (1995), Recent California Water Transfers: Implications for Water Management, *Natural Resour. J.*, 35,.1-32.

Johansson, R. C., Tsur, Y., Roe, T. L., Doukkali, R. and Dinar, A. (2002), Pricing irrigation water: a review of theory and practice, *Water Policy*, 4(2), 173-199.

Knapp, K. C., Weinberg, M., Howitt, R., and Posnikoff, J. F. (2003), Water transfers, agriculture, and groundwater management: a dynamic economic analysis, *J. Enviro. Manage.*, 67, 291-301.

Knapp, K. C. and Olsen, L. J. (1995), The Economics of Conjunctive Groundwater Management with Stochastic Surface Supplies, *J. Enviro. Econ. Manage.*, 28, 340-356.

Loomis, J. B. (1994), Water transfer and major environmental provisions of the Central Valley Project Improvement Act: A preliminary economic evaluation, *Water Resour. Res.,* 30(6), 1865-1871.

Lund, J. R. (1993), Transaction Risk Versus Transaction Cost in Water Transfers*, Water Resour. Res., 29(9), 3103-3107.*

Lund, J. R. (1995), Derived estimation of willingness to pay to avoid probabilistic shortage*, Water Resour. Res*., 31(5): 1367-1372.

Lund, J. R. and Reed, R.U. (1995), Drought water rationing and transferable rations*, J. Water Resour. Plann. Manage*., 121(6), 429-437.

Marques, G. (2004), *Economic Representation of Agricultural Activities in Water Resources System Engineering,* Ph.D Dissertation, University of California, Davis, Calif.

Newlin, B. D., Jenkins, M. W., Lund, J. R. and Howitt, R. E. (2002), Southern California water markets: potential and limitations, *J. Water Resour. Plann. Manage.,* 128(1), 21-32.

Vaux, H. J. and Howitt, R. E. (1984), Managing water scarcity: an evaluation of interregional transfers*, Water Resour. Res*., 20(7), 785-792.

Wilchfort, O. and Lund, J. R. (1997), Shortage Management Modeling for Urban Water Supply Systems, *J. Water Resour. Plann. Manage.*, 123(4), pp. 250-258.

Chapter 6 Summary and Conclusions

This dissertation examines potential climate change impacts on California hydrologic components and explores adaptation methods for flood control and water supply. Based on theoretical analysis and simple case studies, the following conclusions are drawn.

1) Comprehensive representations of inflows to a water management system are important for impact, management, and adaptation studies of climate change. In the California statewide, winter flows would increase and spring snowmelt runoff would decrease due to climate warming. The potential magnitude of water supply effects of climate warming can be very significant, both positive and negative. These changes can be significant even relative to estimates of increased water demands due to population growth. Groundwater flows are especially important for water supply adaptation to climate change.

2) For flood levee planning under static climatic and economic conditions, the optimal tradeoff of levee setback for height is not affected by flood frequency and damageable property value, but determined by channel hydraulics, unit construction cost and marginal floodplain land value loss due to floodway occupation. Levee re-design decision rules are developed for static conditions based on the concepts of *critical height* for a setback and *critical setback* for a river reach.

3) Optimal flood levee height over time under dynamic conditions is studied with optimal control. With linear construction cost, levee construction decision depends on relative present values of marginal construction cost and marginal benefit of levee raising to the remaining period. For nonlinear construction cost case, a numerical approach is given to calculate levee construction decision and the optimal marginal benefit of levee construction over time. Levee raising patterns are discussed for each case.

4) Long term floodplain planning with climate change and urbanization are examined with stochastic dynamic programming. The results demonstrate the economically optimal interaction of multiple flood control decisions over long period. Climate change and urbanization can have major combined effects on flood damage and optimal long-term flood management. The case study shows there is likely to be economic value to expanding lower American River setbacks and levee heights over long periods of time, and making present-day zoning decisions to preserve such options.

5) A multiple stage stochastic optimization model is formulated to examine economic-engineering integration of water demand, conservation, conjunctive use and water transfer decisions for an agricultural district and an urban area with stochastic surface water supply. Water transfers provide incentives to facilitate

coordinated agricultural production arrangement and urban water conservation. Conjunctive use of surface and ground waters and water transfer operations complement each other and improve local water management flexibility.